

RING-FUSED NITROGEN HETEROCYCLES BY
EFFICIENT SYNTHETIC STRATEGIES

By

JOEL KWAME ANNOR-GYAMFI

Bachelor of Science in Chemistry
University of Cape Coast
Cape Coast, Ghana
2012

Master of Science in Chemistry
East Tennessee State University
Johnson City, Tennessee
2016

Submitted to the Faculty of the
Graduate College of the
Oklahoma State University
in partial fulfillment of
the requirements for
the Degree of
DOCTOR OF PHILOSOPHY
May, 2020

RING-FUSED NITROGEN HETEROCYCLES BY
EFFICIENT SYNTHETIC STRATEGIES

Dissertation Approved:

Dr. Richard A. Bunce

Dissertation Adviser

Dr. Kenneth D. Berlin

Dr. Ziad El Rassi

Dr. Toby L. Nelson

Dr. Andrew Mort

ACKNOWLEDGEMENTS

First and foremost, I would like to thank my Lord and savior Jesus Christ for granting me the grace to reach this milestone. A very special thanks to my adviser, Prof. Richard A. Bunce for providing me with great working atmosphere for research. In addition, his guidance and endless support throughout my studies at Oklahoma State University is highly appreciated. I would like to also express my deepest gratitude to Prof. Kenneth D. Berlin and his family for their encouragement and support as well as the many wonderful conversations we shared. I also wish to express my sincere appreciation to the rest of my committee members for being helpful in every way possible as well as to all faculty and staff in the Department of Chemistry. Special thanks are also due Dr. Krishna K. Gnanasekaran for being a tremendous mentor during my first semester, Dr. Kevin Meraz as well as Daniel Bryant for being great colleagues in the lab.

A very special thank you to my parents, Mr. Stephen and Mrs. Margaret Annor-Gyamfi as well as my wonderful family for their prayers and encouragement throughout my entire academic career. I also want to thank Mr. Francis Appah-Aikins and Mrs. Getty Otchere as well as my brothers-in-law for being very helpful in every way possible. A special thank you to all my friends and loved ones. Most importantly, to my beautiful and amazing wife, Mrs. Priscilla Abokuma Annor-Gyamfi, thank you for your immense support, love, prayers, devotion, and companionship during these years. Without you and Christ, none of this would have been possible.

Name: JOEL KWAME ANNOR-GYAMFI

Date of Degree: MAY, 2020

Title of Study: RING-FUSED NITROGEN HETEROCYCLES BY EFFICIENT SYNTHETIC STRATEGIES

Major Field: CHEMISTRY

Abstract: The first part of this work involved the synthesis of small molecules as potential inhibitors of the bacterioferritin B–bacterioferritin-associated ferredoxin (BfrB–Bfd) protein–protein interaction in *Pseudomonas aeruginosa*. BfrB is the main iron storage protein, which is central to bacterial iron homeostasis. The mobilization of iron from BfrB requires binding by a cognate ferredoxin (Bfd), thus BfrB–Bfd interaction is essential to the regulation of cytosolic iron levels in *P. aeruginosa*. The purpose of this project was to develop small molecules which could inhibit this protein–protein interaction and elicit perturbations in iron homeostasis that decrease bacterial fitness. Previous work from our research group involved the synthesis of 4-(alkylamino)isoindoline-1,3-diones which demonstrated promising inhibition of the BfrB–Bfd interaction. The current project focused on the synthesis of analogs that could be effective in a relatively low micromolar range. Consequently, 1- and 3-carbon linker analogs of the 4-(alkylamino)isoindoline-1,3-diones were synthesized and characterized. Based on molecular modeling, the following modifications below led to the synthesis of a series of twelve (12) new compounds.

- Incorporation of new benzaldehyde components: Relatively inexpensive starting materials were used for the reaction. It was envisioned that the incorporation of these functionalities in the analogs of the 4-(alkylamino)isoindoline-1,3-diones would possibly increase the inhibitory effect.
- Altering the carbon linker: Other modifications were made to the 4-(alkylamino)isoindoline-1,3-diones by decreasing the 3-carbon linker to a 1-carbon linker with similar aromatic substitution patterns and comparing their activity data.
- Substitution of the benzaldehyde component with other heterocyclic groups: The benzaldehyde component for both 1- and 3-carbon linkers was replaced with 2- and 3-furaldehyde and tetrahydrofuran analogs.

The second part of this work involved the design of new methods for the synthesis of bioactive heterocyclic scaffolds. A summary of these methods follows:

- An efficient one-pot approach to 1-aryl-5-nitro-1*H*-indazoles and 1-aryl-1*H*-indazoles was developed and optimized.
- A one-pot route to 4*H*-benzo[*d*][1,3]-oxazin-4-ones and dihydro analogs was designed from substituted anthranilic acid and ortho esters.
- An efficient, inexpensive approach to bis-1,3,4-oxadiazoles was established using NH₄Cl as a catalyst.
- An efficient synthesis of naphthalene, dihydroquinoline and naphthyridine carboxylates and carbonitriles as well as quinolones was accomplished using Morita-Baylis-Hillman acetates.

TABLE OF CONTENTS

Chapter	Page
I. SYNTHESIS OF SMALL MOLECULES AS POTENTIAL ANTIBIOTICS	1
1.1 Introduction	1
1.2 Statement of work.....	5
1.3 Screening of fragments that bind BfrB at the Bfd-binding site.....	5
1.4 Results and discussion for synthesis of 4-(alkylamino)isoindoline-1,3-dione derivatives.....	9
1.4.1 Binding effects of 4-(alkylamino)isoindoline-1,3-diones due to the incorporation of new benzaldehydes and altering of 3-carbon linker into 1-linker	11
1.4.2 Incorporation of new substituted benzaldehydes and altering of the 3-carbon linker to a 1-carbon linker	14
1.5 Conclusions	17
1.5.1 Incorporation of new substituted benzaldehyde and heterocyclic groups	17
1.5.2 Altering the carbon linker in 4-(alkylamino)isoindoline-1,3-dione analogs.....	18
1.6 Chemistry	18
1.6.1 Incorporation of new substituted benzaldehydes in BfrB–Bfd chemical probes	18

Chapter	Page
II. SYNTHESIS OF BIOACTIVE HETEROCYCLIC SCAFFOLDS.....	27
2.1 Introduction	27
2.2 Results and Discussion	30
2.2.1 1-Aryl-5-nitro-1 <i>H</i> -indazoles and a general route to 1-aryl-1 <i>H</i> -indazoles.....	30
2.2.1.1 Conclusions	31
2.2.2 4 <i>H</i> -Benzo[<i>d</i>][1,3]oxazin-4-ones and dihydro analogs	37
2.2.2.1 Conclusions	45
2.2.3 Bis- and mono-1,3,4-oxadiazole synthesis promoted by catalytic NH ₄ Cl	46
2.2.3.1 Conclusions	52
2.2.4 Naphthalenes and heterocycles from Morita-Baylis-Hillman (MBH) acetates by domino Michael addition-elimination-S _N Ar reactions.....	52
2.2.4.1 Conclusions	64
2.3 Chemistry	64
2.3.1 1-Aryl-5-nitro-1 <i>H</i> -indazoles and a general route to 1-aryl-1 <i>H</i> -indazoles	65
2.3.2 4 <i>H</i> -Benzo[<i>d</i>][1,3]oxazin-4-ones and dihydro analogs	76
2.3.3 Bis- and mono-1,3,4-oxadiazole synthesis promoted by catalytic NH ₄ Cl.....	84
2.3.4 Naphthalenes and heterocycles from Morita-Baylis-Hillman (MBH) acetates by domino Michael addition-elimination-S _N Ar reactions.....	90
REFERENCES.....	100
APPENDIX	119
X-ray data for ethyl 6-fluoro-4-oxo-1-phenylethyl-1,4-dihydroquinoline-3-carboxy- late	119

LIST OF TABLES

Table	Page
1.0 Structure and binding affinity of 4-(alkylamino)isoindoline-1,3-diones from previous work.....	11
2.0 Structure and binding affinity of current 4-(alkylamino)isoindoline-1,3-dione analogs.....	12
2.1 Yields for the two-step synthesis of 1-aryl-5-nitro-1 <i>H</i> -indazoles.....	33
2.2 Yields for the modified one-pot synthesis of 1-aryl-5-nitro-1 <i>H</i> -indazoles.....	35
2.3 Yields for the general one-pot synthesis of 1-aryl-5-nitro-1 <i>H</i> -indazoles	36
2.4 Formation of 4 <i>H</i> -benzo[<i>d</i>][1,3]oxazin-4-ones	40
2.5 Formation of (±)-1,2-dihydro-4 <i>H</i> -benzo[<i>d</i>][1,3]oxazin-4-ones.....	42
2.6 Optimization results for bis-1,3,4-oxadiazole from terephthalic dihydrazide (1.0 equiv) and triethyl orthoformate	48
2.7 Summary of 1,4-bis-1,3,4-oxadiazole from terephthalic dihydrazide	48
2.8 Summary of 1,3-bis-1,3,4-oxadiazole from isophthalic dihydrazide.....	49
2.9 Summary of 1,4-butyl-bis-1,3,4-oxadiazole from adipic dihydrazide.....	49
3.0 Summary of 1,3,4-oxadiazole from substituted arylhydrazide	51
3.1 Summary of 1,3,4-oxadiazole from nicotinic acid hydrazide	51
3.2 Summary of 1,3,4-oxadiazole from isonicotinic acid hydrazide	51
3.3 Yields for the synthesis of MBH alcohols	56

LIST OF FIGURES

Figure	Page
1.1 Structures of Penicillin and Vancomycin.....	1
1.2 Examples of semi-synthetic antibiotics.....	2
1.3 Maintenance of cellular iron homeostasis under deficient and replete conditions	4
1.4 Protein–protein interaction interface of the BfrB–Bfd complex.....	6
1.5 Schematic summary of the synthetic procedures employed to prepare fragments 6 , 10 and 13 ; ethers 9 derived from 5-hydroxyisoindoline-1,3-dione (6).....	8
1.6 Retrosynthetic route for 4-(alkylamino)isoindoline-1,3-diones.....	11
1.7 Analogs of 4-(alkylamino)isoindoline-1,3-diones with 3- and 1-carbon linker	16
2.1 General mechanism for S _N Ar reaction	30
2.2 Drugs incorporating 1-aryl-1 <i>H</i> -indazoles	31
2.3 4 <i>H</i> -Benzo[<i>d</i>][1,3]oxazin-4-ones with potential drug activity	38
2.4 Conformational options for intermediate D	45
2.5 Drug containing an oxadiazole ring	47
2.6 Scope of Morita-Baylis-Hillman (MBH) reaction	54
2.7 Naphthalene-containing anticancer agents.....	55
2.8 Entries of synthesized MBH acetates.....	57
2.9 Entries of synthesized naphthalene and quinoline derivatives.....	60
3.0 Entries of synthesized dihydroheteroaromatics	62
3.1 X-ray of ethyl 6-fluoro-4-oxo-1-phenyl-1,4-dihydroquinoline-3-carboxylate (104e) ...	63

LIST OF SCHEMES

Scheme	Page
1.1 Synthesis of analogs 27 and 31	14
2.1 Reactions of 46 and 47 with hydrazine hydrate	32
2.2 Formation of 4 <i>H</i> -benzo[<i>d</i>][1,3]oxazin-4-ones and their dihydro analogs from anthranilic acids and orthoesters	39
2.3 Presumed mechanism for the formation of 4 <i>H</i> -benzo[<i>d</i>][1,3]oxazin-4-ones	44
2.4 Presumed mechanism for the formation of 1,3,4-oxadiazole ring system	50
2.5 Synthesis of MBH alcohol 95a	55
2.6 A plausible mechanism for MBH alcohol formation	57
2.7 Results and plausible mechanism for esterification process	58
2.8 Plausible mechanisms for Michael addition-elimination (S _N 2')	59
2.9 A possible mechanism to aromatic compounds	60
3.0 Possible mechanism to dihydroheteroaromatics	61
3.1 Unexpected synthesis of 4-oxo-1,4-dihydroquinolines	63
3.2 Possible extension to fluoroquinoline antibiotics	63

CHAPTER I

SYNTHESIS OF SMALL MOLECULES AS POTENTIAL ANTIBIOTICS

1.1. Introduction

Infections due to antibiotic-resistant bacteria remain a worldwide threat to public health.¹ The ability of bacteria to develop antibiotic-resistant strains has overwhelmed our ability to develop new antibiotics and validate other targets.¹⁻⁴ Hence, new strategies and targets are critical and urgently needed to effectively overcome this challenge. In modern medicine, many achievements, such as organ transplantation, cancer chemotherapy and major surgery, have not received the deserved recognition due to antibiotic resistant infections.¹ The battle between new antibiotics and bacteria resistance mechanisms has always existed since the invention of the first antibiotic, Penicillin (**1**, Figure 1.1).

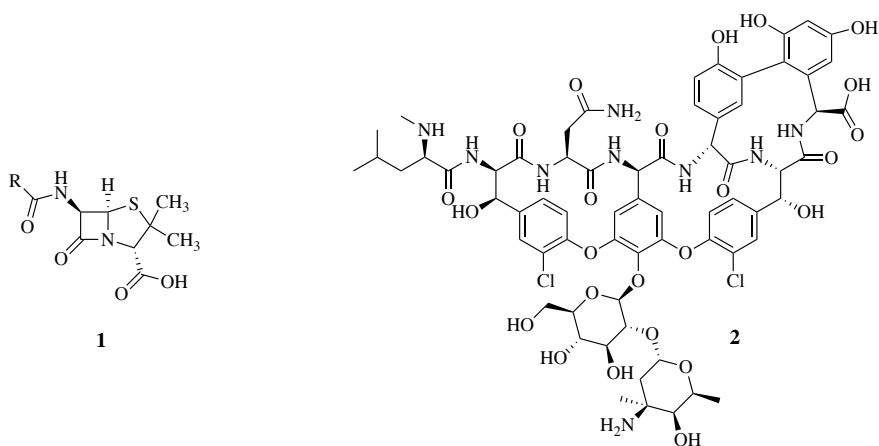


Figure 1.1. Structures of Penicillin and Vancomycin.

Most antibiotics are derived from natural products, and thus, antibacterial defense mechanisms of some sort often already exist. A typical example of an ancient antibiotic resistance is when genes coding for resistance against Vancomycin **2** (Figure 1.1) were observed in bacterial samples isolated from 10,000-year-old permafrost.^{3,5} Modern antibiotics and bacterial resistance are caused by several factors, including diminished pharmaceutical investments, antibiotic misuse by individuals and the food industry, chronic clinical over-prescription and public misconceptions.⁶ In response to this resistance, efforts were channeled towards the design of antibiotics that were semi-synthetically derived from natural products. Within the last 30 years, the majority of the semi-synthetic antibiotics introduced have demonstrated promising activities. These include the β -lactams meropenem **3** and tazobactam **4** as well as the aminoglycoside amikacin **5** (Figure 1.2) among others.^{6,7} Nevertheless, recent resistance developed against natural product antibiotics has necessitated the search for new classes of antibiotics. The ease with which many resistance genes are disseminated has made totally synthetic antibiotics better and attractive options to explore. Until recently, synthetic antibiotics remained extremely rare with sulfa drugs, quinolones, oxazolidinones and diarylquinolines being the only examples.⁶

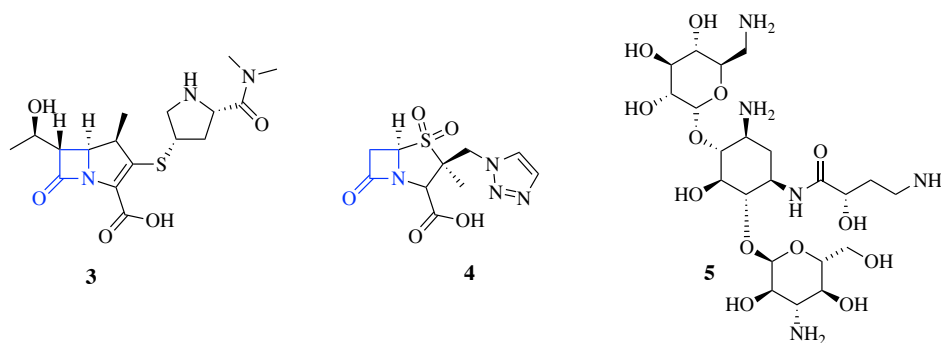


Figure 1.2. Examples of semi-synthetic antibiotics.⁶

Since 2016, the World Health Organization (WHO) has encouraged investment in new drugs by publishing a priority list for research and development of new antibiotics to combat multidrug resistant bacteria. A critical priority has been assigned to the Gram-negative carbapenem-resistant

Acinetobacter baumannii and *Pseudomonas aeruginosa*, and third-generation cephalosporin resistant Enterobacteriaceae.⁸ Gram-negatives are naturally resistant to many antibiotics because their outer membranes are designed to prevent the entry of many amphipathic drugs. Similarly, the inner membranes and highly active efflux pumps often recognize highly hydrophilic molecules. Thus, the issue of bacterial cell penetration poses an immense challenge to finding new synthetic scaffolds.^{6,9,10} *P. aeruginosa* remains one of the leading Gram-negative pathogens associated with hospital infections. Such pathogens easily colonize urinary catheters and endotracheal tubes,^{11,12} and accelerate lung function decay in patients with cystic fibrosis.^{13,14} An effective response to this menace will require vibrant research and continued investment in the early stages of drug development in order to establish a conduit of novel ideas and strategies.¹ In this context, a new therapeutic intervention recently developed involves potential strategies that interfere with bacterial iron acquisition and homeostasis.¹⁵⁻¹⁹ Bacteria rely heavily on iron for multiple metabolic processes such as respiration and fundamental enzymatic reactions.²⁰ The host usually serves as the source of iron for the pathogenic bacteria, however, its nutritional immunity maintains an extremely low concentration of free iron. Thus, the essential nutrient needed by the invading pathogens is denied.^{1,21-24} Typically, iron exists in two oxidation states, Fe³⁺ and Fe²⁺. The ferric iron (Fe³⁺) exhibits reduced bioavailability due to its minimal solubility. Ferrous iron (Fe²⁺), on the other hand, is soluble in aqueous solution, however, it can readily be converted to Fe³⁺ via an oxygen (O₂) or hydrogen peroxide oxidation mechanism. In response to the insufficient availability of iron, bacteria express a variety of uptake systems, and also evolve a number of mechanisms to highly regulate the process of bacterial iron homeostasis (acquisition, storage and utilization) ensuring sufficiency for metabolic needs while preventing iron-induced toxicity.^{25,26} One of the mechanisms involves the production of a ferric-siderophore complex, which plays a key role in the transportation of iron to the bacterial cytoplasm. Siderophores, also known as Fe²⁺ importers, contain oxygen atoms which selectively bind to ferric iron (Fe³⁺), making it water soluble and allowing cellular uptake.²⁷⁻²⁹ Bacteria secrete iron chelating

siderophores *via* an active efflux mechanism which involves inner membrane transporters such as EntS and IroC and the outer protein TolC (Figure 1.3).³⁰

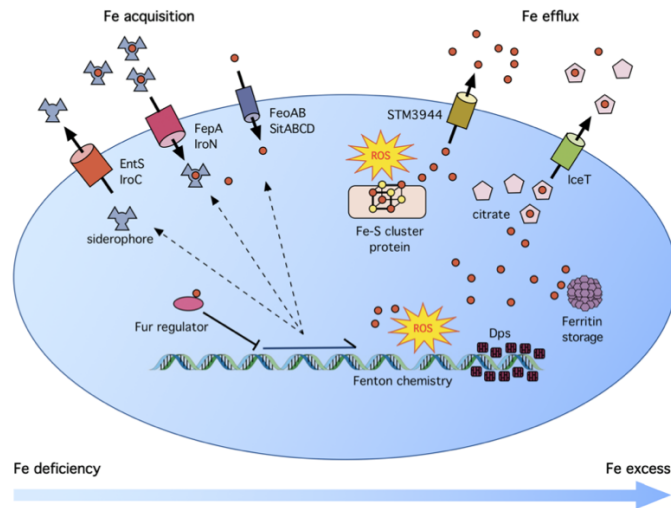


Figure 1.3. Maintenance of cellular iron homeostasis under deficient and replete conditions.³⁰

FeoAB and SitABCD are examples of uptake systems that bacteria employ in the acquisition of Fe^{2+} and/or other transition metals. FeoAB consists of a cytosolic protein and an inner membrane transporter that allows the uptake of only ferrous iron (Fe^{2+})³¹ whereas SitABCD is an ABCD family transporter that enables the acquisition of both Fe^{2+} and manganese.³² Bacteria maintain proper iron storage in several iron storage proteins. Two of the most studied proteins in *P. aeruginosa* cells are the bacterial ferritin (Ftn) and bacterioferritin (Bfr).¹ The *ftnA* and *bfrB* genes encode bacterial ferritin (FtnA) and bacterioferritin B (BfrB), respectively.^{33,34} However, BfrB functions as the main iron storage protein.²⁵ Recent research has shown that the mobilization of iron stored in BfrB requires specific interactions between BfrB and its cognate partner, bacterioferritin-associated ferredoxin (Bfd).^{25,35,36} BfrB stores iron in the form of a Fe^{3+} mineral. When *P. aeruginosa* needs iron, Bfd binds to the outer shell of BfrB and facilitates the transfer of an electron from ferredoxin NADp reductase (Fpr) into BfrB for the reduction of Fe^{3+} to Fe^{2+} . Ferrous iron (Fe^{2+}) is essential for the normal growth and function of the Gram-negative

bacteria, *P. aeruginosa*. Therefore, when the BfrB–Bfd interaction is interrupted, the bacteria are deprived of Fe²⁺, and consequently, bacterial death occurs.^{25,28-30,37,38}

1.2. Statement of work

Recent investigations have established the BfrB–Bfd interaction as a novel target to rationally induce iron homeostasis dysregulation in bacteria.^{1,25} These investigations involved the deleting of the *bfd* gene in *P. aeruginosa* to observe the effect on the bacterial iron metabolism. The outcome of these investigations showed an irreversible accumulation of Fe³⁺ in BfrB with concomitant iron deprivation in the cytosol.²⁵ Consequently, it was imperative to design small molecule inhibitors of the BfrB–Bfd interaction as chemical probes to study iron homeostasis in bacteria and possibly uncover additional vulnerabilities in the bacterial cell.¹ The focus of current work involved the synthesis and optimization of 4-(alkylamino)isoindoline-1,3-diones as chemical probes to dysregulate iron homeostasis in *P. aeruginosa*. These small molecules were designed to block the BfrB–Bfd protein–protein interaction by selectively binding BfrB at the Bfd binding site.

1.3. Screening of fragments that bind BfrB at the Bfd-binding site.

Initial work from our collaborators began with the screening and detection of fragments that bind BfrB at the Bfd-binding site. Structural information obtained from the BfrB–Bfd interaction showed that Bfd residues M1 (i.e. Met 5), Y2 (i.e. Tyr 2), and L5 (i.e. Leu 5) and BfrB residues L68 (i.e. Leu 68) and E81 (i.e. Glu 81) dominate the buried surface area at the protein-protein interface (Figure 1.4) and contribute significantly to the binding energy of the BfrB–Bfd complex.^{1,39} Thus, fragments that may bind at the sites occupied by Y2 and L5 were potential candidates. Moreover, fragments capable of π - π stacking were included with both electron-rich and electron-deficient aromatic rings.¹ Additionally, groups possessing similar chemical properties, such as the aromatic and aliphatic side chains of Tyr and Leu, were of great interest.

To screen for fragments, a competition assay that utilizes STD (saturation transfer difference) NMR spectroscopy was developed.¹ This technique was found to be ideal because only low protein concentrations were required, and also protein resonance assignments were not necessary. Additionally, the large rotational correlation time (τ_c) of BfrB enhanced spin diffusion as well as saturation transfer within the protein and to the ligand.^{1,40}

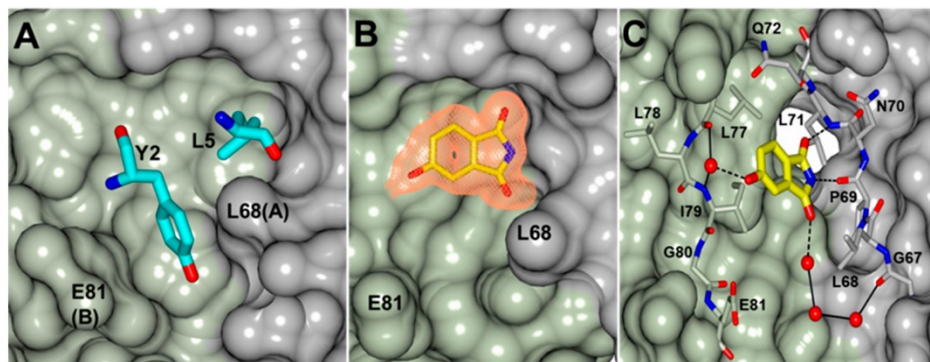
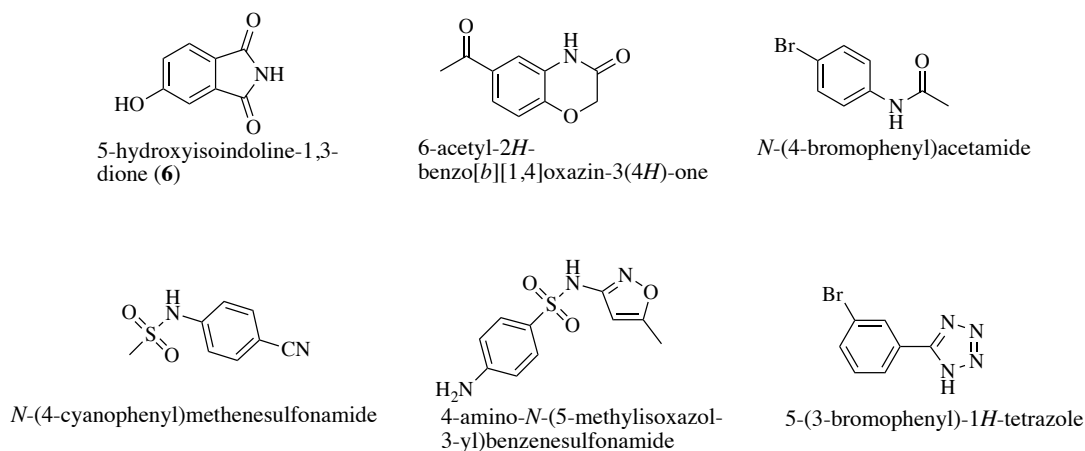


Figure 1.4. Protein–protein interaction interface of the BfrB–Bfd complex. Subunits A and B of a BfrB subunit dimer were colored gray and green, respectively. (A) Residues Y2 and L5 of BfrB (cyan cylinders) are positioned within pockets at the BfrB subunit dimer interface. (B) F_o-F_c omit map (orange mesh) contoured at 3σ showing fragment 6 (Chart 1) bound within the cleft occupied by L5 in the BfrB–Bfd complex. (C) Hydrogen bond interactions (dashed lines) between fragment 6 and BfrB. Water mediated contacts are indicated by the solid lines.¹

An STD spectrum of a solution containing a fragment and BfrB was used to assess each fragment's binding. Eighteen (18) compounds were uncovered, consisting of fragments that bind BfrB specifically at the Bfd-binding site and nonspecific binders.¹ Thus, a displacement strategy that utilizes Bfd as a specific competitor was implemented to identify and separate the specific binders. The strategy involved the acquisition of an STD spectrum from a solution containing fragment, BfrB and Bfd. Nearly complete disappearance of the STD signal indicated that the fragment binds BfrB at the Bfd-binding site. Consequently, of the 18 fragments, six (6) molecules bound BfrB at the Bfd-binding site (Chart 1). A structure-guided approach was further used to

synthetically elaborate these fragment binders into analogs that are capable of binding with higher affinity. The affinity and selectivity of molecules and analogs were investigated by X-ray crystallography, surface plasmon resonance (SPR), and fluorescence polarization methods.¹

Chart 1. Structures of fragments identified to bind BfrB at the Bfd-Binding site.¹



Based on an X-ray analysis, fragments and derived analogs that are shown in Figure 1.5B bound BfrB at the Bfd-binding site. In an effort to identify the “perfect” crystals for the study, crystals obtained from three (3) different BfrB constructs were tested in a ligand soaking experiment. Several analogs of ether **9**, amines **11** and **14**, and amides **12** and **15** were generated using a general synthetic approach as shown in Figure 1.5A. Preparation of the ether analogs **9** involved four steps. Esterification of the acid groups in 4-hydroxyphthalic acid (**7**), followed by alkylation of the phenolic oxygen gave **8**. Subsequently, base cleavage of the ester groups in **8** and cyclization with (NH₄)₂CO₃ afforded the isoindoline-1,3-dione ethers **9**. Reductive amination of **10** and **13**, respectively, with a series of aldehydes afforded the amine analogs **11** and **14**, whereas reactions of **10** and **13**, respectively, with a series of acid chlorides produced the amide analogs **12** and **15**. Although crystal soaking experiments were conducted for each of the analog types shown in Figure 1.5B, structures of analog-bound BfrB were obtained only for analogs **16-21**, which are derivatives of 4-aminoisoindoline-1,3-dione (**13**) with $-(\text{CH}_2)-$ and $-(\text{CH}_2)_3-$ linkers.¹

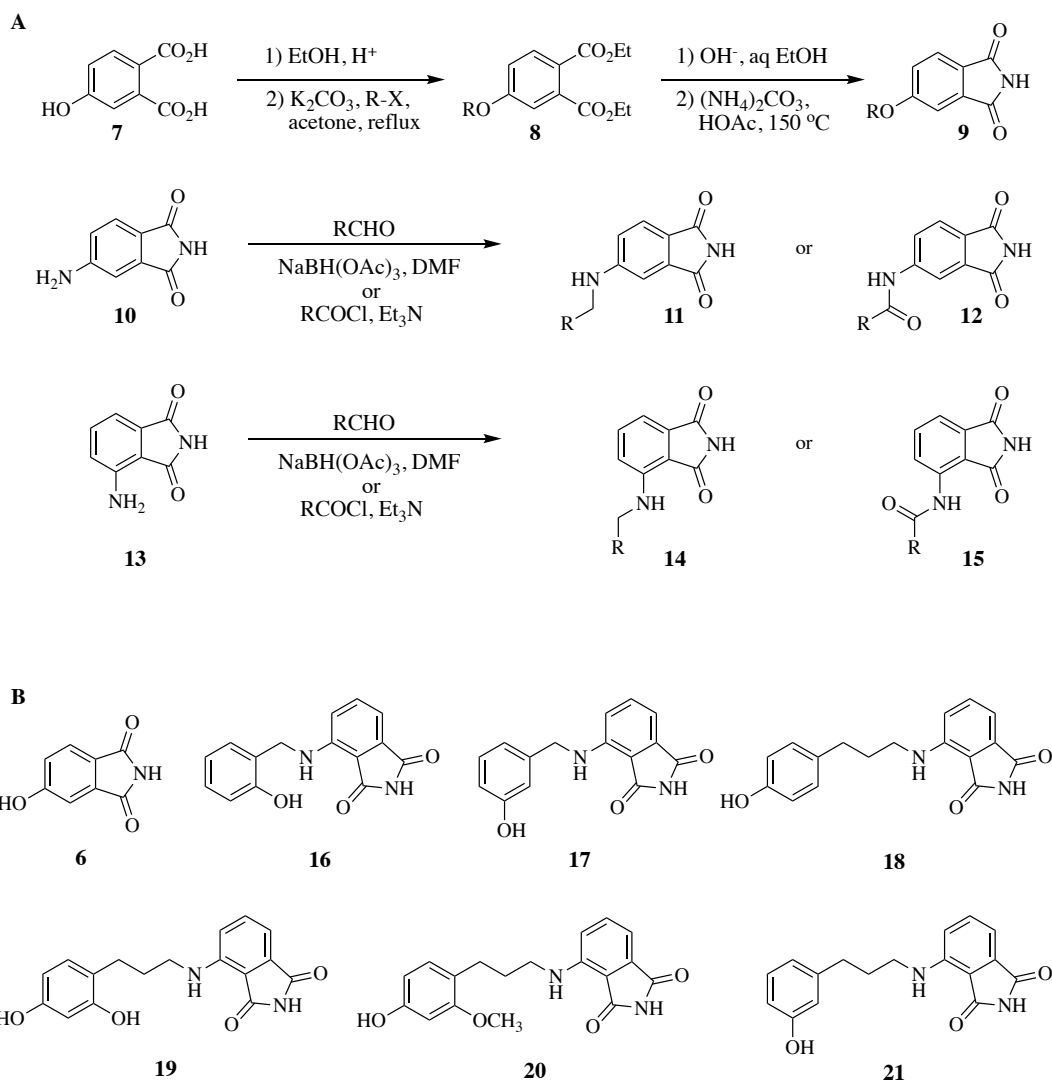
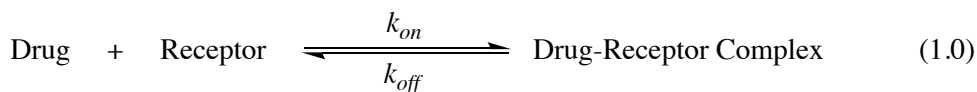


Figure 1.5. (A) Schematic summary of the synthetic procedures employed to prepare analogs of fragments **6**, **10** and **13**; ethers **9** derived from 5-hydroxyisindolinone-1,3-dione (**6**), amines **11** or amides **12** derived from 5-aminoisindolinone-1,3-dione (**10**), or amines **14** or amides **15** derived from 4-aminoisindolinone-1,3-dione (**13**). (B) Structures of fragment **6** and analogs of fragment **13** have been shown by X-ray crystallography to bind BfrB at the Bfd-binding site.¹

The driving force for any drug–receptor interaction can be expressed as a low-energy state of the drug-receptor complex [Eq. (1.0)], where k_{on} represents the rate constant for formation of the drug-receptor complex, and k_{off} is the rate constant for the breakdown of the complex. K_{on}

depends on the concentrations of the drug and receptor, whereas k_{off} depends on the concentration of the drug–receptor complex as well as other forces. Typically, binding affinity is measured and reported by the equilibrium dissociation constant (K_d) [Eq. (1.1)], which is used to evaluate and rank order strengths of the ligand–target interactions. Therefore, the smaller the K_d value, the larger the concentration of the drug–receptor complex, and subsequently, the greater the binding affinity of the drug for the receptor.⁴¹



$$K_d = \frac{[\text{Drug}][\text{Receptor}]}{[\text{Drug - Receptor complex}]} \quad (1.1)$$

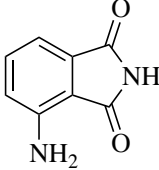
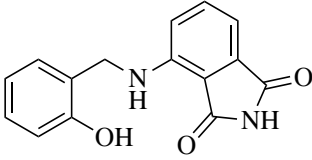
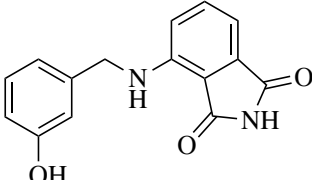
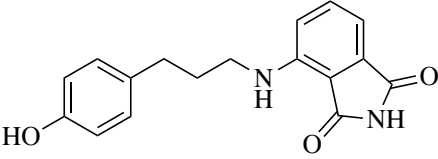
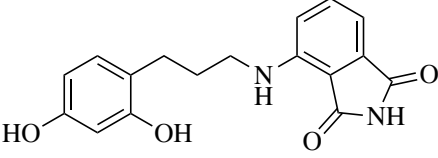
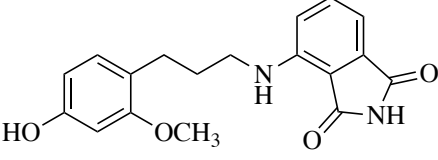
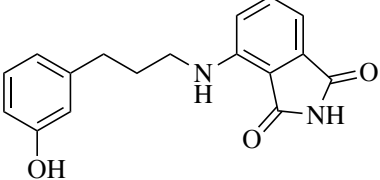
Consequently, the K_d values (Table 1) show that analogs **16-21** exhibited significantly higher affinity than fragment **13**. Importantly, most of these analogs bound BfrB at the Bfd-binding site with a strength comparable to that of BfrB–Bfd association ($K_d = 3 \mu\text{M}$), thus suggesting that they were capable of interfering with the BfrB–Bfd interaction in the cytosol of *P. aeruginosa*.¹ However, analogs with K_d values within the lower micromolar or nanomolar range are desired.

1.4. Results and discussion for synthesis of 4-(alkylamino)isoindoline-1,3-dione derivatives.

Herein, we present the synthesis, characterization and optimization of 4-(alkylamino)isoindoline-1,3-dione analogs that are capable of decreasing the cytosolic iron levels in *P. aeruginosa* cells by inhibiting the BfrB–Bfd interaction within a reduced micromolar concentration range. The following changes were envisioned as a potential approach to improve the activity of the BfrB–Bfd inhibitors:

- 1) Incorporating new substituted benzaldehydes and altering the 3-carbon linker unit into a 1-carbon linker with similar substitution pattern
- 2) Replacing the benzaldehyde component with a furan or tetrahydrofuran group

Table 1. Structure and binding affinity of 4-aminoisindoline-1,3-diones from previous work.¹

Analog	Structure	K_d (μM)
13	 <chem>Nc1ccc2c(c1)c(=O)[nH]c2=O</chem>	300 ± 50
16	 <chem>Oc1ccccc1CNc2ccc3c(=O)[nH]c3=O</chem>	11 ± 1
17	 <chem>Oc1ccc(cc1)CNc2ccc3c(=O)[nH]c3=O</chem>	15 ± 2
18	 <chem>Oc1ccc(cc1)CCCNc2ccc3c(=O)[nH]c3=O</chem>	3 ± 1
19	 <chem>Oc1ccc(O)cc1CCCNc2ccc3c(=O)[nH]c3=O</chem>	4 ± 2
20	 <chem>COc1ccc(O)cc1CCCNc2ccc3c(=O)[nH]c3=O</chem>	5 ± 2
21	 <chem>Oc1ccc(cc1)CCNc2ccc3c(=O)[nH]c3=O</chem>	6 ± 1

Retrosynthetic analysis of potential targets **22** and **23** from precursors **24** and **25** involves a single- and multistep synthesis, respectively, as shown in Figure 1.6.

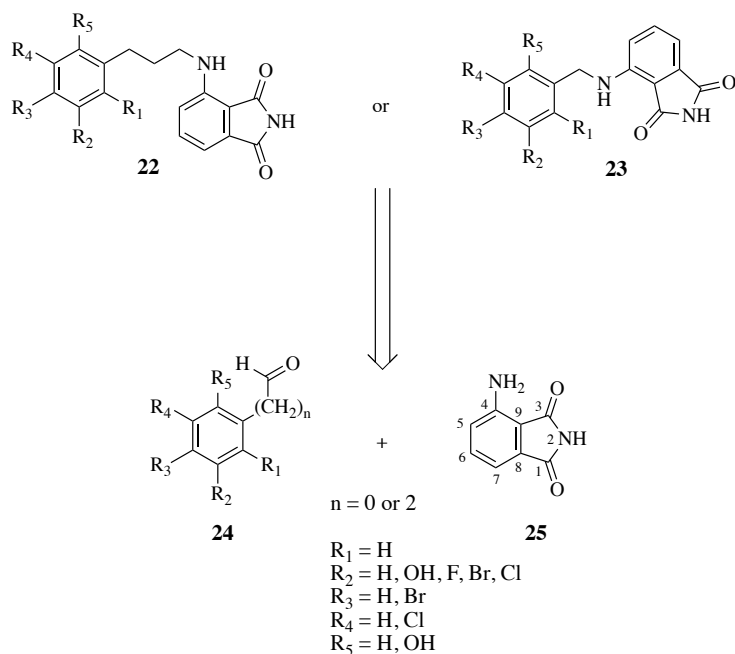
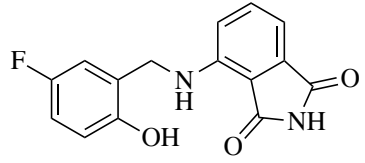
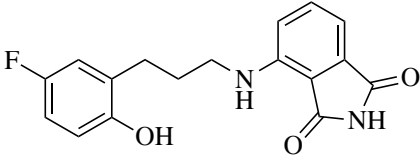
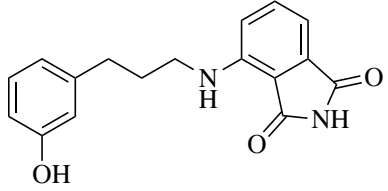
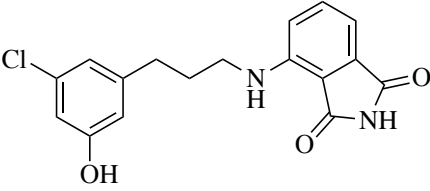
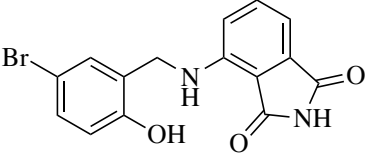
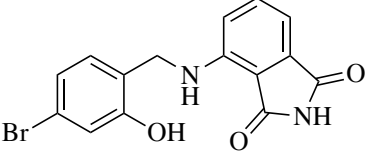
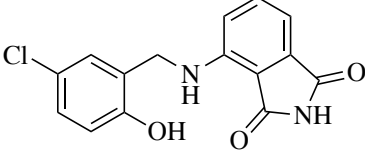


Figure 1.6. Retrosynthetic route for 4-(alkylamino)isoindoline-1,3-diones.

1.4.1. Binding effects of 4-(alkylamino)isoindoline-1,3-diones due to the incorporation of new benzaldehydes and altering of 3-carbon linker into 1-linker.

Modifications to the substituents on the benzaldehyde component **24** have been found to enhance the inhibition of the BfrB–Bfd interaction.^{25,37,38} Careful analysis and consideration led to the utilization of fluorine-, chlorine- and bromine-substituted salicylaldehydes. These halogens have not only increased the molecular weight of our target molecules, but more importantly, allowed selective binding to BfrB at the Bfd binding site. In addition, varying the position of the halogens on **24** was critical to our investigation. Replacing fluorine with chlorine and bromine at the R_2 position of the 1-carbon linker **23** enhanced the inhibitory effect of our target molecule significantly. Similarly, the derivative bearing bromine at the R_3 position exhibited major inhibition.

Table 2. Structure and binding affinity of current 4-(alkylamino)isoindoline-1,3-dione analogs.

Analogue	Structure	K_d (μM)
27		6.50 ± 2.00
31		0.43 ± 0.07
32		1.50 ± 0.25
33		0.35 ± 0.05
35		4.52 ± 0.42
36		1.53 ± 0.21
37		4.07 ± 0.55

Some of the 3-carbon linker analogs of 4-(alkylamino)isoindoline-1,3-diones have also shown promising inhibitory effects. An example is the target 4-(alkylamino)isoindoline-1,3-dione analog which was made from 3-hydroxybenzaldehyde. 5-Fluorosalicylaldehyde also gave a 3-carbon linker target with significant inhibitory ability. Generally, most of the synthesized analogs in Table 2 showed significantly lower K_d values compared to the analogs in Table 1. Thus, these compounds have relatively higher binding affinities for BfrB at the Bfd-binding site. Importantly, comparison of the BfrB-Bfd association ($K_d = 3 \mu\text{M}$) with the lower K_d values of analogs **31**, **32**, **33**, and **36** (Table 2) suggests that these compounds are capable of eliciting greater inhibition by interfering with the BfrB–Bfd interaction in the *P. aeruginosa* cytosol. Halogen and hydroxyl functionalities on the benzaldehyde component may shed light on the potential inhibition effects of hydrogen bonding versus an effect of electron withdrawing groups. A new series of compounds was also designed and synthesized by replacing the benzaldehyde component with 2- or 3-furaldehyde. However, these compounds showed no activity for both 1- and 3-carbon linker analogs. The size of the furaldehyde was presumably too small and prevented effective binding to the BfrB protein. The use of these small molecule inhibitors as chemical probes was necessary for our study because such probes offer dose-dependent, selective and temporal control over target proteins. Therefore, they can be used as complements to other synergistic or antagonistic probes.^{42,43} The novel probes presented herein are capable of the following:

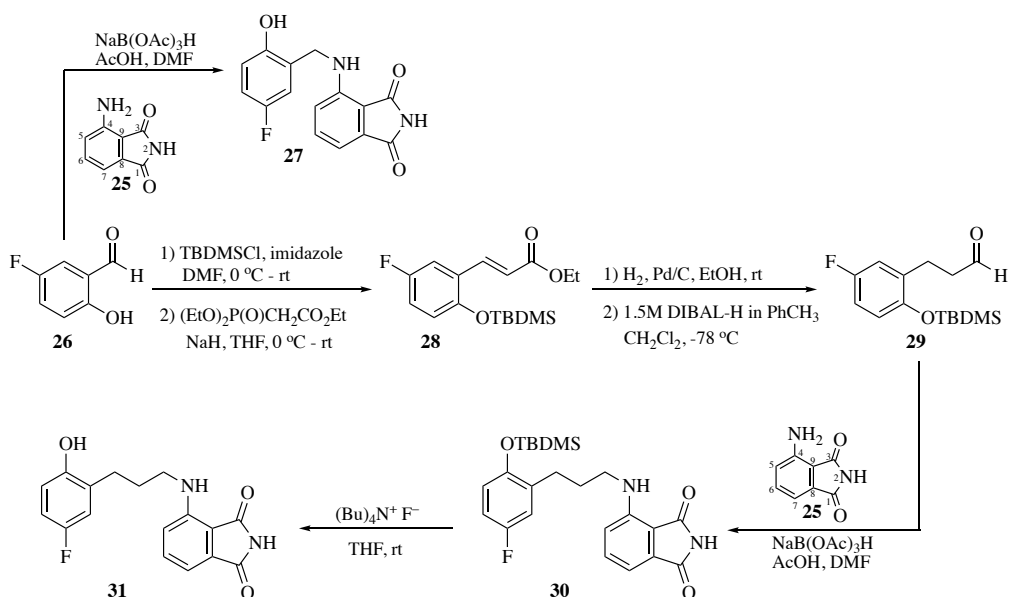
- a) Penetrating the bacteria cells
- b) Inhibiting the mobilization of iron from BfrB by selectively binding at the Bfd binding site
- c) Decreasing bacterial fitness by eliciting perturbations in iron homeostasis
- d) Potentiating the bactericidal activity of fluoroquinolone antibiotics

Current molecular modeling has shown that one of the carbonyl groups (C=O) at position 3 of the 4-aminoisoindoline-1,3-dione (**25**) is not involved in binding or interaction at the BfrB–Bfd site.

Thus, replacing that C=O with a CH₂ group should have no negative influence on the inhibition effect of the target molecule. The reductive amination step for both 1- and 3-carbon linker target molecules was found to give poor yields. Steric hindrance around the amino (NH₂) group of **25** is one of the few explanations for such a poor result. Additionally, the C=O ortho to the amino group reduces the electron density of the amino nitrogen on **25** via resonance and subsequently decrease its nucleophilicity towards the corresponding aldehyde. Therefore, substituting the C=O functionality at position 3 with CH₂ should not only reduce the sterics on **25**, but may also allow an increase in the nucleophilicity of the amino group responsible for the nucleophilic attack towards the aldehyde component. Based on this study, future efforts will be channeled to develop, optimize and synthesize new classes of possible targets.

1.4.2. Incorporation of new substituted benzaldehydes and altering of the 3-carbon linker to a 1-carbon linker.

The syntheses of analogs with 3-carbon linker-substituted 4-(alkylamino)isoindoline-1,3-diones required six steps, and the 1-carbon linker analogs involved only one step (Scheme 1.1).



Scheme 1.1. Synthesis of analogs **27** and **31**.

Protection of the hydroxyl group on **26** with *tert*-butyldimethylsilyl chloride was promoted by imidazole in DMF to afford **28** in 91% yield after purification by silica gel chromatography.⁴⁴⁻⁴⁹ Horner-Wadsworth-Emmons (HWE) conditions were employed to obtain the acrylate intermediate **27**. The HWE reaction required a slight excess of triethyl phosphonoacetate (TEPA) and 60% NaH dispersed in mineral oil to produce predominantly the (*E*)-enolate in good yield.⁵⁰ Importantly, the sequence of addition was critical since an increase in yield was only observed when NaH was added to a solution of TEPA in freshly distilled THF. The crude acrylate **28** was taken directly to the hydrogenation step under anhydrous conditions and with N₂ to give a saturated ester after purification by silica gel column chromatography. The pure intermediate ester was further subjected to DIBAL-H reduction to afford the aldehyde intermediate **29**. Reduction of the ester moiety using DIBAL-H was troublesome if the temperature and mode of addition were not carefully monitored.⁵¹ Slow dropwise addition of the DIBAL-H reagent and a temperature at or below -78 °C (dry ice-acetone) was critical for the success of this reaction. Failure to meet these conditions resulted in a mixture of products (i.e. the desired aldehyde product and an alcohol counterpart due to over reduction). The reductive amination step between **25** and **26** (for 1-linker analogs) or **25** and **29** (for 3-linker analogs) was a one-pot reaction catalyzed by AcOH. The success of this reaction depended on the purity of the aldehyde component, the volume of anhydrous DMF solvent, and the mode of addition of the moisture-free NaB(OAc)₃H reducing agent.⁵²⁻⁵⁵ The use of excess solvent impeded formation of the imine intermediate from **26** or **29**, which was required for reduction by NaB(OAc)₃H to give the desired products **27** or **30**. Thus, it was important to use 1.2-1.5 mL of anhydrous DMF for reactions involving 2-3 mmol of the aldehyde component **26** or **29**. For the 3-linker synthesis, the first part of the amination step, which involved formation of the imine intermediate, required stirring at 23 °C for 1 h prior to the portionwise addition of the reducing agent.⁵² The coupled product **27** or **30** was obtained in 30% yield after column chromatography on silica gel pretreated with 3-hydroxy-2-methyl-4-pyrone to complex metals ions (especially iron). Silyl deprotection of **30** was

achieved by the addition of 2 equivalents of 1 M tetrabutylammonium fluoride (TBAF) in freshly distilled THF at 23 °C. The desired analog **31** was further obtained in 80% yield after purification using pyrone-treated silica gel column chromatography. A similar set of conditions was used to synthesize analogs **32-34** (Figure 1.7). Generally, 4-(alkylamino)isoindoline-1,3-diones (**27**, **30**, **31** and other analogs) have an affinity for iron. Thus, the use of untreated silica gel would deactivate the target molecules and consequently reduce their potency. The low yield recorded at the reductive amination step for both 1- and 3-carbon linker systems leading to **27** and **30**, respectively, could be attributed to two factors:

- a) Steric hindrance around the 4-aminoisoindoline-1,3-dione imine bond
- b) Decreased nucleophilicity of the amino group on **25** due to the presence of two strong electron withdrawing C=O groups

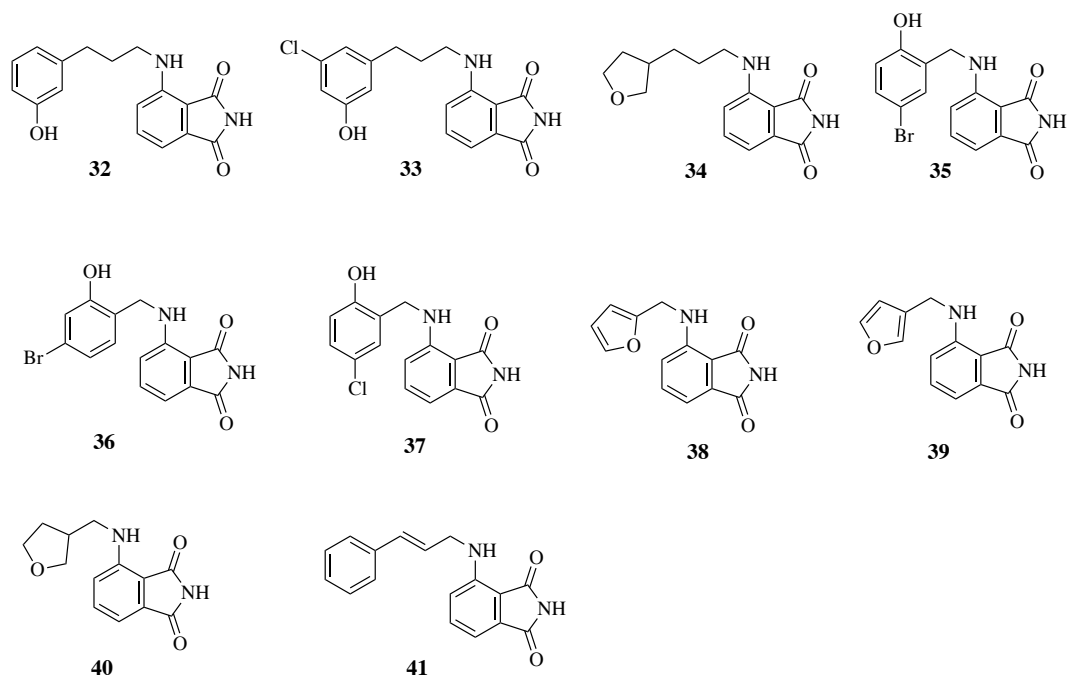


Figure 1.7. Analogs of 4-(alkylamino)isoindoline-1,3-diones with 3- and 1-carbon linker.

Unlike the 3-carbon linker **31**, reductive amination for the 1-carbon linker **27** synthesis did not proceed cleanly at room temperature.⁵² Initial attempts to use the previously mentioned conditions failed to afford **27** in good yield. To ensure maximum conversion, an acid-catalyzed reaction between **26** and **27** was heated at 90 °C for 2 h. Decreased flexibility and reactivity of **26** towards the nucleophilic attack of **25** could be a possible reason. However, the rate of reaction increased in the forward direction at the higher temperature. Addition of **25** to a solution of **26** in DMF under acidic conditions resulted in a thick slurry which turned clear at 90 °C. Heating the reaction at 90 °C for longer than 2 h did not improve the outcome. The mixture was gradually cooled to 0 °C prior to the portion-wise addition of the reducing agent.⁵² The desired product **27** was obtained after purification with pyrone-treated silica gel column chromatography. Similar reaction conditions were used to synthesize analogs **35-41** (Figure 1.7).

1.5. Conclusions

In summary, we have synthesized several 4-(alkylamino)isoindoline-1,3-diones as potential antibiotic candidates that are capable of interfering with the BfrB–Bfd interaction in the cytosol of *P. aeruginosa* and inhibit iron mobilization.

1.5.1. Incorporation of new substituted benzaldehydes and other heterocyclic groups.

In this study, we have successfully prepared new derivatives of **22** and **23** (Figure 1.6) from substituted benzaldehydes. Additionally, analogs **34**, **38**, **39**, and **40** (Figure 1.7) were made from 2- and 3-furaldehyde. The synthesis of the 3-carbon linker derivatives of **22** required six (6) steps, whereas that of the 1-carbon linkers **23** involved a single step. The K_d values for most of the synthesized benzaldehyde derivatives were within the low micromolar concentration range, thus suggesting that they have greater binding affinities for BfrB. Importantly, analogs **31**, **32**, **33** and **36** (Table 2) exhibited smaller K_d values compared to the BfrB–Bfd association ($K_d = 3 \mu\text{M}$), and thus these derivatives are capable of interfering with the BfrB–Bfd interaction to elicit

perturbations in iron homeostasis that decrease bacterial fitness. However, no activity was observed for analogs **34**, **38**, **39**, and **40**, possibly due to the small size of the furan ring.⁵⁶

1.5.2. Altering the carbon linker in the 4-(alkylamino)isoindoline-1,3-dione analogs.

In an attempt to further expand the array of possible active 4-(alkylamino)isoindoline-1,3-diones, the synthesis of 1-carbon linker derivatives was considered. Results from the binding affinity experiment (Table 2) revealed that most of the 1-carbon linker analogs **27**, **35**, and **37** were not as promising as the 3-carbon linkers. Nonetheless, current docking studies have shown that 1-carbon linker analogs of 4-(alkylamino)isoindoline-1,3-dione with benzo-fused six membered heterocyclic components could be potential candidates. Moreover, analogs derived from substituted cinnamaldehydes are of major interest. As such, 4-(cinnamylamino)isoindoline-1,3-dione (**41**) has been prepared from cinnamaldehyde using the one step route in Scheme 1.1, and we are awaiting its biological testing. Consequently, a promising result would facilitate the design, synthesis, and characterization of other potential derivatives.

1.6. Chemistry

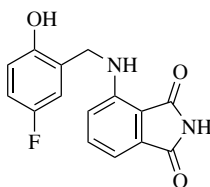
1.6.1 Incorporation of new substituted benzaldehydes in BfrB–Bfd chemical probes.

General procedure for pyrone-treated silica gel: A 3-L, sintered-glass funnel suspended on an O-ring was charged with one-kilogram of silica gel (Sorbent Technologies CA# 40940-25). The silica gel was treated with a solution of 3-hydroxy-2-methyl-4-pyrone (20 mg) in 1 L of MeOH. The initial wash (yellow-orange coloring) was discarded. Additionally, the silica gel was washed with 500 mL of recycled MeOH (old washings) and finally 1.5 L of fresh MeOH was used to rinse the silica gel. The silica gel was transferred to a tray, covered with aluminum foil (poked holes for ventilation) and was set to air dry at room temperature overnight. Subsequently, the silica gel was dried in the oven at 90 °C in 3 h increments. Generally, derivatives of 4-

(alkylamino)isoindoline-1,3-diones have an affinity for iron and earlier work showed that purification with untreated silica gel deactivated the target molecules and reduced their potency.

General methods: Commercial anhydrous *N,N*-dimethylformamide was stored under dry N₂ and transferred by syringe into reactions when needed. Tetrahydrofuran was dried over potassium hydroxide pellets and then distilled from lithium aluminum hydride prior to use. All other commercial reagents and solvents were used as received. Unless otherwise indicated, all reactions were carried out under dry N₂ in oven-dried glassware. Reactions were monitored by thin layer chromatography (TLC, Analtech No 21521) using silica gel GF plates. Preparative separations for all final compounds were performed by column chromatography on silica gel (Davisil[®], grade 62, 60 - 200 mesh) pre-treated with 3-hydroxy-2-methyl-4-pyrone mixed with UV-active phosphor (Sorbent Technologies No UV-05) slurry packed into quartz columns. Band elution for all chromatographic separations was monitored using a hand-held UV lamp. Melting points were uncorrected. IR spectra were run as thin films on NaCl disks. The ¹H- and ¹³C-NMR spectra were measured in the indicated solvent at 400 MHz and 100 MHz, respectively, using tetramethylsilane as the internal standard with coupling constants (*J*) given in Hz.

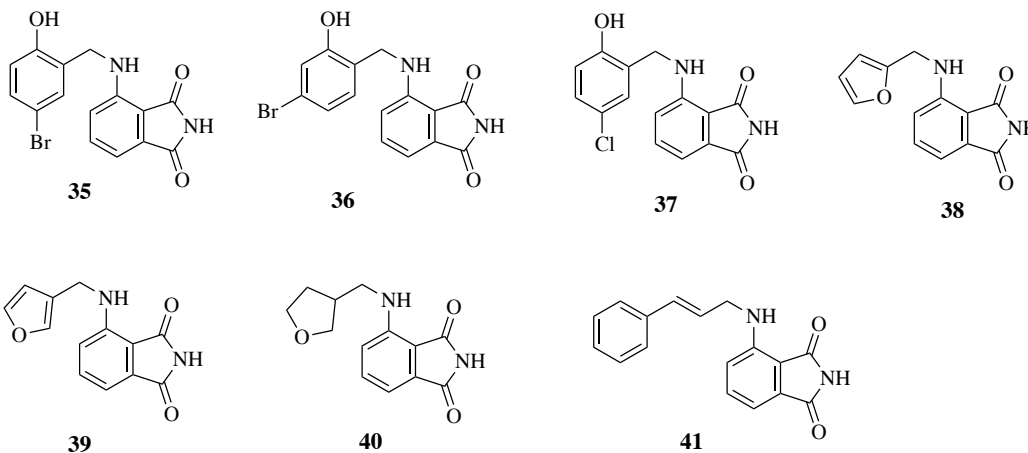
Synthesis of (27)



4-((5-Fluoro-2-hydroxybenzyl)amino)isoindoline-1,3-dione (27). To a solution of 5-fluorosalicylaldehyde (**26**, 0.47 g, 3.34 mmol) in DMF (1.1 mL) was added AcOH (0.8 mL), and the solution was stirred for 10 min. To this reaction mixture, was added 4-aminoisoindoline-1,3-dione (**25**, 0.27 g, 1.67 mmol) and stirring was continued at 23 °C for 1 h. An additional 1 mL of DMF was added bringing the volume to 2.1 mL. The reaction was heated to 90 °C for 2 h and

then cooled to room temperature. NaB(OAc)₃H (1.1 g, 5.01 mmol) was added portionwise to the reaction at 0 °C and stirring was continued at this temperature for 30 min. The reaction was gradually warmed to 23 °C and stirred for 18 h. The crude reaction mixture was poured into de-ionized water, the mixture of which was extracted with EtOAc (3 × 75 mL). The combined organic layers were washed with NaHCO₃ (2 × 50 mL) and NaCl (50 mL). The organic layer was dried (Na₂SO₄) and concentrated under vacuum. The crude product was subjected to column chromatography (using silica gel pre-treated with 3-hydroxy-2-methyl-4-pyrone) eluted with 20% EtOAc/hexane to afford **27** (0.56 g, 58%) as an orange solid, m.p. 216-217 °C. ¹H NMR (400 MHz, DMSO-*d*₆): δ 10.97 (s, 1H), 9.75 (s, 1H), 7.50 (t, *J* = 7.7 Hz, 1H), 7.07 (br t, *J* = 6.4 Hz, 1H), 7.02 (dd, *J* = 9.5, 3.2 Hz, 1H), 6.98-6.86 (complex, 3H), 6.82 (dd, *J* = 8.8, 4.7 Hz, 1H), 4.43 (d, *J* = 6.3 Hz, 2H); ¹³C NMR (101 MHz, DMSO-*d*₆): δ 171.8, 169.8, 155.9 (d, *J* = 233.9), 151.8, 146.4, 136.3, 134.1, 126.9 (d, *J* = 6.6), 117.1, 116.3 (d, *J* = 8.0), 115.1 (d, *J* = 23.3), 114.6 (d, *J* = 22.5), 111.7, 110.6, 41.1.

The following compounds can also be prepared by the procedure above.



4-((5-Bromo-2-hydroxybenzyl)amino)isoindoline-1,3-dione (35). Orange solid, m.p. 219-220 °C. ¹H NMR (400 MHz, DMSO-*d*₆): δ 11.0 (s, 1H), 10.1 (s, 1H), 7.49 (t, *J* = 8.0 Hz, 1H), 7.35 (d, *J* = 2.5 Hz, 1H), 7.23 (dd, *J* = 8.6, 2.5 Hz, 1H), 7.06 (t, *J* = 6.4 Hz, 1H), 6.96 (d, *J* = 8.6 Hz, 1H),

6.93 (d, $J = 7.1$ Hz, 1H), 6.79 (d, $J = 8.6$ Hz, 1H), 4.41 (d, $J = 6.4$ Hz, 2H); ^{13}C NMR (101 MHz, DMSO- d_6): δ 171.8, 169.8, 155.0, 146.4, 136.3, 134.1, 131.1, 128.1, 117.7, 117.1, 111.7, 110.6, 110.5, 41.1 (one aromatic carbon unresolved).

4-((4-Bromo-2-hydroxybenzyl)amino)isoindoline-1,3-dione (36). Yellow solid, m.p. 226-227 °C. ^1H NMR (400 MHz, DMSO- d_6): δ 11.0 (s, 1H), 10.3 (s, 1H), 7.48 (dd, $J = 8.5, 7.1$ Hz, 1H), 7.14 (d, $J = 8.1$ Hz, 1H), 7.01 (t, $J = 6.4$ Hz, 1H), 7.00 (d, $J = 2.0$ Hz, 1H), 6.93 (m, 3H), 4.40 (d, $J = 6.4$ Hz, 2H); ^{13}C NMR (101 MHz, DMSO- d_6): δ 171.8, 169.8, 156.8, 146.4, 136.3, 134.1, 130.6, 124.9, 122.1, 120.6, 118.1, 117.2, 111.7, 110.6, 41.1.

4-((5-Chloro-2-hydroxybenzyl)amino)isoindoline-1,3-dione (37). Orange solid, m.p. 229-230 °C. ^1H NMR (400 MHz, DMSO- d_6): δ 11.0 (s, 1H), 10.1 (s, 1H), 7.49 (dd, $J = 8.2, 7.4$ Hz, 1H), 7.22 (d, $J = 2.6$ Hz, 1H), 7.12 (dd, $J = 8.6, 2.6$ Hz, 1H), 7.07 (t, $J = 6.5$ Hz, 1H), 6.96 (d, $J = 8.6$ Hz, 1H), 6.93 (d, $J = 7.0$ Hz, 1H), 6.84 (d, $J = 8.6$ Hz, 1H), 4.42 (d, $J = 6.4$ Hz, 2H); ^{13}C NMR (101 MHz, DMSO- d_6): δ 171.3, 169.3, 154.1, 145.9, 135.9, 133.6, 127.8, 127.7, 127.0, 122.4, 116.6, 111.3, 111.2, 110.2, 40.6.

4-((Furan-2-ylmethyl)amino)isoindoline-1,3-dione (38). Yellow solid, m.p. 149-150 °C. ^1H NMR (400 MHz, DMSO- d_6): δ 10.98 (s, 1H), 7.59 (br s, 1H), 7.53 (t, $J = 7.8$ Hz, 1H), 7.12 (d, $J = 8.5$ Hz, 1H), 6.97 (d, $J = 7.1$ Hz, 1H), 6.91 (t, $J = 6.4$ Hz, 1H), 6.40 (br s, 1H), 6.34 (d, $J = 3.2$ Hz, 1H), 4.54 (d, $J = 6.3$ Hz, 2H); ^{13}C NMR (101 MHz, DMSO- d_6): δ 171.8, 169.7, 152.6, 145.2, 142.9, 136.2, 134.0, 117.4, 111.8, 110.9, 107.8, 39.3 (one aromatic carbon unresolved).

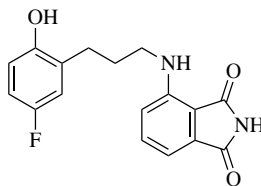
4-((Furan-3-ylmethyl)amino)isoindoline-1,3-dione (39). Yellow solid, m.p. 133-134 °C. ^1H NMR (400 MHz, DMSO- d_6): δ 10.95 (s, 1H), 7.54 (t, $J = 7.8$ Hz, 1H), 7.08 (d, $J = 8.5$ Hz, 1H), 6.94 (d, $J = 7.1$ Hz, 1H), 6.61 (br t, $J = 6.5$ Hz, 1H), 3.78 (m, 1H), 3.72 (t, $J = 8.0$ Hz, 1H), 3.63 (q, $J = 7.7$ Hz, 1H), 3.47 (t, $J = 6.8$ Hz, 2H), 3.35-3.22 (complex, 2H), 1.97 (m, 1H), 1.62 (m,

2H); ^{13}C NMR (101 MHz, $\text{DMSO-}d_6$): δ 171.9, 169.8, 146.7, 136.4, 134.0, 117.0, 111.3, 110.4, 70.8, 67.3, 45.1, 38.8, 29.9.

4-(((Tetrahydrofuran-3-yl)methyl)amino)isoindoline-1,3-dione (40). Yellow solid, m.p. 154-155 °C. ^1H NMR (400 MHz, $\text{DMSO-}d_6$): δ 10.95 (s, 1H), 7.65 (s, 1H), 7.60 (s, 1H), 7.51 (t, J = 7.8 Hz, 1H), 7.13 (d, J = 8.3 Hz, 1H), 6.95 (d, J = 7.1 Hz, 1H), 6.83 (br t, J = 6.1 Hz, 1H), 6.50 (s, 1H), 4.35 (d, J = 6.1 Hz, 2H); ^{13}C NMR (101 MHz, $\text{DMSO-}d_6$): δ 170.7, 168.7, 145.3, 143.0, 139.7, 135.1, 132.9, 122.2, 116.3, 110.6, 109.7, 109.5, 36.3.

(E)-4-((3-(3-Hydroxyphenyl)allyl)amino)isoindoline-1,3-dione (41). Yellow solid, m.p. 187-188 °C. ^1H NMR (400 MHz, $\text{DMSO-}d_6$): δ 10.97 (s, 1H), 7.53 (dd, J = 8.5, 7.1 Hz, 1H), 7.42 (d, J = 8.5 Hz, 2H), 7.31 (t, J = 7.4 Hz, 2H), 7.23 (t, J = 7.3 Hz, 1H), 7.04 (d, J = 8.5 Hz, 1H), 6.95 (d, J = 7.1 Hz, 1H), 6.81 (br t, J = 6.1 Hz, 1H), 6.61 (d, J = 16.0 Hz, 1H), 6.36 (dt, J = 16.0, 5.5 Hz, 1H), 4.12 (dt, J = 5.8, 1.6 Hz, 2H); ^{13}C NMR (101 MHz, $\text{DMSO-}d_6$): δ 170.7, 168.8, 145.5, 135.8, 135.2, 133.0, 130.0, 128.0, 126.9, 126.2, 125.6, 116.4, 110.5, 109.5, 43.3.

Synthesis of 4-((3-(5-fluoro-2-hydroxyphenyl)propyl)amino)isoindoline-1,3-dione (31).



***tert*-Butyldimethylsilyl chloride (TBDMSCl) protection and Horner-Wadsworth-Emmons reaction.**

Ethyl (E)-3-(2-((*tert*-Butyldimethylsilyl)oxy)-5-fluorophenyl)acrylate (28). A stirred solution of 5-fluoro-2-hydroxybenzaldehyde (**26**, 1.21 g, 8.65 mmol) in DMF (10 mL) was cooled to 0 °C under nitrogen atmosphere, and imidazole (1.18 g, 17.3 mmol) was added. The resulting solution was stirred for 20 min, and *tert*-butyldimethylsilyl chloride (1.96 g, 12.98 mmol) was added dropwise as a solution in DMF (10 mL) over a period of 15 min. The reaction mixture was

warmed to 23 °C and stirred until TLC analysis indicated the complete conversion of the phenolic compound. The crude reaction was poured into water (50 mL) and extracted with ether (3 × 40 mL). The combined organic layers were washed with saturated NaCl (50 mL), dried (Na₂SO₄) and concentrated under vacuum. The crude product was purified by silica gel column chromatography to give 2-((*tert*-butyldimethylsilyl)oxy)-5-fluorobenzaldehyde (2.01 g, 91%) as a colorless oil.

To a stirred, ice-cold solution of triethyl phosphonoacetate (2.05 g, 1.83 mL, 9.16 mmol) in THF (5.0 mL) was added 60% NaH dispersed in mineral oil (367 mg, 9.16 mmol), and the mixture was stirred for 15 min. To the resulting reaction mass was added dropwise TBS protected 5-fluorobenzaldehyde (1.96 g, 7.70 mmol) in THF (15 mL), and the stirred reaction was allowed to warm to 23 °C. After the TLC (5% ether/hexane) analysis indicated the complete consumption of starting material (2 h), the reaction mass was cooled and quenched by dropwise addition of ice-cold water. The product was extracted with ether (2 × 25 mL), and the organic layer was washed with saturated NaCl (15 mL), dried (Na₂SO₄) and evaporated to afford the acrylate (**28**, 2.25 g, 90%) as colorless oil. This compound was carried forward without further purification.

Hydrogenation and DIBAL-H ester reduction.

3-(2-((*tert*-Butyldimethylsilyl)oxy)-5-fluorophenyl)propanal (29). A solution of ethyl (*E*)-3-(2-((*tert*-butyldimethylsilyl)oxy)-5-fluorophenyl)acrylate (**28**, 2.23 g, 6.87 mmol) in ethanol (200 proof, 15 mL) was flushed twice with nitrogen, and 10 wt% of PtO₂ (223 mg) was added. The reaction was stirred at room temperature under hydrogen gas (1 atm) for 12 h until TLC (5% ether/hexane) indicated complete reaction. The reaction mass was filtered through Celite[®] bed and washed with ethanol (2 × 40 mL). The filtrate was concentrated under vacuum and subjected to column chromatography to afford the ethyl 3-(2-((*tert*-butyldimethylsilyl)oxy)-5-fluorophenyl)propanoate (2.03 g, 91%) as a colorless oil.

The ethyl 3-(2-((*tert*-butyldimethylsilyloxy)-5-fluorophenyl)propanoate (1.03 g, 3.17 mmol) prepared above was dissolved in DCM (10 mL), and cooled to $-78\text{ }^{\circ}\text{C}$ under N_2 . The solution was treated via dropwise addition of 1.5 M DIBAL-H in toluene (2.11 mL, 3.17 mmol) over a period of 30 min. Stirring was continued for 2 h at $-78\text{ }^{\circ}\text{C}$ until TLC (5% ether/hexane) analysis indicated the complete absence of starting material. The reaction was quenched by dropwise addition of methanol (10 mL), followed by addition of 1 M HCl (15 mL). The organic layer was separated, and the aqueous layer was further extracted with DCM ($2 \times 50\text{ mL}$). The combined organic layers were washed with saturated NaCl and dried (Na_2SO_4). Removal of the solvent under reduced pressure afforded the 3-(2-((*tert*-butyldimethylsilyloxy)-5-fluorophenyl)propanal (**29**, 0.76 g, 85%) as a colorless oil.

Reductive amination procedure

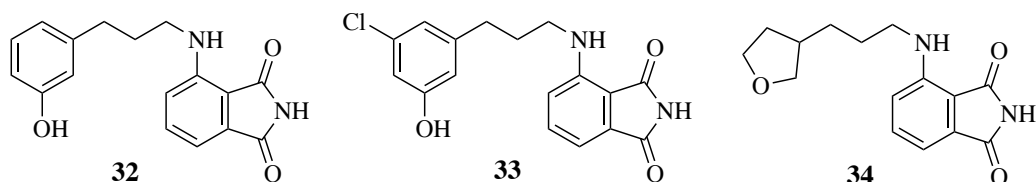
4-((3-(2-((*tert*-Butyldimethylsilyloxy)-5-fluorophenyl)propyl)amino)isoindoline-1,3-dione (**30**). To a solution of 3-(2-((*tert*-butyldimethylsilyloxy)-5-fluorophenyl)propanal (**29**, 1.16 g, 4.11 mmol) in DMF (1.2 mL) was added AcOH (0.8 mL) and the solution was stirred for 10 min at room temperature. To this mixture, was added 4-aminoisoindoline-1,3-dione (**25**, 0.33 g, 2.05 mmol), and stirring was continued at $23\text{ }^{\circ}\text{C}$ for 1 h. An additional 3.8 mL of DMF was added to bring the volume to 5.0 mL over the 1 h period. The reaction was cooled to $0\text{ }^{\circ}\text{C}$ and $\text{NaB}(\text{OAc})_3\text{H}$ (1.31 g, 6.16 mmol) was added portion-wise to the reaction over 25 min. The reaction was further stirred at this temperature for 30 min, and then gradually warmed to $23\text{ }^{\circ}\text{C}$. Stirring was continued for 18 h until TLC (5-20% EtOAc/hexane) indicated complete conversion of the aldehyde. The crude reaction mixture was poured into de-ionized water, extracted with EtOAc ($3 \times 75\text{ mL}$) and the combined organic layers were washed with NaHCO_3 ($2 \times 50\text{ mL}$), followed by saturated NaCl (50 mL). The organic layer was dried (Na_2SO_4) and concentrated under vacuum. The crude product was subjected to column chromatography (using silica gel pre-treated with 3-hydroxy-2-methyl-4-pyrone) and eluted with 20% EtOAc/hexane to afford 4-((3-

(2-((*tert*-butyldimethylsilyl)oxy)-5-fluorophenyl)propyl)amino)isoindoline-1,3-dione (**30**, 0.69 g, 30%) as a yellow solid.

Silyl deprotection

4-((3-(5-Fluoro-2-hydroxyphenyl)propyl)amino)isoindoline-1,3-dione (31). A solution of **30** (0.39 g, 0.92 mmol) in 7 mL of freshly distilled THF was stirred under N₂ at 23 °C, then 1.0 M TBAF in THF (1.84 mL, 1.84 mmol) was added. Stirring was continued for 1 h and when TLC analysis (5-20% EtOAc/hexane) indicated the complete consumption of the silyl ether, de-ionized water (5.0 mL) was added. The THF was evaporated under vacuum and the aqueous layer was extracted with EtOAc (3 × 40 mL). The combined organic layers were washed with saturated NaCl (50 mL), dried (Na₂SO₄), and concentrated under vacuum. The crude product was purified by column chromatography (using silica gel pre-treated with 3-hydroxy-2-methyl-4-pyrone) using 20% EtOAc/hexane as the mobile phase to afford **31** (0.33 g, 80%) as an orange solid, m.p. 163-164 °C. ¹H NMR (400 MHz, DMSO-*d*₆): δ 10.9 (s, 1H), 9.33 (s, 1H), 7.51 (t, *J* = 7.8 Hz, 1H), 6.98 (d, *J* = 8.5 Hz, 1H), 6.92 (d, *J* = 7.0 Hz, 2H), 6.81 (td, *J* = 8.5, 3.2 Hz, 1H), 6.76 (dd, *J* = 8.6, 5.2 Hz, 1H), 6.58 (t, *J* = 6.0 Hz, 1H), 3.28 (q, *J* = 6.6 Hz, 2H), 2.59 (t, *J* = 7.5 Hz, 2H), 1.83 (quintet, *J* = 7.3 Hz, 2H); ¹³C NMR (101 MHz, DMSO-*d*₆): δ 171.9, 168.8, 155.9 (d, *J* = 238.9 Hz), 151.1 (d, *J* = 7.3 Hz), 146.7, 136.3, 134.1, 126.9 (d, *J* = 2.4 Hz), 117.2, 116.9, 115.1 (d, *J* = 23.3 Hz), 111.2, 110.2, 41.9, 28.9, 27.2.

The following compounds can also be prepared using the above procedures.



4-((3-(3-Hydroxyphenyl)amino)isoindoline-1,3-dione (32). Yellow solid, m.p. 160-162 °C. ¹H NMR (400 MHz, DMSO-*d*₆): δ 10.94 (s, 1H), 9.23 (s, 1H), 7.52 (dd, *J* = 8.4, 7.0 Hz, 1H), 7.06 (t,

$J = 7.7$ Hz, 1H), 6.97 (d, $J = 8.5$ Hz, 1H), 6.93 (d, $J = 7.0$ Hz, 1H), 6.65-6.55 (complex, 3H), 6.52 (t, $J = 6.0$ Hz, 1H), 3.27 (q, $J = 6.7$ Hz, 2H), 2.57 (t, $J = 7.6$ Hz, 2H), 1.85 (quint, $J = 7.8$ Hz, 2H); ^{13}C NMR (101 MHz, DMSO- d_6): δ 171.9, 169.8, 157.8, 146.7, 143.3, 136.4, 134.1, 129.7, 119.3, 116.9, 115.6, 113.3, 111.2, 110.3, 41.8, 32.8, 30.7.

4-((3-(3-Chloro-5-hydroxyphenyl)propyl)amino)isoindoline-1,3-dione (33). Yellow solid, m.p. 186-188 °C; ^1H NMR (400 MHz, DMSO- d_6): δ 10.93 (s, 1H), 9.77 (s, 1H), 7.52 (dd, $J = 8.2, 7.4$ Hz, 1H), 6.98 (d, $J = 8.5$ Hz, 1H), 6.93 (d, $J = 7.0$ Hz, 1H), 6.70 (m, 1H), 6.61 (t, $J = 2.0$ Hz, 1H), 6.57 (m, 1H), 6.52 (t, $J = 5.8$ Hz, 1H), 3.27 (q, $J = 6.7$ Hz, 2H), 2.57 (t, $J = 7.5$ Hz, 2H), 1.84 (quint, $J = 7.4$ Hz, 2H); ^{13}C NMR (101 MHz, DMSO- d_6): δ 170.8, 168.7, 157.8, 145.6, 144.2, 135.3, 133.0, 132.6, 118.2, 115.9, 113.5, 112.2, 110.2, 109.2, 40.7, 31.4, 29.3.

4-((3-(Tetrahydrofuran-3-yl)propyl)amino)isoindoline-1,3-dione (34). Yellow solid, m.p. 111-112 °C. ^1H NMR (400 MHz, DMSO- d_6): δ 10.93 (s, 1H), 7.53 (t, $J = 7.7$ Hz, 1H), 7.02 (d, $J = 8.5$ Hz, 1H), 6.93 (d, $J = 7.0$ Hz, 1H), 6.48 (t, $J = 6.0$ Hz, 1H), 3.79 (t, $J = 7.6$ Hz, 1H), 3.72 (m, 1H), 3.61 (q, $J = 7.7$ Hz, 1H), 3.35-3.18 (complex, 3H), 2.14 (septet, $J = 7.4$ Hz, 1H), 1.98 (m, 1H), 1.57 (m, 2H), 1.40 (m, 3H); ^{13}C NMR (101 MHz, DMSO- d_6): δ 171.9, 169.8, 146.7, 136.4, 134.1, 116.9, 111.1, 110.2, 72.9, 67.5, 42.3, 38.9, 32.4, 30.5, 28.2.

CHAPTER II

SYNTHESIS OF BIOACTIVE HETEROCYCLIC SCAFFOLDS

2.1 Introduction

Heterocyclic compounds remain a fundamental division of organic chemistry accounting for nearly two-thirds of modern publications. These classes of compounds are cyclic and contain mostly carbon and hydrogen atoms, with at least one heteroatom in a ring formation. Although the most common heteroatoms are nitrogen, oxygen and sulfur, heterocyclic rings containing other heteroatoms such as phosphorus are also widely known.⁵⁷ Heterocycles can be classified as aromatic or aliphatic. The aromatic analogs have properties similar to that of benzene in that they fulfill Huckel's rule for aromaticity. Typical examples are pyrimidine and purine, the major components of DNA and RNA.⁵⁸ Moreover, chlorophyll and heme, the oxygen carriers in plants and animals respectively, are also derivatives of large porphyrin rings.⁵⁹ The aliphatic heterocycles, in contrast, are cyclic analogs of amines, ethers, thio-ethers and amides. Generally, these compounds consist of 3-7 membered ring systems, and the strain in the rings influence their properties.⁶⁰ Among the various clinical applications, heterocycles are present in a wide variety of drugs, most vitamins, many natural products, and a wide range biological active compounds including anti-bacterial,^{61,62} anti-viral,⁶³ anti-fungal,⁶⁴ anti-inflammatory,⁶⁵ and anti-tumor agents.⁶⁶⁻⁶⁸ Moreover, heterocycles are considered as useful synthetic intermediates,⁶⁹ chiral auxiliaries,⁷⁰ and metal ligands⁷¹ in catalytic asymmetric synthesis. Other important areas of application of heterocyclic compounds include polymer chemistry⁷² and materials science.⁷³

Therefore, substantial attention has been directed towards the synthesis and optimization of biologically active heterocyclic scaffolds. Synthetic chemists are in constant search of the most viable and cost-effective alternatives to simplify the synthesis of heterocyclic targets. More importantly, the development of high atom economy and eco-friendly methods to access these heterocyclic frameworks have recently been the primary focus of most researchers. In past years, transition metal catalysts have proven efficient in the synthesis of organic compounds especially heterocycles. However, the use of such catalysts in late-stage drug synthesis requires special purification techniques to completely remove these toxic metals from the final products. Thus, simple transition metal-free methodologies are necessary for the preparations of useful heterocyclic scaffolds. Sildenafil citrate, an active ingredient in Revatio™ is popular for the treatment erectile dysfunction and pulmonary arterial hypertension in adults and children. Evidently, an alternative strategy in a new synthetic route to Sildenafil citrate avoided tin (II) chloride and thus eliminated 30,000 tons of chemical waste between 1997 and 2003.⁷⁴ In addition, the improvement in the synthesis of Zolpidem, a sedative, is noteworthy. The previous synthesis involved a 4-step reaction route using 4-methylacetophenone as a starting material to give Zolpidem in 66% yield.⁷⁵ However, an improved strategy involving the reaction of 2-aminopyridines and Morita-Baylis-Hillman (MBH) acetates of nitroalkenes afforded Zolpidem in 96% yield.⁷⁶

Over the years, the design and optimization of new drug molecules as anti-cancer and antibiotic candidates has been the primary focus of our research group. Importantly, our expertise involves the development of cost-effective and atom efficient synthetic approaches to essential bioactive scaffolds such as quinazolinones, chromanones and isoquinolines. As an extension, this dissertation designed and optimized new methods to prepare 1-aryl-5-nitro-1*H*-indazoles, 4*H*-benzo[*d*][1,3]oxazin-4-ones, bis-1,3,4-oxadiazoles, nitro-, cyano- or fluoro-substituted 2-naphthoates, 1,8-naphthyridines, 1,2-dihydroquinolines, and 4-oxo-1,4-dihydroquinolines, as well as quinoline carboxylates and carbonitriles. These methods were developed using readily

available and economical starting materials. Thus, an alternative strategy to access most of these bioactive building blocks has been formulated without the use of transition metals. Initially, nucleophilic aromatic substitution (S_NAr) reactions were adopted to generate 1-aryl-5-nitro-1*H*-indazoles in good to excellent yields. In addition, a one-pot sequential protocol for a 1-aryl-1*H*-indazole assembly, without the limiting substitution patterns required for S_NAr cyclization, was achieved in decent yields.⁷⁷ Encouraged by this outcome, we extended the S_NAr mechanism to prepare nitro-, cyano- and fluoro-substituted 2-naphthoates, 1,2-dihydroquinolines, and 4-oxo-1,4-dihydroquinolines as well as carboxylates and carbonitriles using Morita-Baylis-Hillman (MBH) acetates. The S_NAr reaction has been known for more than 150 years, and its relevance is justified by its wide application in organic synthesis and industry.⁷⁸ In this type of reaction, a nucleophile displaces a leaving group (usually a fluoride or chloride) on an electron deficient arene. Generally, substitution in S_NAr reaction occurs by a two-step mechanism involving, an addition-elimination sequence. The first step is the rate determining (slow) step which involves a nucleophilic attack on the aromatic carbon that bears the halogen to form a resonance-stabilized carbanion intermediate known as a Meisenheimer complex. The second (fast) step involves elimination of the leaving group to restore aromaticity.⁷⁹ For the S_NAr mechanism to proceed, strong electron-withdrawing groups on the aromatic ring must be positioned ortho or para to the leaving group. The stronger the electron-withdrawing substituent, the easier it is for the S_NAr reaction to occur (Figure 2.1). Similarly, the order of reactivity for the leaving group (X) is fluoride > chloride > bromide > iodide.

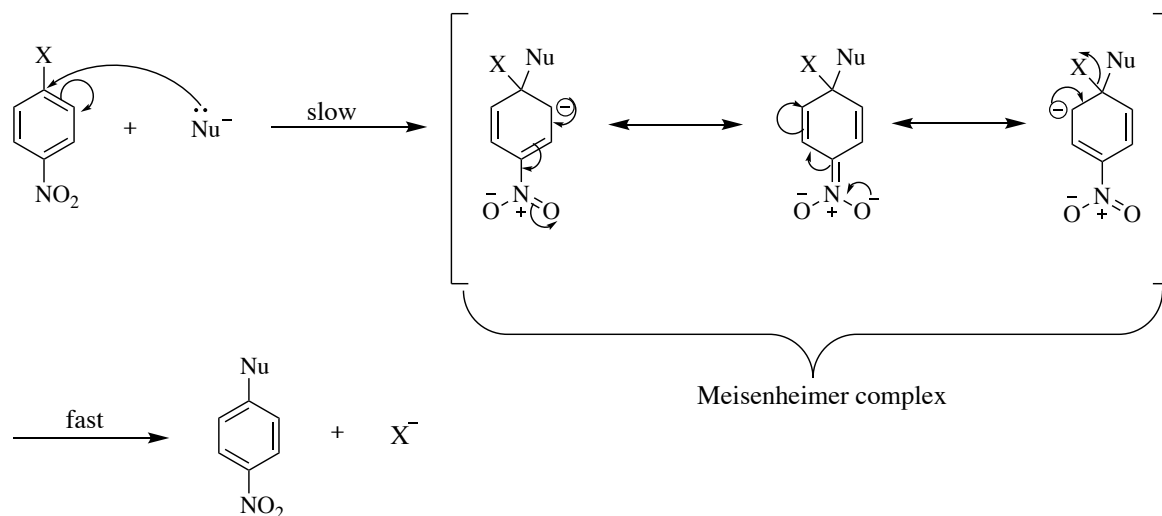


Figure 2.1. General mechanism for S_NAr reaction.⁸⁰

2.2. Results and Discussion

2.2.1. 1-Aryl-5-nitro-1*H*-indazoles and a general sequential route to 1-aryl-1*H*-indazoles.

Our synthetic methods program has recently focused on the use of nucleophilic aromatic substitution (S_NAr)-terminated tandem reactions as a means to prepare heterocyclic compounds.⁸⁰ This project has developed a synthesis of 1-aryl-1*H*-indazoles⁷⁷, which are core ring structures in a broad range of biologically active compounds (Figure 2.2). Among the compounds pictured, benzydamine (**42**) is a well-known NSAID drug,⁸¹ while alcohol **43** has likewise shown promise as an anti-inflammatory agent.⁸² The urea-based structure **44** has recently been judged to possess significant tumor antiproliferative properties.⁸³ Similarly, amide **45** has also demonstrated anticancer activity.^{84,85}

Several strategies have previously been disclosed as routes to 1-aryl-1*H*-indazoles. All required multiple steps. The closest work to that presented here utilized a two-step sequence involving acid catalyzed formation of the arylhydrazone, followed by a copper(I)-catalyzed Ullmann-type coupling to close the ring.⁸⁶ Two related accounts described (1) the base-promoted S_NAr displacement of the nitro group from arylhydrazones derived from 2-nitrosubstituted

benzaldehydes⁸⁷ and (2) the reaction of salicylaldehydes with arylhydrazine hydrochlorides.⁸⁸ Additional work examined the condensation of *N*-aroyl-*N'*-arylhyaazines with 2-bromoaryl ketones or aldehydes,⁸⁹ and arylhydrazines with 2-haloaroyl esters,⁹⁰ both followed by copper(I)-assisted ring closure. Along a different line, another study has reported a [3+2]-type annulation involving arynes generated in the presence of hydrazones under mild basic conditions.⁹¹ Finally, syntheses promoted by palladium⁹² and rhodium⁹³ catalysts have also furnished these targets. A full listing of methods to prepare 1*H*-indazoles, with and without the N1 aryl group, have been cataloged in three published reviews.⁹⁴⁻⁹⁶

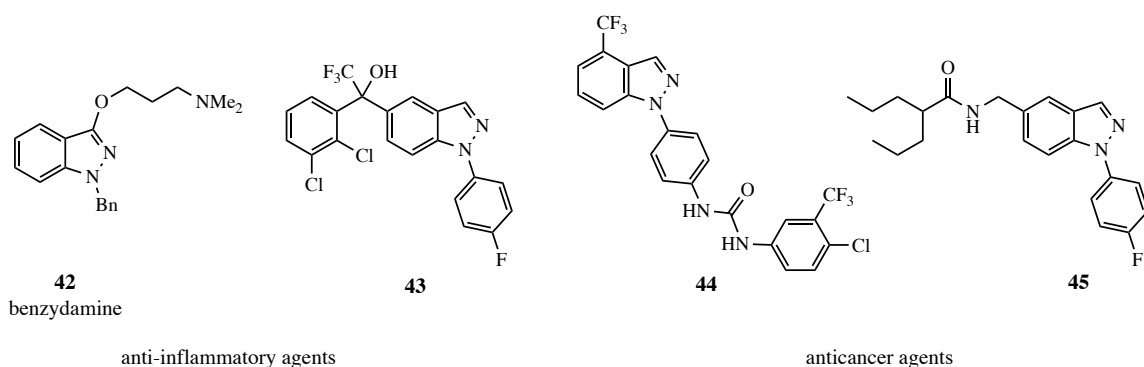
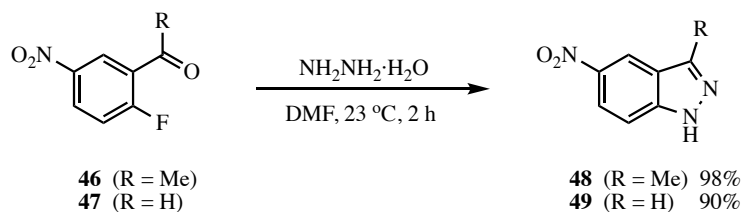


Figure 2.2. Drugs incorporating 1-aryl-1*H*-indazoles.

A logical route to 1*H*-indazoles would involve the ring closure of an arylhydrazone anion derived from an appropriately substituted aromatic ketone or aldehyde. Although the arylhydrazones would form as two isomers, with the *E* isomer (less favorable for cyclization) predominating, these should readily interconvert with heat⁹⁷ and allow access to the *Z* isomer required for ring closure. Furthermore, the p*K*_a of the phenylhydrazone proton (Ar = Ph) is 21.5,⁹⁸ and with slight variations due to substituents on the aromatic ring, should permit the use of K₂CO₃ in a polar aprotic solvent as the deprotonating agent.⁹⁹ Optimally, these annulations would proceed in one pot, but we initially sought to determine the feasibility of the sequence by evaluating each transformation separately. Once each step was optimized, attempts were made to merge the two processes into a single laboratory operation. Finally, since this generated structures with limited

substitution patterns, we also aspired to generalize the process to include structures without S_NAr activating groups. Although there are numerous examples of S_NAr -type reactions to generate five-membered rings fused to a benzene, some strain would be expected in ring formations involving closure of a fragment incorporating three sp^2 atoms onto an aromatic nucleus.^{100,101} Thus, 2'-fluoro-5'-nitroacetophenone (**46**) and 2-fluoro-5-nitrobenzaldehyde (**47**) were initially reacted with hydrazine hydrate ($NH_2NH_2 \cdot H_2O$) to assess the feasibility of forming indazoles in this manner. Due to the α -effect,¹⁰² hydrazine is an exceptionally potent nucleophile and might be expected to react without added base. Indeed, treatment of **46** and **47** with $NH_2NH_2 \cdot H_2O$ (3.0 equiv for **46** and 2.0 equiv for **47**) in DMF at 23 °C for 2 h resulted in high yields of targets **48** and **49**, respectively (see Scheme 2.1). Encouraged by this result, we forged ahead to prepare 1-aryl-5-nitro-1*H*-indazoles.

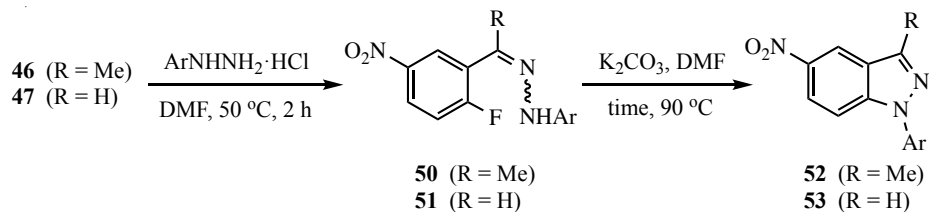


Scheme 2.1. Reaction of **46** and **47** with hydrazine hydrate.

Formation of the intermediate arylhydrazones **50** and **51** (see Table 2.1) was initially addressed. This involved warming a DMF solution of the carbonyl compound with an arylhydrazine hydrochloride ($ArNHNH_2 \cdot HCl$) at 50 °C for 2-3 h. DMF was used as a solvent for this process since we anticipated that a one-pot procedure where the hydrazone was prepared, deprotonated, and cyclized would likely require the use of a polar aprotic solvent. Optimization studies indicated that DMF was a suitable medium and the use of 3.0 equiv of $ArNHNH_2 \cdot HCl$ with acetophenone **46** and 2.0 equiv with benzaldehyde **47** afforded the highest yields of **50** and **51**. In all cases, the intermediate hydrazones were isolated in $\geq 70\%$ yield from **46** and $\geq 50\%$ yield from **47**. Interestingly, compounds arising from direct S_NAr displacement of fluoride by the

arylhazirine were not observed to any significant extent under these conditions. While the product of addition-elimination by hydrazine is known to cyclize to a 1*H*-indazole,¹⁰³ ring closure of the analogous product from arylhydrazine would likely give a 2-aryl-2*H*-indazole, and this was not detected.

Table 2.1. Yields for the two-step synthesis of 1-aryl-5-nitro-1*H*-indazoles.



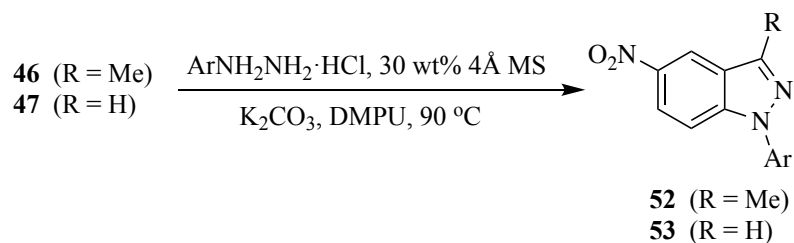
Substrate	Ar	Time (h) ^a	Pdt	%Yield ^b
46	a Ph-	2	52a	95
46	b 2-MeOPh-	2	52b	82
46	c 3-MeOPh-	2	52c	81
46	d 4-MeOPh-	2	52d	94
46	e 4-BrPh-	2	52e	95
46	f 3-ClPh-	2	52f	87
46	g 4-ClPh-	2	52g	93
46	h 2,4-Cl ₂ Ph-	36	52h	80
46	i 3-CF ₃ Ph-	2	52i	88
46	j 4-CF ₃ Ph-	2	52j	70
46	k 4-CNPh-	2	52k	80
46	l 4-H ₂ NSO ₂ Ph-	10	52l	70
46	m 4-HO ₂ CPh-	24	52m	75
47	a Ph-	2	53a	72
47	b 2-MeOPh-	2	53b	0 ^c
47	c 3-MeOPh-	2	53c	67
47	d 4-MeOPh-	2	53d	70
47	e 4-BrPh-	2	53e	70
47	f 3-ClPh-	2	53f	60
47	g 4-ClPh-	2	53g	70
47	h 2,4-Cl ₂ Ph-	2	53h	60
47	i 3-CF ₃ Ph-	2	53i	62
47	j 4-CF ₃ Ph-	2	53j	68
47	k 4-CNPh-	3	53k	60
47	l 4-H ₂ NSO ₂ Ph-	2	53l	50
47	m 4-HO ₂ CPh-	2	53m	50

^aAll hydrazones were generated in 2 h. Times given are for the final cyclization. ^bIsolated yield of 1*H*-indazole for the two-step sequence. ^cOnly the hydrazone was isolated.

Cyclization of hydrazones **50** and **51** required base, higher temperature and occasionally extended reaction times. This reaction was performed in DMF at 90 °C and found to work best using 3.0 equiv of K₂CO₃. Yields were slightly lower from the benzaldehyde since this substrate led to a product that was unhindered at C3 and possibly susceptible to nucleophilic attack by various species in the reaction. The results of our two-step synthesis of 1-aryl-5-nitro-1*H*-indazoles are summarized in Table 2.1.

Modification of the protocol to allow for a one-pot procedure had to overcome several problems that could lead to unwanted impurities. Since water is produced during hydrazone formation, some conversion of the K₂CO₃ to KOH would be expected. Furthermore, KOH could hydrolyze the DMF solvent to form Me₂NH. Both of these nucleophiles (OH⁻ and Me₂NH) could potentially undergo competitive S_NAr addition to the carbonyl containing substrate. While no significant product resulting from OH⁻ addition was observed, some of the Me₂NH addition product was noted when prolonged heating was required. These side reactions were suppressed by adding 30 wt% (relative to **46** or **47**) of powdered 4Å molecular sieves to scavenge water produced during the initial condensation and using anhydrous 1,3-dimethyl-3,4,5,6-tetrahydro-2(1*H*)-pyrimidinone (DMPU) as the solvent to minimize hydrolysis (see Table 2.2).

The one-step tandem process was successful for the conversion of ketone **46** to indazoles **52**, and in most cases, the yield was superior to the two-step sequence. Reactions of aldehyde **47** to give **53**, however, were more limited and several of the substrates bearing acidic functions on the aromatic ring failed to react. For aldehydes that did generate a product, sequential treatment with ArNHNH₂·HCl and base afforded yields that also surpassed the two-step process (see Table 2.2). In both one-pot procedures, it was often noted that the cyclization required a longer reaction time when the aryl group of the hydrazone was substituted by an electron-withdrawing group. This would be expected since the arylhydrazone anion would be less nucleophilic with a stabilizing group at C2 or C4 of the hydrazone aromatic ring.¹⁰⁴ Conversely, this same anion with electron-donating substituents at C2 or C4 should be more reactive with potentially shorter reaction times.

Table 2.2. Yields for the modified one-pot synthesis of 1-aryl-5-nitro-1*H*-indazoles.

Substrate	Ar	Time (h) ^a	Pdt	% Yield ^b
46	a Ph-	1.5	52a	96
46	d 4-MeOPh-	1.5	52d	95
46	g 4-ClPh-	1.5	52g	94
46	h 2,4-Cl ₂ Ph-	72	52h	85
46	m H ₂ NSO ₂ Ph-	16	52m	85
46	n HO ₂ CPh-	45	52n	73
47	a Ph-	3.5	53a	73
47	d 4-MeOPh-	3.5	53d	74
47	g 4-ClPh-	3.5	53g	71
47	l 4-NCPH-	6.5	53l	63
47	m H ₂ NSO ₂ Ph-	8.5	53m	0
47	n HO ₂ CPh-	8.5	53n	0

^aFor **46**, time is the total reaction time. For **47**, the hydrazone was allowed to form for 1.5 h at 90 °C before base was added; time is for the final cyclization. ^bIsolated yield.

Finally, we sought to develop a general approach to 1*H*-indazoles unrestricted by the substitution patterns needed for the S_NAr ring closure (see Table 2.3). Protocol development efforts indicated that this variant of the reaction required sequential addition of the reagents. The hydrazone was initially generated using 1.5 equiv of the ArNHNH₂·HCl and then cyclized by addition of 20 mol% of copper(I) iodide (CuI) and 2.5 equiv of K₂CO₃, all in the same flask at 90 °C. Again, the key to success in this transformation was the inclusion of 30 wt% of powdered 4Å molecular sieves and the use of DMPU as the solvent. Without activating groups on the ring, Ullmann conditions (CuI and base) for the final ring closure were essential. An earlier paper noted that this copper(I)-catalyzed ring closure was facilitated by the addition of 20 mol% of L-proline or 4-hydroxy-L-proline.⁹² In the current procedure, however, addition of these ligands had no impact

on the yield of the reaction. The cyclization using 2'-bromoacetophenone (**54**), 2-bromobenzaldehyde (**55**) and 2-chloronicotinaldehyde (**56**) was performed using phenylhydrazine as well as electron-rich and electron-poor arylhydrazines in relatively uniform yields. Though it was expected that the nicotinaldehyde derivatives would not need a copper catalyst, since it could directly cyclize by a S_NAr reaction, this ring closure failed to proceed to completion without this additive. Overall, our procedure permits the rapid construction of 1-aryl-1*H*-indazoles in a single reaction vessel without isolation or purification of intermediates.

Table 2.3. Yields for the general one-pot synthesis of 1-aryl-1*H*-indazoles.

54 (X = Br, Y = CH; R = Me)
55 (X = Br, Y = CH; R = H)
56 (X = Cl, Y = N; R = H)

57 (Y = CH; R = Me)
58 (Y = CH; R = H)
59 (Y = N; R = H)

Substrate	Ar	Product	% Yield ^a
54	a Ph-	57a	81
54	d 4-MeOPh-	57d	83
54	l 4-CNPh-	57l	87
55	a Ph-	58a	77
55	d 4-MeOPh-	58d	72
55	l 4-CNPh-	58l	79
56	a Ph-	59a	68
56	d 4-MeOPh-	59d	62
56	l 4-CNPh-	59l	78

^aIsolated yield.

2.2.1.1. Conclusions

We have developed and optimized a two-step synthesis to prepare 1-aryl-5-nitro-1*H*-indazoles from 2'-fluoro-5'-nitroacetophenone (**46**) and 2-fluoro-5-nitrobenzaldehyde (**47**). We have further modified the conditions to allow a one-pot conversion of **46** to **52** (tandem reaction) and **47** to **53**

(sequential reaction) in yields that surpassed those of the two-step sequence. Our strategy involved initial formation of the hydrazone, followed by deprotonation and S_NAr ring closure. Yields were 73-96% from **46** and 70-74% from **47** for the one-pot version of the synthesis, though two examples involving **47** failed to give an indazole product. We have also developed a general one-pot sequential approach to 1-aryl-1*H*-indazoles that is not limited by the substitution patterns normally required for the S_NAr ring closure. Treatment of 2'-bromoacetophenone (**54**), 2-bromobenzaldehyde (**55**) and 2-chloronicotinaldehyde (**56**) with ArNHNH₂·HCl and 30 wt% of powdered 4Å molecular sieves in DMPU at 90 °C, followed by addition of CuI and K₂CO₃, afforded 1*H*-indazoles bearing phenyl as well as electron-rich and electron-poor aromatic groups at N1 in 62-87% yields. The current work provides access to a selection of 1-aryl-1*H*-indazoles in a single laboratory operation without isolation or purification of intermediates. We are continuing our work to devise new and efficient approaches to a broad range of heterocyclic systems.

2.2.2. 4*H*-Benzo[*d*][1,3]oxazin-4-ones and dihydro analogs.

We recently reported the high-yield synthesis of quinazolin-4(3*H*)-ones by reaction of 2-aminobenzamides with orthoesters in ethanol promoted by acetic acid.¹⁰⁵ These heterocycles have received considerable attention as they have demonstrated diverse biological activities. With the success of this previous study, we sought to evaluate a similar strategy for the synthesis of 2-alkyl and 2-aryl-4*H*-benzo[*d*][1,3]oxazin-4-ones (also known as 4*H*-3,1-benzoxazin-4-ones).¹⁰⁶ These compounds are less stable, and thus, have been less well studied. An early account noted that several substituted structures related to compound **57** exhibited hypolipidemic activity.¹⁰⁷ Other benzoxazinones demonstrated potential as protease inhibitors. In particular, 4*H*-benzo[*d*][1,3]-oxazin-4-one **58** was shown to have substrate inhibitory activity towards the serine protease human leukocyte elastase which is the presumed tissue degenerating agent in the pathogenesis of several diseases.¹⁰⁸ Two additional studies revealed that **59** and **60** interfered with the action of intramembrane serine proteases known as rhomboids that are important in the progression of

diseases such as cancer, diabetes, invasion of apicomplexan parasites, and Parkinson's disease.^{109,110} Thus, access to these drug candidates would allow further study of the etiology of these diseases and could lead to new drugs to treat them. Structures **57-60** are shown in Figure 2.3. Apart from investigations of their potential use as drugs, 4*H*-benzo[*d*][1,3]oxazin-4-ones have also been used as precursors to new heterocycles¹¹¹ as well as interesting peptide based oligomers.¹¹²

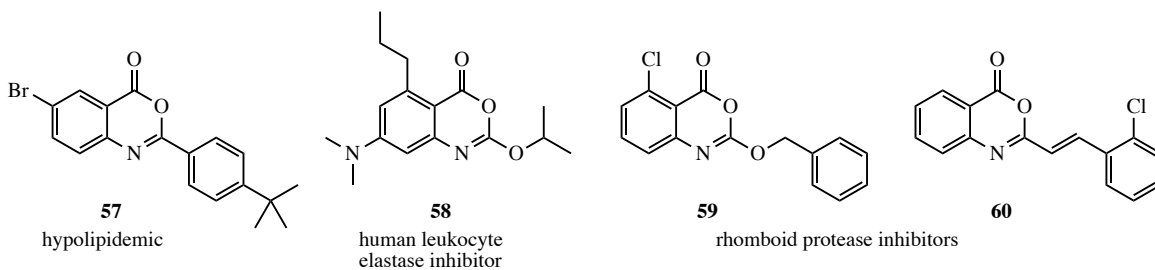
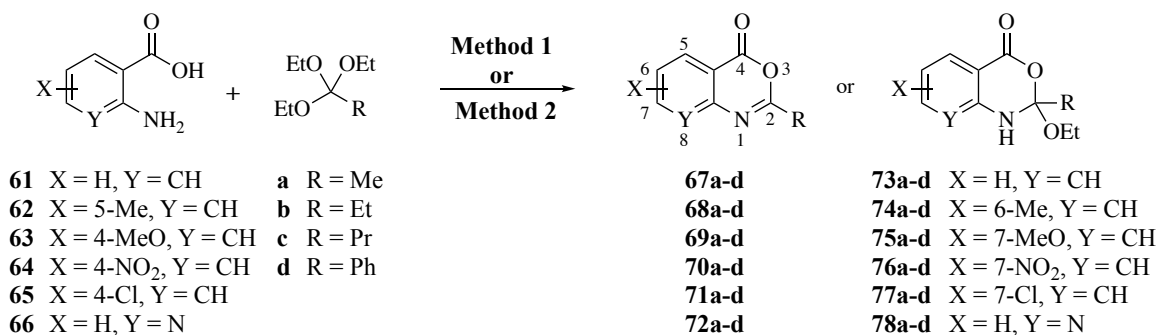


Figure 2.3. 4*H*-Benzo[*d*][1,3]oxazin-4-ones with potential drug activity.

Classic approaches to 4*H*-benzo[*d*][1,3]oxazin-4-ones involved reaction of anthranilic acid with two equivalents of benzoyl chloride in pyridine to afford >90 % of 2-aryl-4*H*-benzo[*d*][1,3]oxazin-4-ones.¹⁰⁷ Similarly, treatment of substituted anthranilic acids with one equivalent of various acid chlorides to give the 2-amidobenzoic acid, followed by boiling in acetic anhydride, also afforded these products in good yields.^{113,114} A later synthesis of 4*H*-benzo[*d*][1,3]oxazin-4-ones described a high-yield palladium-catalyzed cyclocarbonylation of *o*-iodoanilines with acid chlorides.¹¹⁵ Furthermore, three oxidative approaches to these aryl-fused heterocycles have also been reported. In the first example, copper was used to promote the conversion of 2-alkynylanilines to 2-aryl-4*H*-benzo[*d*][1,3]oxazin-4-ones using base conditions under oxygen atmosphere.¹¹⁶ Another approach utilized oxone in nitromethane at 100 °C to accomplish the oxidation of 2-arylindoles to these same targets. A third oxidative procedure involved the water assisted oxidation of 2-arylindoles to 2-aryl-4*H*-benzo[*d*][1,3]oxazin-4-ones using (diacetoxyiodo)benzene.¹¹⁷ Finally, a method related to the current procedure was reported

for a small series of compounds substituted by phenyl at C2. This procedure utilized microwave energy to promote the formation of 2-phenyl-4*H*-benzo[*d*][1,3]oxazin-4-ones from four anthranilic acids and triethyl orthobenzoate.¹¹⁸ The yields varied in this reaction, but no problems were noted. In the current study, we have attempted to expand the scope of this transformation examining the reaction of additional aryl-substituted anthranilic acids with four orthoesters. The results of our study are detailed below.

Scheme 2.2 depicts the focus and scope of the current study. We have explored the synthesis of a range of 4*H*-benzo[*d*][1,3]oxazin-4-ones from reaction of six anthranilic acids with a range of commercially available orthoesters (Tables 2.4 and 2.5). The reaction was run under two sets of conditions: one under thermal conditions promoted by acid and the other under microwave conditions. The acid promoted conditions involved heating anthranilic acid (1 equiv) with the orthoester (4.5 equiv) in the presence of AcOH (2.6 equiv), neat, at 100 °C, for 4-48 h. The microwave reaction was run using anthranilic acid (1 equiv) and the orthoester (2.0-2.7 equiv), neat, without AcOH, at 100 °C (400 W), for 0.75-3 h. Upon cooling, the products from both procedures crystallized from the crude reaction mixtures and were purified by trituration from 5% pentane in ether.



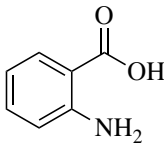
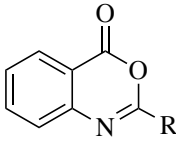
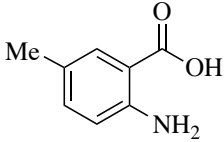
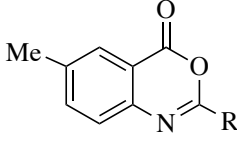
Method 1: anthranilic acid (1 equiv), orthoester (4.5 equiv), AcOH (2.6 equiv), neat, 100 °C, 4-48 h

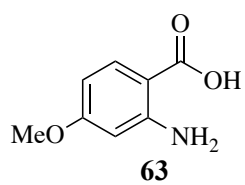
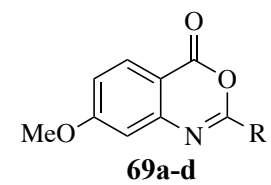
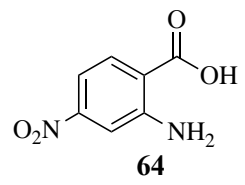
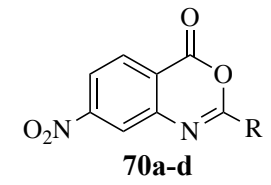
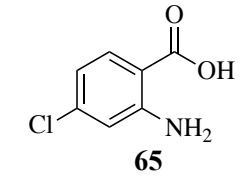
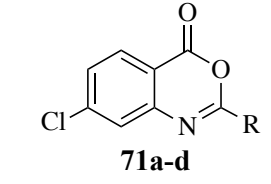
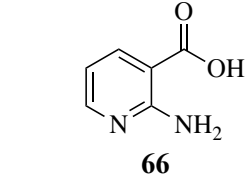
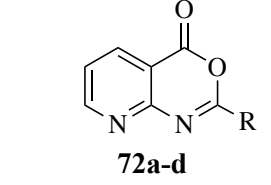
Method 2: anthranilic acid (1 equiv), orthoester (2.0-2.7 equiv), neat, MW, 100 °C (400 W), 0.75-3 h

Scheme 2.2. Formation of 4*H*-benzo[*d*][1,3]oxazin-4-ones and their dihydro analogs from anthranilic acids and orthoesters.

Contrary to what has been reported in related studies to date, we found that not all of the thermal reactions produced the target heterocycles cleanly. In several cases, (\pm)-2-substituted-1,2-dihydro-4*H*-benzo[*d*][1,3]oxazin-4-ones, resulting from ring closure without elimination of the final molecule of ethanol, were isolated. This led us to expand our study to evaluate microwave reactions in addition to the standard acid-promoted thermal reactions; however, both protocols afforded the intermediate dihydro compounds from specific substrates. In several cases, it was possible to isolate either product by modification of the procedure. For example, the reaction of anthranilic acid (**61**) with triethyl orthobenzoate (**d**, Scheme 2.2) for 24 h under thermal conditions afforded dihydro product **73d**, while extending the reaction to 48 h yielded 4*H*-benzo[*d*][1,3]oxazin-4-one **67d**. In several other examples, however, it was not possible to induce the final elimination reaction.

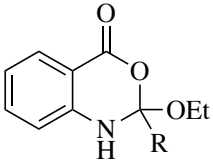
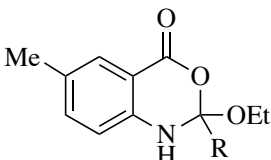
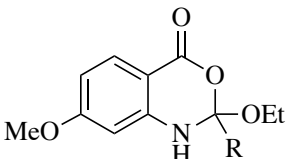
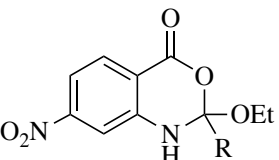
Table 2.4. Formation of 4*H*-benzo[*d*][1,3]oxazin-4-ones.

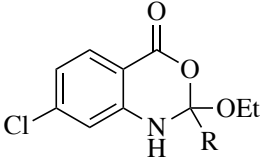
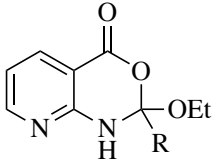
Substrate	Product	R	Method ^a	Time (h)	Yield (%)
 61	 67a-d	a: Me	1(2)	48(0.75)	81(82)
		b: Et	1(2)	7(0.75)	80(83)
		c: Pr	1(2)	4(0.75)	b
		d: Ph	1(2)	48(0.75)	78(80)
 62	 68a-d	a: Me	2	0.75	68
		b: Et	2	0.75	66
		c: Pr	1(2)	24(0.75)	c
		d: Ph	2	0.75	85

		a: Me	1(2)	24(0.75)	87(88)
		b: Et	1(2)	24(0.75)	86(88)
		c: Pr	1(2)	24(0.75)	86(87)
		d: Ph	1(2)	48(0.75)	83(85)
		a: Me	1(2)	24(0.75)	c
		b: Et	1(2)	24(0.75)	c
		c: Pr	1(2)	24(0.75)	c
		d: Ph	2	3	91
		a: Me	2	0.75	85
		b: Et	1(2)	48(0.75)	c
		c: Pr	1(2)	48(0.75)	c
		d: Ph	2	1.5	92
		a: Me	1	24	c
		b: Et	2	0.75	d
		c: Pr	2	0.75	d
		d: Ph	2	0.75	d

(a) For anthranilic acid (1 equiv): **Method 1:** orthoester (4.5 equiv), AcOH (2.6 equiv), neat, 100 °C, for the indicated time; **Method 2:** orthoester (2.0-2.7 equiv), neat, MW, 100 °C, for the indicated time; (b) An inseparable mixture of the 4*H*-benzo[*d*][1,3]oxazin-4-one and the dihydro product was formed; (c) The dihydro product formed; (d) Only ethyl 2-aminonicotinate was formed from esterification of the substrate acid.

Table 2.5. Formation of (±)-1,2-dihydro-4*H*-benzo[*d*][1,3]oxazin-4-ones.

Substrate	Product	R	Method ^a	Time (h)	Yield (%)
61	 73a-d	a: Me			b
		b: Et			b
		c: Pr			c
		d: Ph	1	24	86
62	 74a-d	a: Me	1	24	88
		b: Et	1	24(0.75)	87
		c: Pr	1(2)	24	88(89)
		d: Ph	1	48	89
63	 75a-d	a: Me			b
		b: Et			b
		c: Pr			b
		d: Ph			b
64	 76a-d	a: Me	1(2)	24(1.5)	84(87)
		b: Et	1(2)	24(1.5)	86(88)
		c: Pr	1(2)	24(1.5)	85(88)
		d: Ph	1	24	90

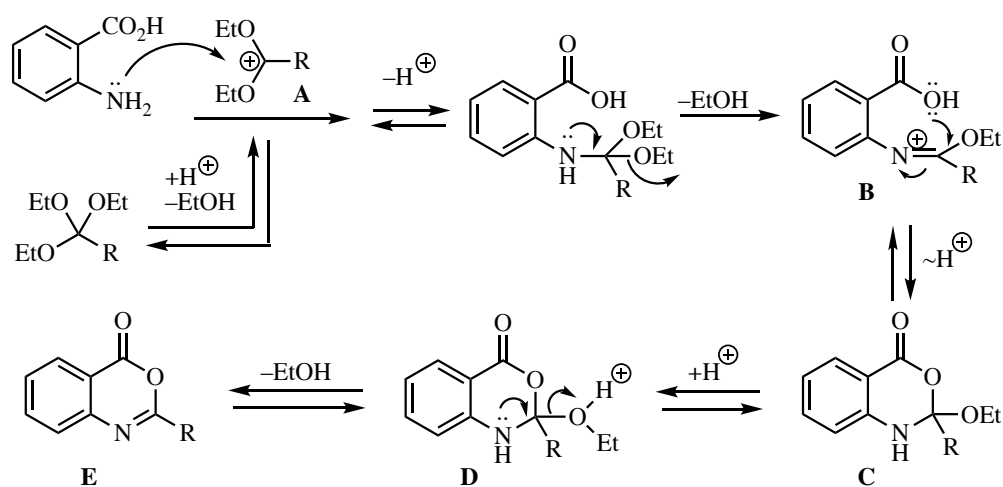
65	 77a-d	a: Me	1	24	84
		b: Et	1(2)	48(0.75)	84(86)
		c: Pr	1(2)	48(0.75)	83(84)
		d: Ph	1	48	85
66	 78a-d	a: Me	1	24	85
		b: Et			d
		c: Pr			d
		d: Ph			d

(a) For anthranilic acid (1 equiv): **Method 1:** orthoester (4.5 equiv), AcOH (2.6 equiv), neat, 100 °C, for the indicated time; **Method 2:** orthoester (2.0-2.7 equiv), neat, MW, 100 °C, for the indicated time; (b) Only the 4*H*-benzo[*d*][1,3]oxazin-4-one product was formed; (c) An inseparable mixture of the 4*H*-benzo[*d*][1,3]oxazin-4-one and the dihydro product was formed; (d) Only ethyl 2-aminonicotinate was formed from esterification of the substrate acid.

The outcome of the reaction appeared to correlate with the electron density in the aromatic ring of the anthranilic acid. For rings substituted with electron donating groups (OMe, Me) or hydrogen, the 4*H*-benzo[*d*][1,3]oxazin-4-one product predominated. More electron-poor aromatic rings bearing a second electron-withdrawing group on the aromatic ring (NO₂ and Cl), in addition to the ortho carbonyl group, showed a tendency to give the 1,2-dihydro-4*H*-benzo[*d*][1,3]oxazin-4-one product. Changing the benzene ring of the anthranilic acid to an electron-deficient pyridine, as in 2-aminonicotinic acid (**66**), almost completely shut down the reaction. In most cases, it was possible to isolate at least one of the products in pure form. The lone exception was the attempted conversion of **61** to **73c** with triethyl orthobutyrate (**c**), which gave an inseparable mixture of the benzoxazinone and dihydro product under all conditions. Attempts to drive the reaction to the benzoxazinone using 5 equiv of AcOH or spiking the reaction with H₂SO₄ failed to alter the outcome, while treatment with base (K₂CO₃, EtOH, molecular sieves), resulted in ring opening to the *N*-acylanthranilic acid. Finally, in attempted reactions of 2-aminonicotinic acid (**66**), triethyl

orthoacetate (**a**) proceeded to give dihydro product **77a**, but all others afforded only ethyl 2-aminonicotinate resulting from esterification of the substrate acid.

The presumed mechanism for the formation of 4*H*-benzo[*d*][1,3]oxazin-4-ones is shown in Scheme 2.3. The process involves initial protonation of the orthoester and loss of ethanol to afford the stabilized carbocation **A**. Attack on **A** by the anthranilic acid amino group, proton exchange and loss of a second molecule of ethanol would then yield iminium ion **B**. Subsequent closure of the acid oxygen on the iminium carbon and proton exchange would give the ring-closed, dihydro product **C**. Finally, protonation of **C** to give **D** and loss of ethanol would then generate the desired heterocycle **E**.



Scheme 2.3. Presumed mechanism for the formation of 4*H*-benzo[*d*][1,3]oxazin-4-ones.

Difficulty was noted in the final elimination of ethanol when the aromatic ring carried a second electron-withdrawing group (EWG) in addition to the adjacent ester carbonyl. For this elimination, the availability of the unshared electron pair on N1 and its ability to align antiperiplanar to the departing alcohol were assumed to be keys to the success of this elimination. The availability of these electrons, however, would be diminished in substrates with a strongly electron-deficient ring. Relatively little seems to be known about the necessity for the

antiperiplanar alignment of the unshared pair for efficient elimination in this system. This anomeric effect has been extensively studied in acetals and hemiacetals,¹¹⁹ but much less so for their nitrogen analogs since elimination is normally facile. If achievable, conformation **D1** would result in good overlap for elimination of ethanol (see Figure 2.4). Placement of the C2 ethoxy group in a pseudo-axial position for this elimination should be favorable since this group is considered to be sterically smaller than an alkyl group.^{120,121} However, this conformation also maximizes overlap of the N1 electron pair with the aromatic ring as well as the ortho carbonyl, and this could slow the elimination if the aromatic ring bears an additional electron-withdrawing substituent. The alternative conformation **D2** is not optimally aligned for elimination (see Figure 2.4). If the ring closure and protonation steps led to this conformation, conversion to **D1** could occur, but would likely be sluggish since flexibility in this rigid system is allowed only at the saturated atoms of the benzoxazinone.

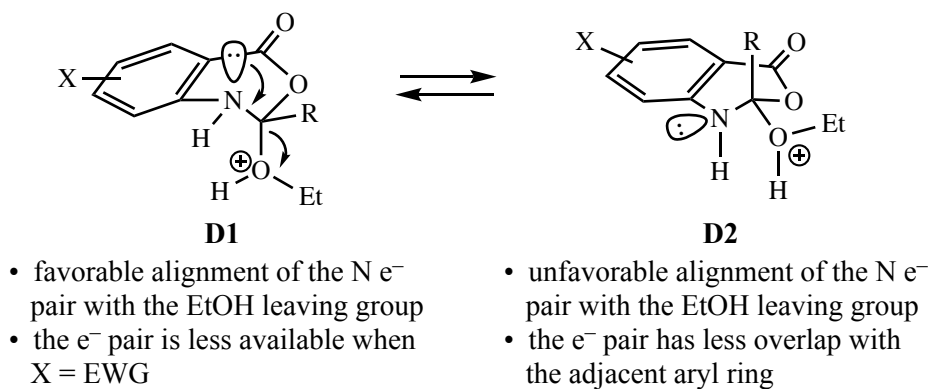


Figure 2.4. Conformational options for intermediate **D**.

2.2.2.1. Conclusions

We have studied the formation of 4*H*-benzo[*d*][1,3]oxazin-4-ones under thermal conditions with acetic acid as well as microwave conditions without acid. In most cases, the target heterocycle was formed in high yield. The reaction was performed with no solvent, and the desired products

were isolated by crystallization and trituration. The microwave reaction proceeded much faster (0.75-3 h) than the thermal reactions (4-48 h) and did not require extra acid. Thus, the microwave protocol represents the superior procedure. Stereoelectronic effects strongly impacted the outcome of the reaction. In addition to the benzoxazinone products, a dihydro intermediate, resulting from failure to undergo the final elimination, was observed in some substrates. The formation of the dihydro compound arose in reactants where the fused aromatic ring possessed a second electron-withdrawing group in addition to the conjugated carbonyl on the ortho carbon. This could deactivate the electron pair on N1 and slow the elimination process, even if the C2 ethoxy group was able to adopt the required pseudo-axial conformation. The formation of these dihydro systems provides access to a new substitution pattern in this family of compounds and could yield additional candidates for biological testing. This finding, coupled with the fact that orthoesters are easily prepared from nitriles,^{122,123} should provide a route to many members of this novel class of structures.

2.2.3. Bis- and mono-1,3,4-oxadiazole synthesis promoted by catalytic NH₄Cl.

We recently reported the high-yield synthesis of 1,3,4-oxadiazoles promoted by NH₄Cl in absolute ethanol.¹²⁴ These heterocyclic scaffolds have received considerable attention in the field of medicinal chemistry as they possess diverse biological activities (Figure 2.5). Encouraged by the outcome of this previous study, we sought to evaluate a similar strategy for the synthesis of bis-1,3,4-oxadiazoles. Over the years, numerous methods for the synthesis of the 1,3,4-oxadiazole ring core have been developed as a result of their broad commercial potential. Most approaches involve either a multi-step strategy or the cyclization of hydrazides using harsh reagents such as phosphorus oxychloride, thionyl chloride, sulfuric acid, zirconium(IV) chloride, XtalFluor-E[®], Burgess reagent, Deoxo-Fluor[®], acid chlorides, Nafion[®] NR50, or acetic acid, under reflux or microwave heating.¹²⁵ Consequently, sensitive functional groups are often intolerable with these earlier methods due to the caustic nature of these reagents. To address this problem, we

developed a mild alternative, which involves the formation of 1,3- and 1,4-bis-1,3,4-oxadiazoles from aryl or aliphatic dihydrazides and orthoesters using NH_4Cl as a catalyst.

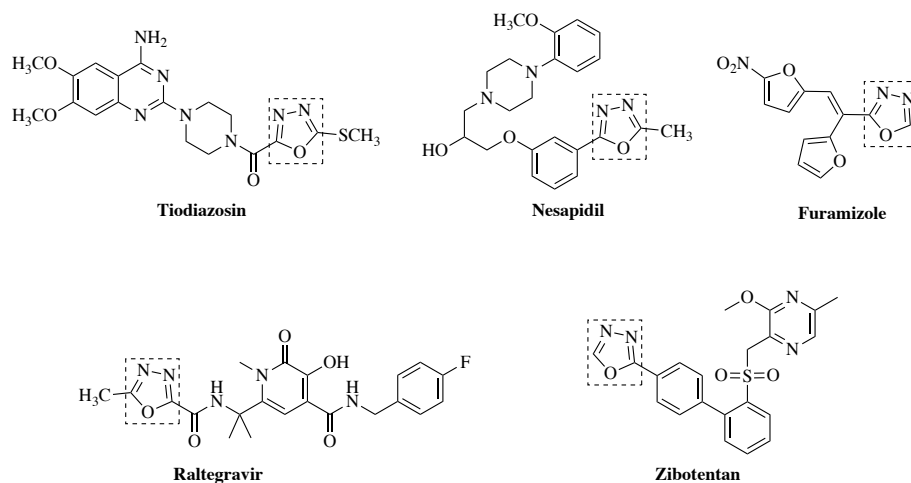


Figure 2.5. Drug containing an oxadiazole ring.

In recent years, NH_4Cl has proven to be a highly efficient and mild catalyst for the synthesis of benzo-fused heterocycles such as benzimidazoles, benzoxazoles, and benzothiazoles.¹²⁶ Moreover, the usefulness of NH_4Cl has been extended to the preparation of α -aminonitriles using a variant of the Strecker synthesis.¹²⁷ The scope of this catalyst was broadened by performing optimization studies for the current reaction using terephthalic dihydrazide (1.0 equiv) and triethyl orthoformate (2.2 equiv). The optimized transformation occurred using 60 mol% of NH_4Cl in DMSO at 100 °C, which afforded an 85% yield of the corresponding 1,4-bis-1,3,4-oxadiazole in 90 minutes (Table 2.6). Lower catalyst loadings resulted in slow and often incomplete reaction, while more catalyst had no impact on the outcome of the reaction. Replacing DMSO with absolute EtOH gave similar yields, but at a much slower rate (twice as much time). Attempts to use other solvents (DMF, MeOH, THF, CH_3CN) either produced lower yields or no detectable product. Moreover, the use of acetic acid (1.69 equiv) afforded only trace amounts of product (Table 2.6).

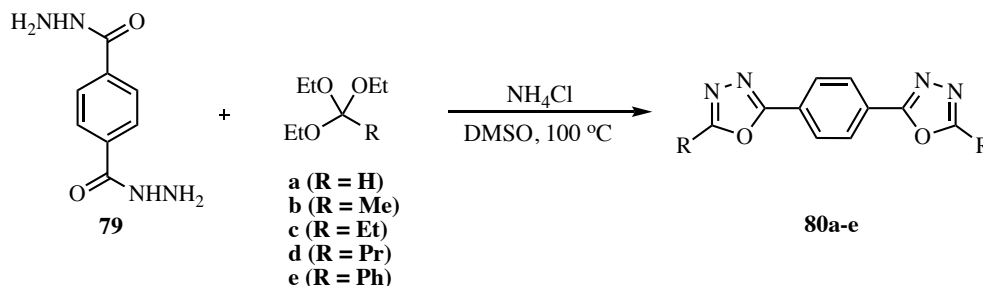
Table 2.6. Optimization results for bis-1,3,4-oxadiazole from terephthalic dihydrazide (1.0 equiv) and triethyl orthoformate.

Trial Exp.	Equiv. of triethyl orthoformate	Proton source/Acid	Equiv. of Acid	Solvent	Time (h)	Yield (%)
1	3.0	NH ₄ Cl	80 mol%	EtOH	3.0	85
2	2.2	NH ₄ Cl	60 mol%	EtOH	3.0	85
3	2.2	NH ₄ Cl	60 mol%	DMF	1.5	45
4	2.2	NH ₄ Cl	60 mol%	Acetonitrile	4.0	ND ^a
5	2.2	NH ₄ Cl	60 mol%	THF	4.0	ND ^a
6	2.2	NH ₄ Cl	60 mol%	MeOH	4.0	ND ^a
7	2.2	Acetic acid	1.69	DMSO	1.5	Trace
8	2.2	NH₄Cl	60 mol%	DMSO	1.5	85
9	2.0	NH ₄ Cl	60 mol%	DMSO	1.5	76
10	2.2	NH ₄ Cl	50 mol%	DMSO	5.0	42

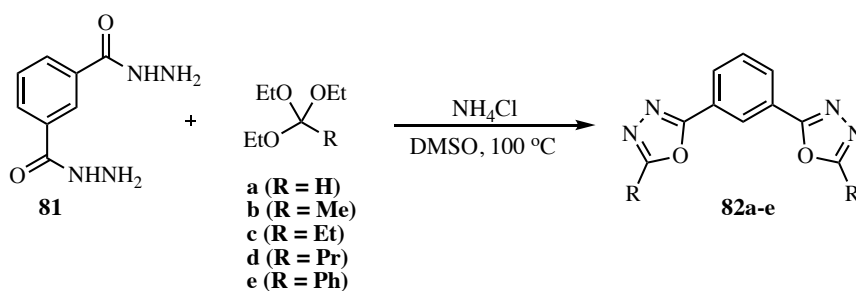
^aND = no detectable product.

The scope of this reaction was extended to a series of aryl and aliphatic dihydrazides using various orthoesters and 60 mol% NH₄Cl in DMSO at 100 °C. Our results are summarized in Tables 2.7–2.9. Additionally, the reaction of various orthoesters with substituted arylhydrazides, nicotinic and isonicotinic acid hydrazides (Tables 3.0–3.2) was also examined under similar optimized conditions. The reaction was tolerant of and successful with both electron-donating (methoxy) and electron-withdrawing (nitro) substituents on the arylhydrazide reactant.

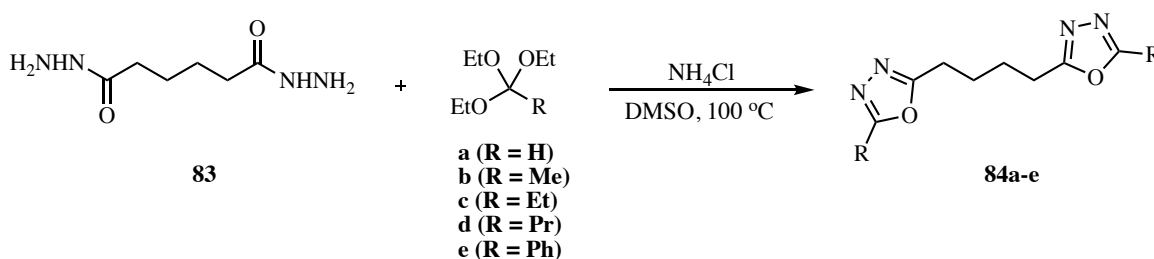
Table 2.7. Summary of 1,4-bis-1,3,4-oxadiazoles from terephthalic dihydrazide.



Substrate	R	Time (h)	Product	Yield (%)
79	a: H	1.5	80a	85
79	b: Me	11.0	80b	89
79	c: Et	6.0	80c	81
79	d: Pr	4.0	80d	80
79	e: Ph	20.0	80e	76

Table 2.8. Summary of 1,3-bis-1,3,4-oxadiazoles from isophthalic dihydrazide.

Substrate	R	Time (h)	Product	Yield (%)
81	a: H	2.5	82a	84
81	b: Me	12.0	82b	88
81	c: Et	8.0	82c	86
81	d: Pr	6.0	82d	85
81	e: Ph	22.0	82e	77

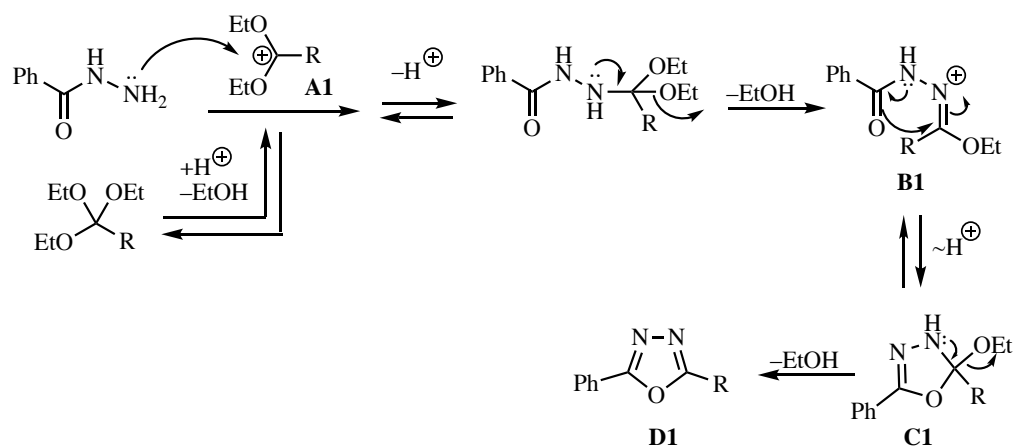
Table 2.9. Summary of 1,4-butyl-bis-1,3,4-oxadiazoles from adipic dihydrazide.

Substrate	R	Time (h)	Product	Yield (%)
83	a: H	1.5	84a	53
83	b: Me	96.0	84b	20
83	c: Et	4.0	84c	79
83	d: Pr	6.0	84d	ND ^a
83	e: Ph	22.0	84e	56

^aND = no detectable product.

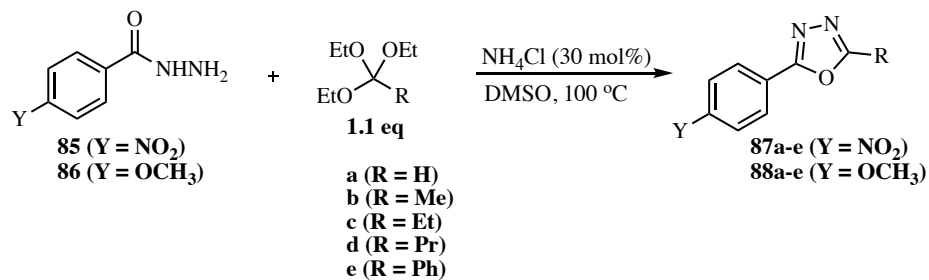
Generally, adipic dihydrazide (**83**) gave low yields of bis-1,3,4-oxadiazoles (Table 2.9). In addition, the yield of the target molecule from isophthalic dihydrazide (**81**) as shown in Table 2.8 were lower in some cases than those from the terephthalic dihydrazide (**79**) in Table 2.7.

Moreover, bis-1,3,4-oxadiazoles from **81** required much longer reaction times, and this presumably results from a steric effect. The proximity of the hydrazide groups in the 1,3 position of **81** may result in steric hindrance, which could potentially impact the reactivity of **81**. Conversely, **79** should be more reactive because the two hydrazide groups are reasonably far apart (1,4) thus only minimal or no steric hindrance may be experienced. A proposed mechanism for the formation of the oxadiazole ring system is given in Scheme 2.4. The process involves initial protonation of the orthoester and loss of ethanol to afford the ether-stabilized carbocation **A1**. Attack on **A1** by the hydrazide amino group, proton exchange and loss of a second molecule of ethanol, would then yield iminium ion **B1**. Subsequent closure of the amide oxygen on the iminium carbon and proton exchange would give the ring-closed dihydro product **C1**. Finally, loss of ethanol would then generate the desired heterocycle **D1**.

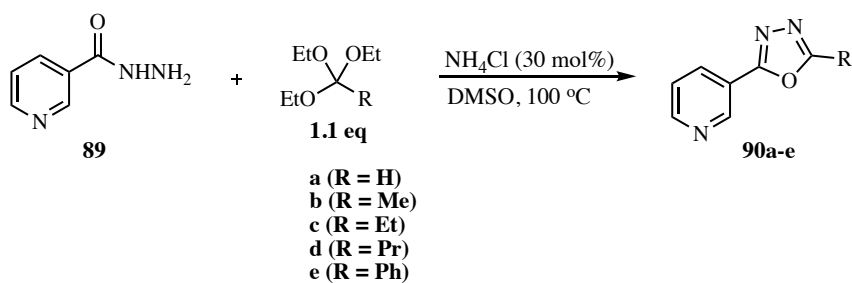


Scheme 2.4. Proposed mechanism for the formation of 1,3,4-oxadiazole ring system.

Extension of the current protocol to substituted aryl, nicotinic and isonicotinic hydrazides required 30 mol% NH_4Cl and orthoesters (1.1 equiv) to afford mono 1,3,4-oxadiazoles in high yields (Tables 3.0–3.2). While a strong electron-releasing group such as methoxy (OCH_3) at the para position of the arylhydrazide gave 1,3,4-oxadiazoles in high yield, the opposite was true for an electron-withdrawing group (NO_2). This may be due to an electronic effect, which should exert a greater impact on the carbonyl reactivity from the para position.

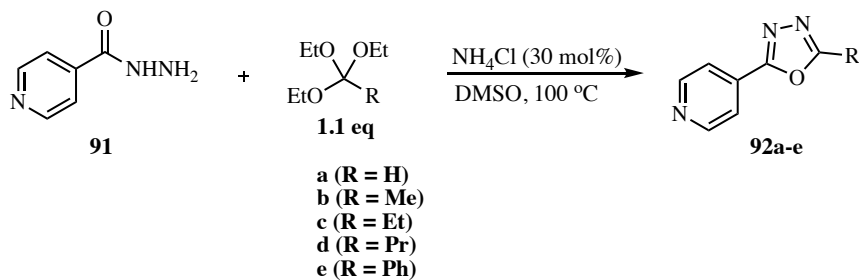
Table 3.0. Summary of 1,3,4-oxadiazoles from substituted arylhydrazide.

Substrate	R	Time (h)	Product	Yield (%)
85	a: H	1.5	87a	92
85	b: Me	10.0	87b	85
85	c: Et	5.0	87c	88
85	d: Pr	4.0	87d	90
85	e: Ph	18.0	87e	78
86	a: H	2.0	88a	94
86	b: Me	10.0	88b	93
86	c: Et	5.5	88c	92
86	d: Pr	5.0	88d	88
86	e: Ph	27.0	88e	80

Table 3.1. Summary of 1,3,4-oxadiazoles from nicotinic acid hydrazide.

Substrate	R	Time (h)	Product	Yield (%)
89	a: H	5.0	90a	96
89	b: Me	28.0	90b	70
89	c: Et	12.0	90c	80
89	d: Pr	26.0	90d	83
89	e: Ph	72.0	90e	80

Table 3.2. Summary of 1,3,4-oxadiazoles from isonicotinic acid hydrazide.



Substrate	R	Time (h)	Product	Yield (%)
91	a: H	24.0	92a	85
91	b: Me	48.0	92b	86
91	c: Et	48.0	92c	85
91	d: Pr	48.0	92d	86
91	e: Ph	72.0	92e	88

2.2.3.1. Conclusions

We have modified the approach from our previous study for the synthesis of bis-1,3,4-oxadiazoles using NH_4Cl as an efficient catalyst. Moreover, the scope of this strategy was broadened for the formation of 4-substituted aryl, nicotinic and isonicotinic 1,3,4-oxadiazoles. The conditions were mild, and thus, compatible with a variety of functional groups. The optimized reaction involved the use of 30 mol% and 60 mol% of NH_4Cl in DMSO for hydrazide and dihydrazide substrates respectively, and in most cases, the yields were high.

2.2.4. Naphthalenes and heterocycles from Morita-Baylis-Hillman (MBH) acetates by domino Michael addition-elimination- $\text{S}_{\text{N}}\text{Ar}$ reactions.

Recent studies in our research group have focused on methodology development which involved a number of domino cyclizations terminated by nucleophilic aromatic substitution reactions.¹²⁸

The current work extends these previous results to the preparation of naphthalene carboxylates and carbonitriles, quinolines, 1,2-dihydroquinolines and 1,2-dihydro-1,8-naphthyridines. Earlier

approaches to the naphthalene framework have been reported.^{129,130} Most recently, Balamurugan and co-workers have developed a process for the synthesis of naphthalenes from *o*-alkynylacetophenone derivatives via tandem acetal formation-intramolecular heteroalkyne metathesis/annulation.¹³¹ Che and co-workers have also reported a method for the synthesis of quinolines and 1,2-dihydroquinolines from aromatic amines and alkynes by a Au(I)-catalyzed tandem hydroamination-hydroarylation under microwave-assisted conditions.¹³² Moreover, Tamariz and co-workers have also developed a process for the regioselective synthesis of 1,2-dihydroquinolines. The method involved a solvent-free MgBr₂-catalyzed reaction between substituted aniline and two ketones.¹³³ Microwave-mediated reactions of 3-aminomethylpyridines with acetylenedicarboxylates have also been reported by Ivachtchenko and co-workers as a novel synthetic route to dihydronaphthyridine and naphthyridine-1-ones.¹³⁴ These protocols yielded modest to good results, but generally subjected substrates to strongly acidic reagents and harsh reaction conditions. Our current reaction provides a straightforward route to these heterocycles in good yields under mild reaction conditions. The target heterocycles are valuable building blocks for the synthesis of drugs used as antibacterial,¹³⁵ antidiabetic¹³⁶ and antioxidant agents¹³⁷ as well as for the treatment of several other medical afflictions.¹³⁸

Formation of the naphthalene and quinoline derivatives resulted from the Michael addition-elimination-S_NAr reaction of active methylene compounds with Morita-Baylis-Hillman (MBH) acetates of 2-fluoro-5-nitrobenzaldehyde and 2-fluoronicotinaldehyde, respectively. Similar reaction of the above-mentioned acetates with primary (1°) alkyl or aromatic amines afforded the respective 1,2-dihydroquinolines and 1,2-dihydro-1,8-naphthyridines. Moreover, an unexpected formation of 4-oxo-1,4-dihydroquinolines was observed from the Michael addition-elimination-S_NAr reaction of 1° amines with MBH acetates of 2,5-difluorobenzaldehyde at high temperature. The MBH reaction was first introduced in 1941 and has since proven to be a valuable source of wide variety of pharmaceutically important scaffolds. As shown in Figure 2.6, synthetic chemists

have dramatically broadened the scope of the MBH reaction through extensive exploitation of its versatility.¹³⁹⁻¹⁴³

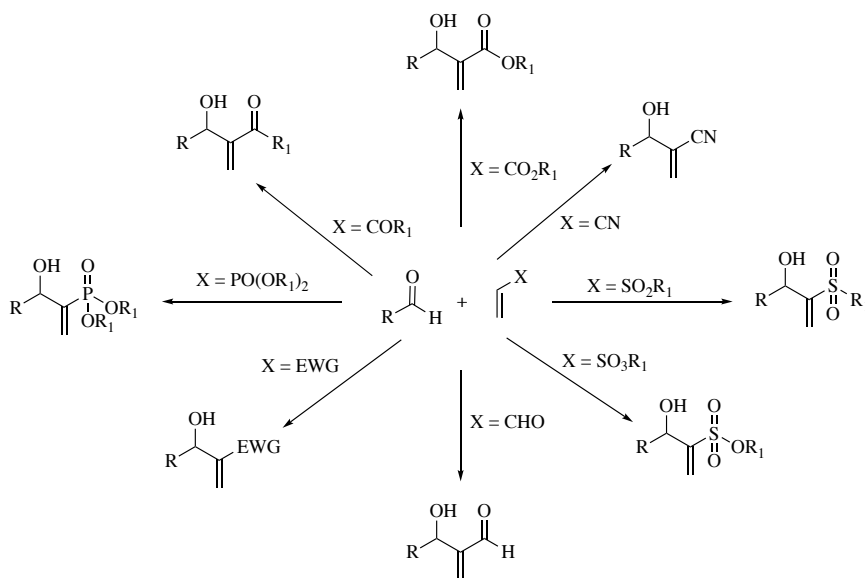


Figure 2.6. Scope of Morita-Baylis-Hillman (MBH) reaction.

The reaction involves a carbon-carbon bond formation between electrophiles and activated alkenes in the presence of a tertiary amine or phosphine catalyst to afford allylic alcohols, also known as MBH adducts or alcohols.^{27, 140-143} Acylation of these adducts gives the MBH acetates which are viable Michael acceptors. Both adducts and acetates have proven to be attractive synthons for building more complex molecular frameworks.¹⁴⁰ A thorough review on the impact and importance of the MBH reaction in medicinal chemistry has been recently reported by Reddy and co-workers.¹⁴¹

The goal of the current study was to provide naphthalene building blocks and other attractive heterocyclic scaffolds from MBH acetates using domino Michael addition-elimination-S_NAr reactions. Naphthalene is the simplest bicyclic aromatic ring, and is frequently found in the molecular frameworks of anticancer agents (Figure 2.7).¹⁴⁴ Earlier approaches to the synthesis of naphthalene-containing molecules involved transition metal catalysts such as PdCl₂, GaCl₃ and

TiCl₄.¹⁴⁵⁻¹⁴⁷ Consequently, some type of special purification procedures were likely required to reduce metal contamination in the final products.

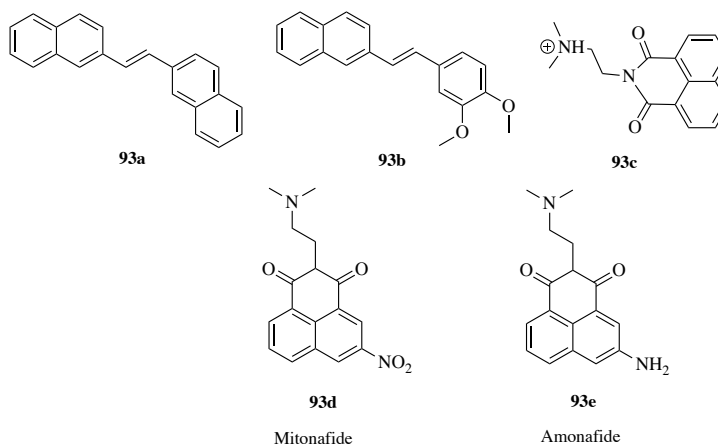
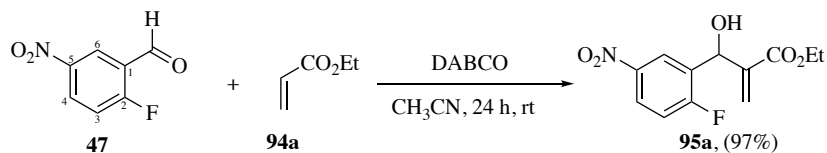


Figure 2.7. Naphthalene-containing anticancer agents.

Our strategy to prepare highly substituted naphthalene derivatives began with the MBH reaction between 2-fluoro-5-nitrobenzaldehyde (**47**) and ethyl acrylate (**94a**) in the presence of 1,4-diazabicyclo[2.2.2]octane (DABCO) to afford the desired MBH alcohol **95a** in excellent yield (Scheme 2.5).

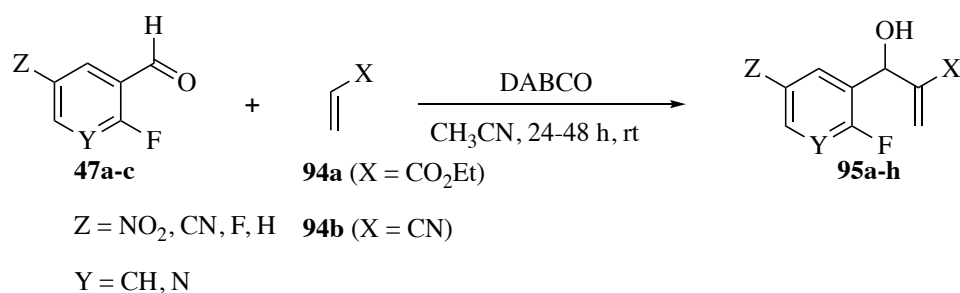


Scheme 2.5. Synthesis of MBH alcohol **95a**.

Initially, the reaction was performed at 23 °C using equimolar amounts of **47**, **94a**, and DABCO. Extractive work-up, followed by ¹H NMR analysis of the product, indicated the presence of **95a** along with some other impurities. A clean conversion to the MBH alcohol was necessary to minimize purification steps enroute to our target naphthalene compounds. Previous methods involved the use of **94a** as a solvent and reactant, however, column chromatography was still required to obtain pure adducts.¹⁴⁸ Moreover, recent studies have shown that the use of a polar aprotic solvent and a slight excess of the activated alkene component affords the MBH adducts in

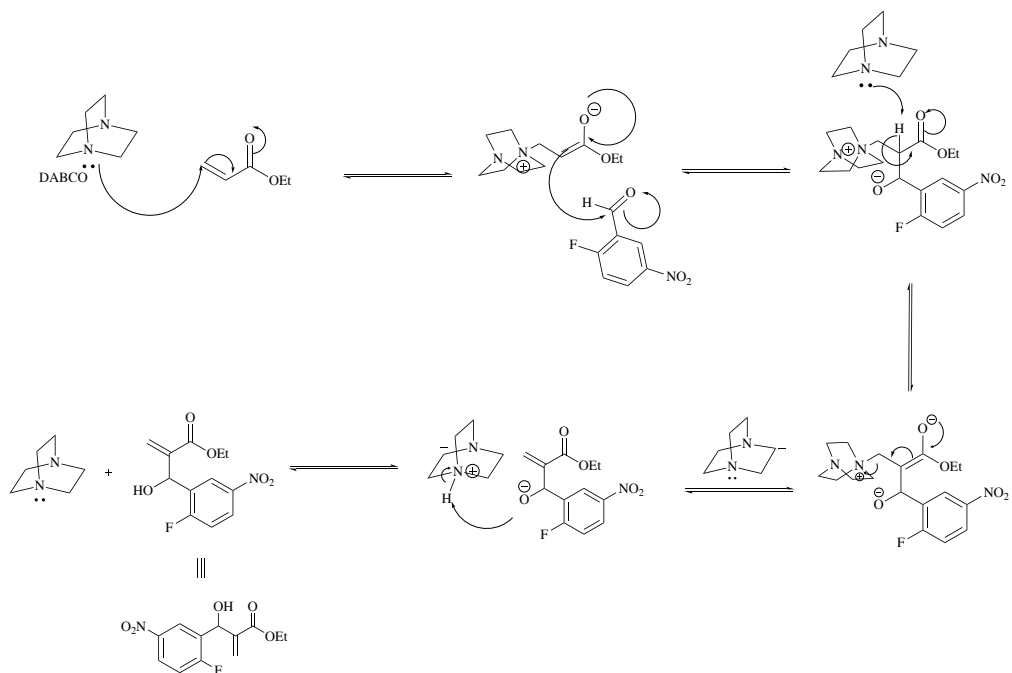
good yield.¹⁴⁹ Therefore, our current strategy involves the use of equimolar equivalents of **47** and **94a** with 1.2 equivalents of DABCO in a polar aprotic solvent (i.e. CH₃CN). In addition, strong electron-withdrawing groups at the C5 position of the aromatic electrophile (Scheme 2.5) proved crucial in maximizing conversion to the corresponding adduct. Moreover, introduction of an electron-withdrawing atom, such as nitrogen in the aromatic ring, also resulted in a similar observation. Encouraged by the success of the reaction between 2-fluoro-5-nitrobenzaldehyde (**47**) and ethyl acrylate (**94a**) to afford adduct **95a**, the scope of the reaction was extended to access new MBH alcohols from their respective electrophiles and activated alkenes in good to excellent yields (Table 3.3).

Table 3.3. Yields for the synthesis of MBH alcohols.



Z	Entry	Alkene	MBH adduct/Yield
NO ₂	Y = CH, 47	94b	95b , (98%)
CN	Y = CH, 47a	94b	95c , (96%)
CN	Y = CH, 47a	94a	95d , (94%)
F	Y = CH, 47b	94b	95e , (92%)
F	Y = CH, 47b	94a	95f , (90%)
H	Y = N, 47c	94b	95g , (88%)
H	Y = N, 47c	94a	95h , (86%)

An extensive review on the mechanism of the MBH reaction has been reported.^{76,142-150} Thus, a plausible mechanism pertaining to our work is demonstrated in Scheme 2.6.



Scheme 2.6. A plausible mechanism for MBH alcohol formation.

In order to successfully access the target naphthalene analogs, the MBH alcohols **95a-h** were converted to their respective acetates **96a-h** (Scheme 2.7 and Figure 2.8).

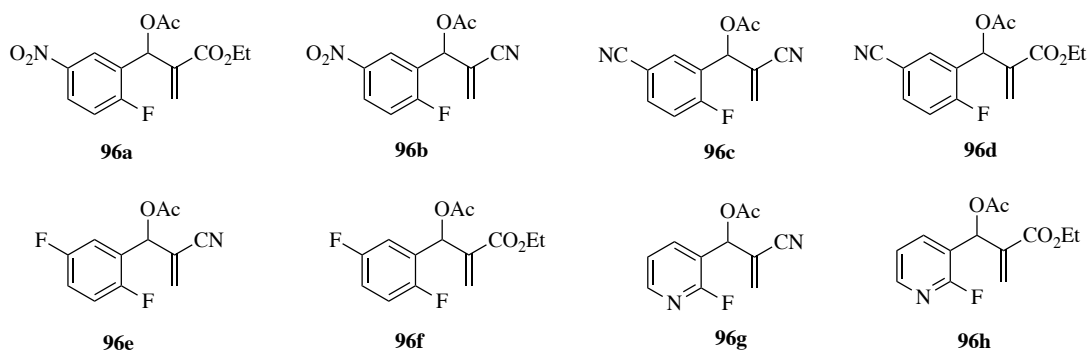
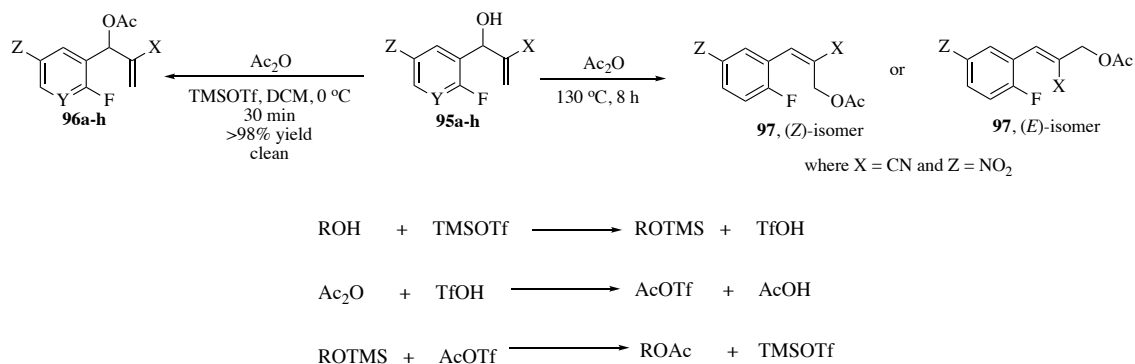


Figure 2.8. Entries of synthesized MBH acetates.

Generally, the MBH acetates are more reactive towards Michael addition-elimination reactions than their alcohol counterparts. Common acylation procedures involved the utilization of acetyl

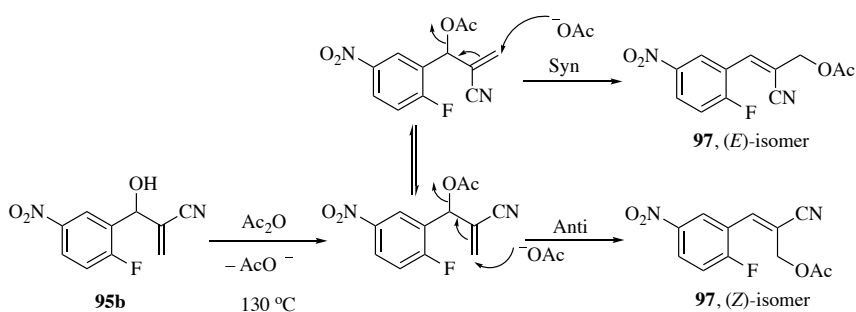
chloride or acetic anhydride in dichloromethane with pyridine as a base.¹³⁹⁻¹⁴⁸ Current esterification strategy for our study involved the use of 1.5 mmol of acetic anhydride (for 1 mmol of MBH alcohol) in the presence of a catalytic amount of trimethylsilyl trifluoromethanesulfonate (TMSOTf, 1 M; 20 μ L).¹⁵¹ The optimum condition for this reaction proved to be dichloromethane at 0 °C and afforded quantitative yields of the desired MBH acetates in 30 minutes (Scheme 2.7). However, MBH alcohols derived from 2-fluoronicotinaldehyde required stoichiometric amounts (6 equivalents) of the TMSOTf catalyst added portionwise over 1 h. In this reaction, nitrogen in the aromatic ring may be nucleophilic enough to react with the TMSOTf. A plausible reaction mechanism for the acylation process is shown in Scheme 2.7.



Scheme 2.7. Results and plausible mechanism for esterification process.

The MBH alcohol reacts with TMSOTf to give the TMS-ether (ROTMS) and triflic acid (TfOH). The latter further reacts with the acetic anhydride to form an active acylating species (AcOTf), which could possibly be a mixed anhydride or the acylium ion. Reaction of the active species with the TMS-ether gives the target ester compound, regenerating the TMSOTf catalyst which reenters the catalytic cycle. The silicon is thought to play a crucial role in the last step by forming a pentacoordinate silicon species which could potentially facilitate the remarkable reaction rate.¹⁵¹ Consequently, all MBH acetates **96a-h** (Figure 2.8) were furnished in >98% yields after extractive work-up without further purification.

Conversely, refluxing MBH alcohol **95b** in acetic anhydride for 8 h afforded an unexpected product **97** (Scheme 2.7), which could result from a possible allylic inversion process on the supposed MBH acetate due to high temperature. Two isomers (*Z* or *E*) were initially considered as possible outcomes for **97** (Scheme 2.7). However, the ¹H NMR indicated the presence of only one isomer, thus an X-ray crystallographic analysis will be required to determine the absolute stereochemistry of the product. An allylic inversion is a type of bimolecular nucleophilic substitution (S_N2') which involves a Michael addition of a nucleophile (OAc) at the allylic double-bond carbon to eliminate a leaving group, all in a single step. Usually, this reaction goes with *syn*¹⁵² arrangement of the nucleophile and leaving group which, in this case, should afford the *E*-isomer. However, *anti*¹⁵³ arrangement could also occur to give the *Z*-isomer (Scheme 2.8).



Scheme 2.8. Plausible mechanisms for Michael addition-elimination (S_N2').

Our target naphthalene compounds **98a-c** were synthesized *via* a domino Michael addition-elimination-S_NAr reaction from **96b** and active methylene compounds, e.g. ethyl cyanoacetate, ethyl nitroacetate and methyl phenylsulfonylacetate (Figure 2.9). The reaction proceeded at room temperature in the presence of K₂CO₃ in 1 mL of DMF to afford the desired products in good yields after extractive work-up, followed by silica gel column chromatography. Initially, the reaction was anticipated to give dihydronaphthalenes, however, the elimination of nontraditional leaving groups such as CO₂Et, SO₂Ph and NO₂ afforded the aromatic naphthalene analogs. Although SO₂Ph and NO₂ are reasonable leaving groups, CO₂Et is a relatively rare one. However, there are precedents for the elimination of CO₂Et,¹⁵⁴ SO₂Ph¹⁵⁵ and NO₂.¹⁵⁶ A similar observation

was made when MBH acetate **96h** reacted with active methylene compounds under the same conditions (Figure 2.9). Quinoline derivatives **99a** and **99b** were formed instead of their dihydro analogs. A possible mechanism to these aromatic products is shown in Scheme 2.9.

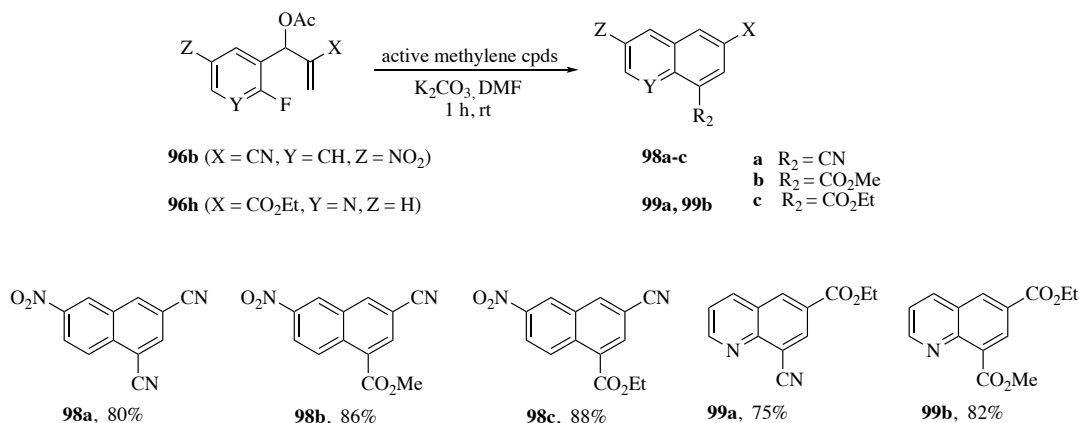
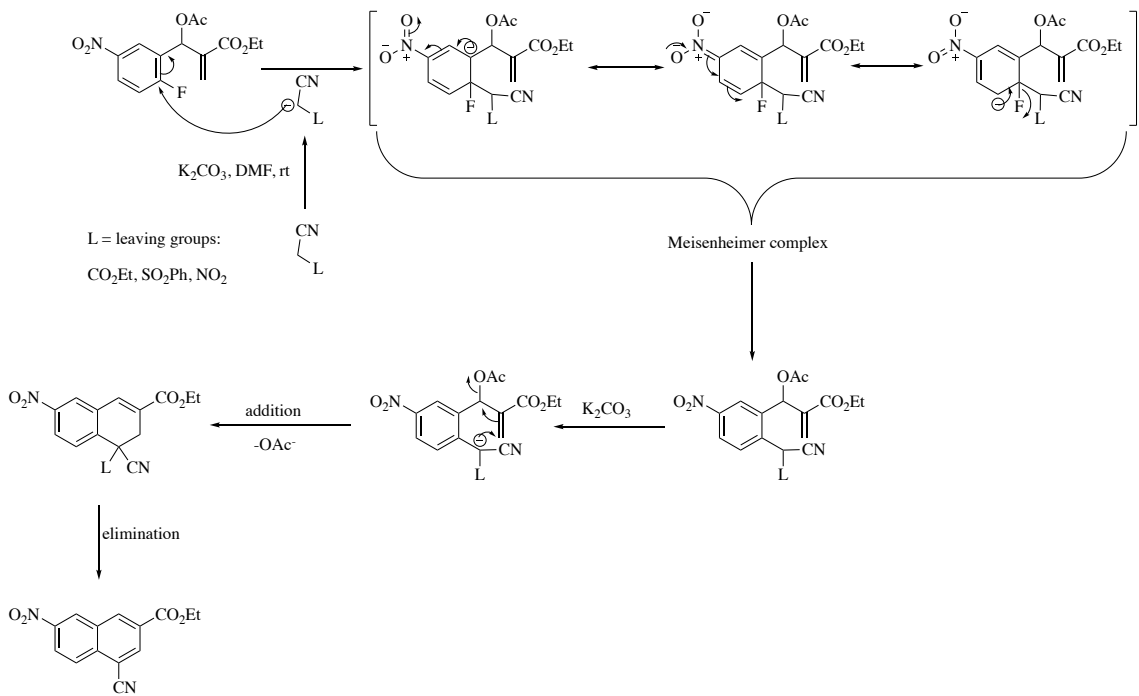


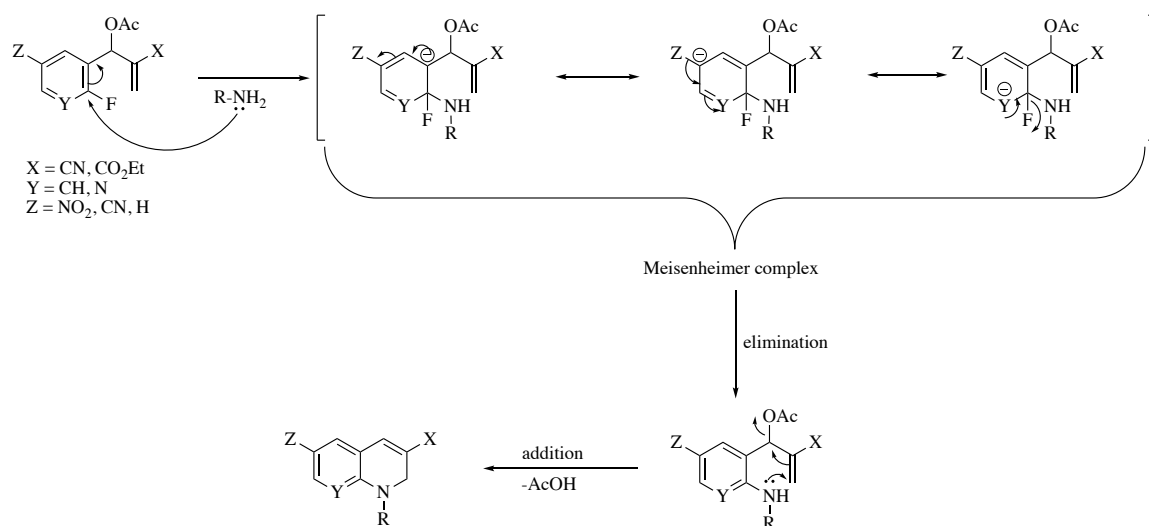
Figure 2.9. Entries of synthesized naphthalene and quinoline derivatives.



Scheme 2.9. A Possible mechanism to aromatic compounds.

The strong electron-withdrawing NO₂ group para to fluoride (F⁻) on the aromatic ring activates the ring towards a nucleophilic aromatic substitution (S_NAr). Thus, the active methylene compound would first add to the ring resulting in a formation of a NO₂-stabilized carbanion called a Meisenheimer complex (Scheme 2.9). Typically, the addition step is the rate determining (or slowest) step as aromaticity is lost, and thus the energy barrier is very high. However, since fluorine has a high negative inductive effect due to its electronegativity, resonance stabilization of the Meisenheimer complex is enhanced. Thus, the activation barrier of the addition step is lowered for addition to occur a bit faster. Subsequent elimination of the F⁻ ion restores aromaticity while Michael addition leads to the formation of the dihydro intermediate, which upon elimination of the leaving group, results in the target aromatic product (Scheme 2.9).

Encouraged by the success of the aromatic products, we forged on to synthesize analogs of 1,2-dihydroquinoline **100a-e**, **101a-c** and **102a,e,f** and 1,2-dihydro-1,8-naphthyridine **103b,e** by reacting the MBH acetates **96b-d,g** with excess of alkyl or aryl amines in 1 mL DMF at 50 °C for 4 h (Figure 3.0). The product was formed with or without the addition of K₂CO₃. Subsequently, extractive work-up, followed by column chromatography, afforded the target compounds in good yields. A plausible mechanism to these dihydroheteroaromatics is also shown in Scheme 3.0.



Scheme 3.0. Possible mechanism to dihydroheteroaromatics.

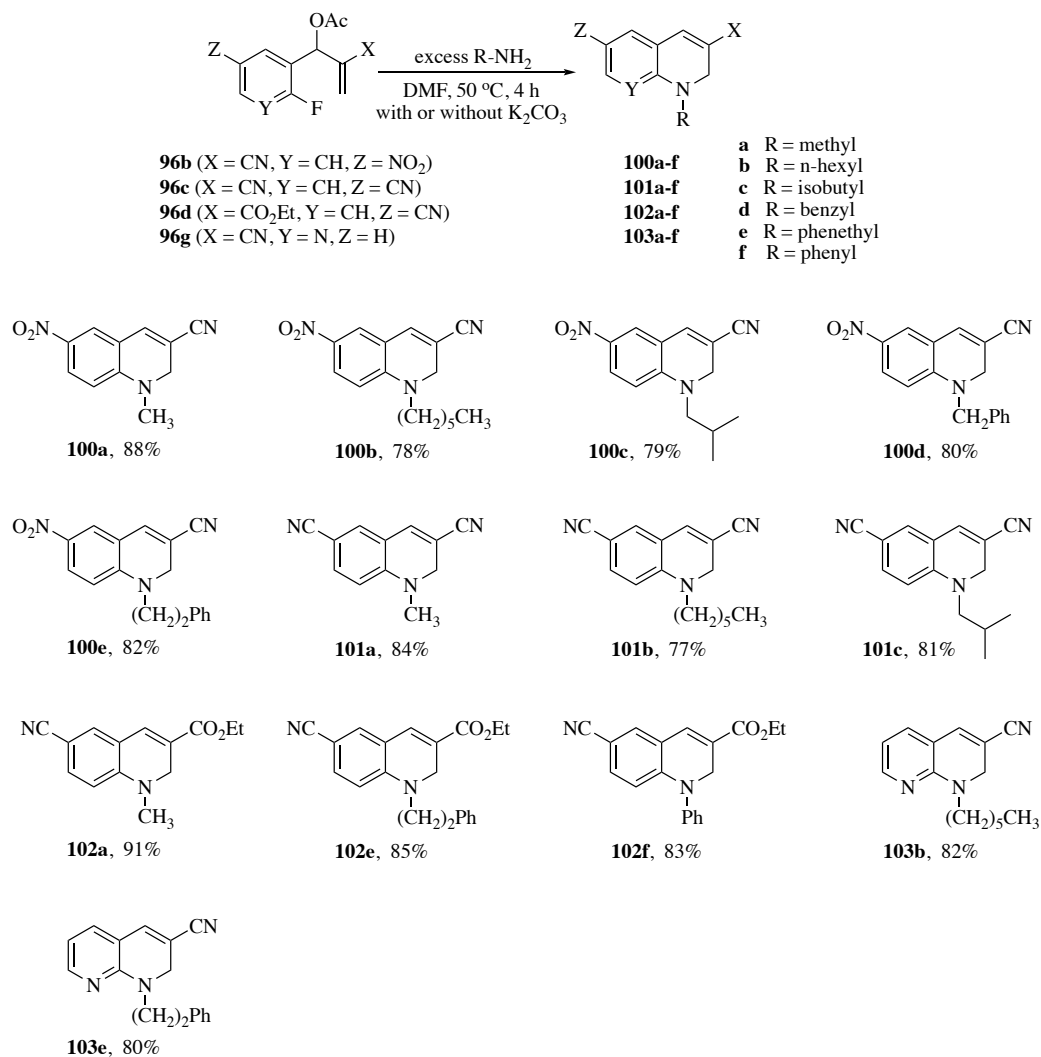
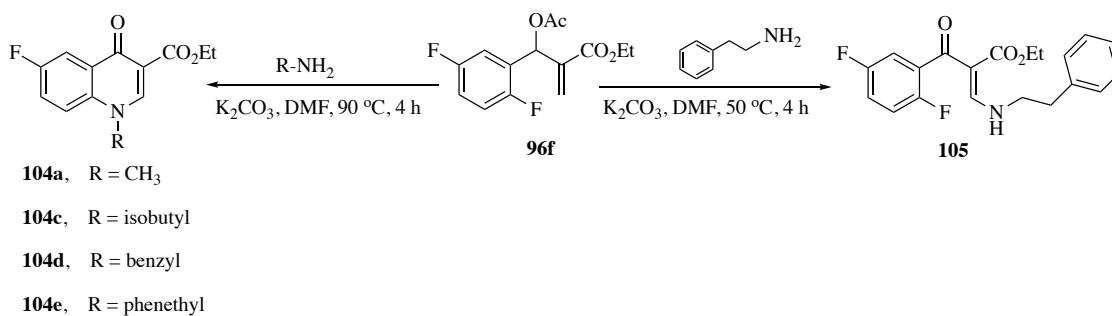


Figure 3.0. Entries of synthesized dihydroheteroaromatics.

Conversely, an unexpected outcome was observed when acetate **96f** reacted with phenethylamine in 1 mL DMF in the presence of K₂CO₃ at 90 °C. An oxidation product, ethyl 6-fluoro-4-oxo-1-phenylethyl-1,4-dihydroquinoline-3-carboxylate (**104e**) was obtained after extractive work-up, followed by trituration with 5% ether/pentane (Scheme 3.1). X-ray analysis of a crystal of this product confirmed the structure (Figure 3.1). Since the reaction was run under nitrogen for the most part, the source of oxygen required to facilitate the oxidation process is unknown. However, this reaction could offer an efficient synthetic route to ciprofloxacin (a fluoroquinolone antibiotic) as well as other related bioactive structures (Scheme 3.2). Moreover, the 2,5-difluoro aromatic

ring is not as activating, thus the S_NAr reaction could possibly precede the conjugate Michael addition only at a higher temperature. This analogy was further confirmed when the reaction was performed at 50 °C to give an uncyclized ethyl-2-(2,5-difluorobenzoyl) acrylate **105** as shown in Scheme 3.1. Although the S_NAr reaction did not occur for obvious reasons, the conjugate addition and oxidation steps still proceeded to give the uncyclized product. The result seems to show that the Michael addition occurs first at a lower temperature.



Scheme 3.1. Unexpected synthesis of 4-oxo-1,4-dihydroquinolines.

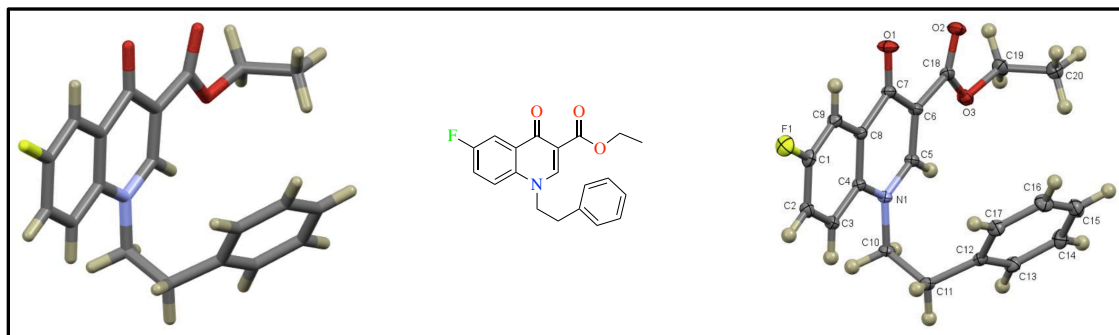
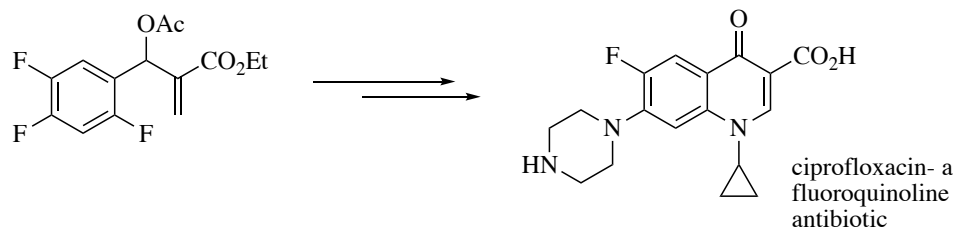


Figure 3.1. X-ray of ethyl 6-fluoro-4-oxo-1-phenylethyl-1,4-dihydroquinoline-3-carboxylate (**104e**).



Scheme 3.2. Possible extension to fluoroquinolone antibiotics.

2.2.4.1. Conclusions

We have studied the formation of naphthalenes and a wide range of heterocyclic compounds from Morita-Baylis-Hillman (MBH) acetates by a domino Michael addition-elimination-S_NAr reaction. The MBH acetates were prepared in quantitative yields under mild conditions without allylic rearrangement. The use of TMSOTf as a catalyst facilitated the acylation process to give unrearranged product in quantitative yield in 30 minutes. The reaction of MBH acetates with active methylene compounds involved the elimination of several nontraditional leaving groups to afford naphthalenes and quinolines. Reaction with 1° alkyl or aromatic amines afforded the dihydroheteroaromatic compounds in good yields. These heterocycles include dihydroquinolines and dihydronaphthyridines. In all cases, the target naphthalene and heterocycle were formed in high yields. In addition, difluorosubstituted MBH acetates reacted with alkyl or aryl amines at higher temperature to afford 4-oxo-1,4-dihydroquinolines upon efficient oxidation. These oxidation products still formed in good yields even after all controls to exclude oxygen from the reaction system were performed. While the mechanism for this reaction is unclear, these 4-oxo-1,4-dihydroquinolines are reminiscent of fluoroquinolone antibiotics and other related active compounds.

2.3. Chemistry

General Methods: All reactions were run under dry nitrogen in oven-dried glassware. Reactions were monitored by thin layer chromatography on silica gel GF plates (Analtech, No. 21521). Preparative separations were performed by one of the following methods: (1) preparative thin layer chromatography (PTLC) on 20-cm × 20-cm silica gel GF plates (Analtech, No. 02015) or (2) column chromatography on silica gel (grade 62, 60–200 mesh) containing UV-active phosphor (Sorbent Technologies, No. UV-05) packed into quartz columns. Band elution for all chromatographic methods was monitored using a hand-held UV lamp. Melting points were

uncorrected. FT-IR spectra were run as thin films on NaCl disks or as nujol mulls. Unless otherwise indicated, ^1H and ^{13}C NMR spectra were measured in CDCl_3 using $(\text{CH}_3)_4\text{Si}$ as the internal standard; coupling constants (J) are given in Hertz. Low-resolution mass spectra (electron impact/direct probe) were obtained at 70 eV. Elemental analyses ($\pm 0.4\%$) were performed by Atlantic Microlabs, Inc., Norcross, GA 30071.

2.3.1. 1-Aryl-5-nitro-1*H*-indazoles and a general sequential route to 1-aryl-1*H*-indazoles.

Indazoles from 2'-fluoro-5'-nitroacetophenone (46) or 2-fluoro-5-nitrobenzaldehyde (47) with $\text{NH}_2\text{NH}_2 \cdot \text{H}_2\text{O}$.

To a stirred solution of **46** or **47** (1.0 mmol) in DMF (5 mL) at 23 °C was added $\text{NH}_2\text{NH}_2 \cdot \text{H}_2\text{O}$ (3.0 mmol for **46**, 2.0 mmol for **47**). The solution was stirred at 23 °C for 2 h at which time TLC (20% EtOAc in hexanes) indicated complete consumption of the starting carbonyl compound. The crude mixture was added to water and extracted with EtOAc (2×15 mL). The combined organic layers were washed with water and saturated aq NaCl, dried (MgSO_4), filtered, and concentrated under vacuum to give the pure indazole products.

3-Methyl-5-nitro-1*H*-indazole (48). Yield: 173 mg (0.98 mmol, 98%) as a yellow solid; m.p. 213-214 °C; IR: 1517, 1332 cm^{-1} ; ^1H NMR ($\text{DMSO}-d_6$): δ 13.1 (br s, 1H), 8.79 (s, 1H), 8.18 (d, $J = 9.1$ Hz, 1H), 7.64 (d, $J = 9.1$ Hz, 1H), 2.59 (s, 3H); ^{13}C NMR ($\text{DMSO}-d_6$): δ 145.4, 143.1, 141.3, 121.9, 121.3, 118.8, 111.2, 12.1; MS: m/z 177 (M^+). Anal. Calcd for $\text{C}_8\text{H}_7\text{N}_3\text{O}_2$: C, 54.24; H, 3.98; N, 23.72. Found: C, 54.29; H, 4.01; N, 23.59.

5-Nitro-1*H*-indazole (49). Yield: 147 mg (0.90 mmol, 90%) as a tan solid; m.p. 207-208 °C; IR: 1534, 1341 cm^{-1} ; ^1H NMR ($\text{DMSO}-d_6$): δ 13.7 (br s, 1H), 8.84 (s, 1H), 8.41 (s, 1H), 8.19 (d, $J = 9.0$ Hz, 1H), 7.74 (d, $J = 9.0$ Hz, 1H); ^{13}C NMR ($\text{DMSO}-d_6$): δ 142.3, 142.0, 137.2, 122.5, 121.3, 119.3, 111.5; MS: m/z 163 (M^+). Anal. Calcd for $\text{C}_7\text{H}_5\text{N}_3\text{O}_2$: C, 51.54; H, 3.09; N, 25.76. Found: C, 51.85; H, 3.15; N, 25.54.

Indazoles from 46 or 47 with ArNHNH₂·HCl. Method A. Representative two-step procedure.

To a stirred solution of the carbonyl compound (1.0 mmol) in DMF (5 mL) at 50 °C (oil bath) was added ArNHNH₂·HCl (3.0 mmol for **46**, 2.0 mmol for **47**) and the solution was stirred until TLC (20% EtOAc in hexanes) indicated complete conversion (ca 2 h). The crude reaction mixture was added to water and extracted with EtOAc (2 × 15 mL). The combined organic layers were washed with water and saturated aq NaCl, dried (MgSO₄), filtered, and concentrated under vacuum to give the crude hydrazones. The crude products were stirred with 20% ether/pentane for 1 h, filtered and dried to give arylhydrazones **50** and **51**. Characterization data for these materials are given in the ESI.

To a stirred solution of the arylhydrazone (1.00 mmol) in DMF (5 mL) at 90 °C (oil bath) was added anhydrous K₂CO₃ (3.0 mmol) and the mixture was stirred for the time indicated in Table 1. The reaction mixture was added to water, extracted with EtOAc, dried (MgSO₄), filtered, and concentrated under vacuum to afford the crude product. Indazoles from **46** were stirred with 20% ether in pentane, filtered and dried, while those from **47** were purified by silica gel chromatography on a 20 cm × 2 cm column eluted with increasing concentrations of EtOAc in hexanes. Yields as well as physical and spectral data are given below.

Indazoles from 46 or 47 with ArNHNH₂·HCl. Method B. Representative one-pot procedure.

To a stirred solution of the carbonyl compound (1.0 mmol) in DMPU (5 mL) were added powdered 4Å molecular sieves (30 wt% relative to the carbonyl substrate), ArNHNH₂·HCl (3.0 mmol for **46**, 2.0 mmol for **47**), and K₂CO₃ (3.0 mmol for **46**, 2.0 mmol for **47**). For **46**, all reagents were placed in the flask and heated to 90 °C; for **47**, the hydrazone was allowed to form at 90 °C (1.5 h) before K₂CO₃ was added. The reaction was stirred at 90 °C for the time indicated in Table 2.2. Workup was performed as described in Method A.

3-Methyl-1-phenyl-5-nitro-1*H*-indazole (52a). Yield: 240 mg, (0.95 mmol, 95%) as a brown solid; m.p. 115-117 °C; IR: 1516, 1336 cm⁻¹; ¹H NMR (DMSO-*d*₆): δ 8.89 (d, *J* = 2.2 Hz, 1H), 8.28 (dd, *J* = 9.3, 2.2 Hz, 1H), 7.93 (d, *J* = 9.3 Hz, 1H), 7.77 (d, *J* = 7.8 Hz, 2H), 7.62 (t, *J* = 7.7 Hz, 2H), 7.46 (t, *J* = 7.4 Hz, 1H), 2.69 (s, 3H); ¹³C NMR (DMSO-*d*₆): δ 147.3, 142.2, 141.1, 139.2, 130.3, 127.8, 124.4, 122.9, 122.8, 119.3, 111.7, 12.1; MS: m/z 253 (M⁺). Anal. Calcd for C₁₄H₁₁N₃O₂: C, 66.40; H, 4.38; N, 16.59. Found: C, 66.33; H, 4.34; N, 16.42.

1-(2-Methoxyphenyl)-3-methyl-5-nitro-1*H*-indazole (52b). Yield: 232 mg (0.82 mmol, 82%) as a light brown solid; m.p. 128-130 °C; IR: 2838, 1519, 1338 cm⁻¹; ¹H NMR (DMSO-*d*₆): δ 8.86 (s, 1H), 8.21 (d, *J* = 9.3 Hz, 1H), 7.55 (t, *J* = 8.0 Hz, 1H), 7.49 (d, *J* = 7.8 Hz, 1H), 7.38-7.28 (overlapping signals, 2H), 7.16 (t, *J* = 7.7 Hz, 1H), 3.78 (s, 3H), 2.66 (s, 3H); ¹³C NMR (DMSO-*d*₆): δ 154.0, 146.6, 143.0, 141.9, 130.8, 128.6, 127.1, 123.2, 122.0, 121.4, 119.0, 113.4, 112.2, 56.2, 12.1; MS: m/z 283 (M⁺). Anal. Calcd for C₁₅H₁₃N₃O₃: C, 63.60; H, 4.63; N, 14.83. Found: C, 63.49; H, 4.61; N, 14.88.

1-(3-Methoxyphenyl)-3-methyl-5-nitro-1*H*-indazole (52c). Yield: 229 g (0.81 mmol, 81%) as a light brown solid; m.p. 105-106 °C; IR: 2836, 1518, 1338 cm⁻¹; ¹H NMR (DMSO-*d*₆): δ 8.90 (s, 1H), 8.29 (d, *J* = 9.3 Hz, 1H), 7.96 (d, *J* = 9.3 Hz, 1H), 7.52 (t, *J* = 8.1 Hz, 1H), 7.34 (d, *J* = 8.1 Hz, 1H), 7.28 (s, 1H), 7.04 (d, *J* = 8.3 Hz, 1H); ¹³C NMR (DMSO-*d*₆): δ 160.6, 147.3, 142.3, 141.2, 140.3, 131.2, 124.4, 122.9, 119.3, 114.9, 113.7, 111.9, 108.6, 56.0, 12.1; MS: m/z 283 (M⁺). Anal. Calcd for C₁₅H₁₃N₃O₃: C, 63.60; H, 4.63; N, 14.83. Found: C, 63.52; H, 4.55; N, 14.71.

1-(4-Methoxyphenyl)-3-methyl-5-nitro-1*H*-indazole (52d). Yield: 266 mg (0.94 mmol, 94%) as a tan solid; m.p. 159-160 °C. IR: 2836, 1514, 1346 cm⁻¹; ¹H NMR (DMSO-*d*₆): δ 8.88 (d, *J* = 2.2 Hz, 1H), 8.26 (dd, *J* = 9.3, 2.2 Hz, 1H), 7.79 (d, *J* = 9.3 Hz, 1H), 7.65 (d, *J* = 8.1 Hz, 2H), 7.15 (d, *J* = 8.1 Hz, 2H), 3.85 (s, 3H), 2.69 (s, 3H); ¹³C NMR (DMSO-*d*₆): δ 158.9, 146.7, 142.0, 141.2, 132.2, 124.8, 123.9, 122.5, 119.3, 115.3, 111.4, 56.0, 12.1; MS: m/z 283 (M⁺). Anal. Calcd for C₁₅H₁₃N₃O₃: C, 63.60; H, 4.63; N, 14.83. Found: C, 63.57; H, 4.60; N, 14.76.

1-(4-Bromophenyl)-3-methyl-5-nitro-1*H*-indazole (52e). Yield: 314 mg, (0.95 mmol, 95%) as a tan solid; m.p. 202-203 °C; IR: 1512, 1345 cm⁻¹; ¹H NMR (DMSO-*d*₆): δ 8.90 (d, *J* = 2.2 Hz, 1H), 8.31 (dd, *J* = 9.2, 2.2 Hz, 1H), 7.96 (d, *J* = 9.2 Hz, 1H), 7.80 (d, *J* = 8.8 Hz, 2H), 7.75 (d, *J* = 8.8 Hz, 2H), 2.69 (s, 3H); ¹³C NMR (DMSO-*d*₆): δ 147.7, 142.4, 141.1, 138.5, 133.1, 124.7, 124.6, 123.0, 120.1, 119.3, 111.8, 12.1; MS: m/z 331 (M⁺). Anal. Calcd for C₁₄H₁₀BrN₃O₂: C, 50.62; H, 3.03; N, 12.65. Found: C, 50.44; H, 2.99; N, 12.73.

1-(3-Chlorophenyl)-3-methyl-5-nitro-1*H*-indazole (52f). Yield: 250 mg, (0.87 mmol, 87%) as a tan solid; m.p. 135-136 °C; IR: 1517, 1339 cm⁻¹; ¹H NMR (DMSO-*d*₆): δ 8.89 (d, *J* = 2.2 Hz, 1H), 8.31 (dd, *J* = 9.3, 2.2 Hz, 1H), 7.98 (d, *J* = 9.3 Hz, 1H), 7.83 (t, *J* = 2.2 Hz, 1H), 7.78 (d, *J* = 8.4 Hz, 1H), 7.64 (t, *J* = 8.1 Hz, 1H), 7.52 (d, *J* = 8.0 Hz, 1H), 2.69 (s, 3H); ¹³C NMR (DMSO-*d*₆): δ 146.8, 141.1, 139.3, 133.4, 130.8, 126.4, 123.6, 122.0, 121.4, 120.1, 118.2, 110.9; MS: m/z 287 (M⁺). Anal. Calcd for C₁₄H₁₀ClN₃O₂: C, 58.45; H, 3.50; N, 14.61. Found: C, 58.58; H, 3.59; N, 14.53.

1-(4-Chlorophenyl)-3-methyl-5-nitro-1*H*-indazole (52g). Yield: 267 mg (0.93 mmol, 93%) as a tan solid; m.p. 217-218 °C; IR: 1511, 1339 cm⁻¹; ¹H NMR (DMSO-*d*₆): δ 8.91 (d, *J* = 2.2 Hz, 1H), 8.31 (dd, *J* = 9.3, 2.2 Hz, 1H), 7.95 (d, *J* = 9.3 Hz, 1H), 7.82 (d, *J* = 8.7 Hz, 2H), 7.67 (d, *J* = 8.7 Hz, 2H), 2.69 (s, 3H); ¹³C NMR (DMSO-*d*₆): δ 147.7, 142.4, 141.1, 138.1, 131.8, 130.2, 124.6, 124.5, 123.0, 119.4, 111.8, 12.1; MS: m/z 287 (M⁺). Anal. Calcd for C₁₄H₁₀ClN₃O₂: C, 58.45; H, 3.50; N, 14.61. Found: C, 58.42; H, 3.49; N, 14.48.

1-(2,4-Dichlorophenyl)-3-methyl-5-nitro-1*H*-indazole (52h). Yield: 257 mg (0.80 mmol, 80%); m.p. 144-145 °C; IR: 1516, 1338 cm⁻¹; ¹H NMR (DMSO-*d*₆): δ 8.92 (d, *J* = 2.1 Hz, 1H), 8.27 (dd, *J* = 9.2, 2.1 Hz, 1H), 8.01 (d, *J* = 2.2 Hz, 1H), 7.74 (d, *J* = 8.5 Hz, 1H), 7.69 (dd, *J* = 8.5, 2.2 Hz, 1H), 7.44 (d, *J* = 9.2 Hz, 1H), 2.68 (s, 3H); ¹³C NMR (DMSO-*d*₆): δ 147.5, 143.1, 142.4, 135.3, 135.0, 132.0, 131.5, 130.7, 129.3, 123.5, 122.8, 119.3, 111.6, 12.1; MS: m/z 321 (M⁺). Anal. Calcd for C₁₄H₉Cl₂N₃O: C, 52.20; H, 2.82; N, 13.04. Found: C, 52.11; H, 2.91; N, 13.09.

3-Methyl-5-nitro-1-(3-(trifluoromethyl)phenyl)-1H-indazole (52i). Yield: 282 mg (0.88 mmol, 88%) as a white solid; m.p. 112-113 °C; IR: 1520, 1339 cm⁻¹; ¹H NMR (DMSO-*d*₆): δ 8.90 (s, 1H), 8.32 (d, *J* = 9.3 Hz, 1H), 8.13 (d, *J* = 7.8 Hz, 1H), 8.07 (s, 1H), 7.99 (d, *J* = 9.3 Hz, 1H), 7.90-7.77 (complex, 2H), 2.70 (s, 3H); ¹³C NMR (DMSO-*d*₆): δ 148.0, 142.5, 141.1, 139.8, 131.6, 130.9 (q, *J* = 32.6 Hz), 126.2, 124.8, 124.2 (q, *J* = 272.6 Hz), 124.0 (q, *J* = 6.7 Hz), 123.1, 119.2 (2C), 111.8, 12.0; MS: *m/z* 321 (M⁺). Anal. Calcd for C₁₅H₁₀F₃N₃O₂: C, 56.08; H, 3.14; N, 13.08. Found: C, 56.02; H, 3.18; N, 13.11.

3-Methyl-5-nitro-1-(4-(trifluoromethyl)phenyl)-1H-indazole (52j). Yield: 225 mg, (0.70 mmol, 70%) as a white solid; m.p. 167-168 °C; IR: 1525, 1331 cm⁻¹; ¹H NMR (DMSO-*d*₆): δ 8.89 (d, *J* = 2.2 Hz, 1H), 8.31 (dd, *J* = 9.3, 2.2 Hz, 1H), 8.05 (d, *J* = 9.3 Hz, 1H), 8.02 (d, *J* = 8.6 Hz, 2H), 7.95 (d, *J* = 8.6 Hz, 2H), 2.69 (s, 3H); ¹³C NMR (DMSO-*d*₆): δ 148.3, 142.6, 142.3, 141.1, 127.4 (q, *J* = 4.0 Hz), 127.1, 125.1, 124.5 (q, *J* = 269.1 Hz), 123.2, 122.6, 119.2, 112.0, 12.1; MS: *m/z* 321 (M⁺). Anal. Calcd for C₁₅H₁₀F₃N₃O₂: C, 56.08; H, 3.14; N, 13.08. Found: C, 55.98; H, 3.19; N, 13.04.

1-(4-Cyanophenyl)-3-methyl-5-nitro-1H-indazole (52k). Yield: 222 mg (0.80 mmol, 80%) as a brown solid; m.p. ≥194 °C (sub), ≥260 °C (dec); IR: 2226, 1516, 1338 cm⁻¹; ¹H NMR (DMSO-*d*₆): δ 8.93 (d, *J* = 2.2 Hz, 1H), 8.35 (dd, *J* = 9.1, 2.2 Hz, 1H), 8.11 (d, *J* = 9.1 Hz, 1H), 8.08 (d, *J* = 8.9 Hz, 2H), 8.04 (d, *J* = 8.9 Hz, 2H), 2.71 (s, 3H); ¹³C NMR (DMSO-*d*₆): δ 148.7, 142.8, 142.7, 141.1, 134.5, 125.3, 123.3, 122.6, 119.3, 118.9, 112.3, 109.4, 12.1; MS: *m/z* 278 (M⁺). Anal. Calcd for C₁₅H₁₀N₄O₂: C, 64.74; H, 3.62; N, 20.13. Found: C, 64.69; H, 3.67; N, 20.06.

4-(3-Methyl-5-nitro-1H-indazol-1-yl)benzenesulfonamide (52l). Yield: 1249 mg (0.75 mmol, 75%); m.p. 265-266 °C; IR: 3422, 1515, 1331, 1320, 1123 cm⁻¹; ¹H NMR (DMSO-*d*₆): δ 8.92 (d, *J* = 2.2 Hz, 1H), 8.34 (dd, *J* = 9.3, 2.2 Hz, 1H), 8.09 (d, *J* = 9.3 Hz, 1H), 8.04 (d, *J* = 8.4 Hz, 2H), 8.01 (d, *J* = 8.4 Hz, 2H), 7.51 (s, 2H), 2.71 (s, 3H); ¹³C NMR (DMSO-*d*₆): δ 148.2, 142.54, 145.50, 141.6, 141.0, 127.9, 125.0, 123.1, 122.3, 119.2, 112.0, 12.0; MS: *m/z* 332 (M⁺). Anal. Calcd for C₁₄H₁₂N₄O₄S: C, 50.60; H, 3.64; N, 16.86. Found: C, 50.70; H, 3.63; N, 16.78.

4-(3-Methyl-5-nitro-1H-indazol-1-yl)benzoic acid (52m). Yield: 208 mg (0.70 mmol, 70%) as a tan solid; m.p. ≥ 240 °C (sub), ≥ 320 °C (dec). IR: 3441-2352, 1697, 1514, 1346 cm^{-1} ; ^1H NMR (DMSO- d_6): δ 12.8 (br s, 1H), 8.93 (d, $J = 2.2$ Hz, 1H), 8.34 (dd, $J = 9.3, 2.2$ Hz, 1H), 8.16 (d, $J = 8.6$ Hz, 2H), 8.09 (d, $J = 9.3$ Hz, 1H), 7.95 (d, $J = 8.6$ Hz, 2H), 2.71 (s, 3H); ^{13}C NMR (DMSO- d_6): δ 167.1, 148.2, 142.6, 142.5, 141.1, 131.5, 125.0, 123.1, 122.0, 119.4, 119.3, 112.2, 12.1; MS: m/z 297 (M^+). Anal. Calcd for $\text{C}_{15}\text{H}_{11}\text{N}_3\text{O}_4$: C, 60.61; H, 3.73; N, 14.14. Found: C, 60.53; H, 3.68; N, 14.22.

1-Phenyl-5-nitro-1H-indazole (53a). Yield: 172 mg (0.72 mmol, 72%) as a tan solid; m.p. 169-170 °C; IR: 1534, 1341 cm^{-1} ; ^1H NMR (DMSO- d_6): δ 8.95 (s, 1H), 8.70 (s, 1H), 8.30 (d, $J = 9.3$ Hz, 1H), 7.98 (d, $J = 9.3$ Hz, 1H), 7.81 (d, $J = 7.9$ Hz, 2H), 7.65 (d, $J = 7.7$ Hz, 2H), 7.51 (t, $J = 7.4$ Hz, 1H); ^{13}C NMR (DMSO- d_6): δ 142.8, 140.5, 139.1, 138.9, 130.3, 128.2, 124.8, 123.3, 122.7, 119.9, 111.9; MS: m/z 239 (M^+). Anal. Calcd for $\text{C}_{13}\text{H}_9\text{N}_3\text{O}_2$: C, 65.27; H, 3.79; N, 17.56. Found: C, 65.16; H, 3.77; N, 17.57.

1-(2-Methoxyphenyl)-5-nitro-1H-indazole (53b). This reaction stopped at the hydrazone stage and did not give an indazole.

1-(3-Methoxyphenyl)-5-nitro-1H-indazole (53c). Yield: 180 mg (0.67 mmol, 67%) as a yellow solid; m.p. 127-128 °C; IR: 1516, 1344 cm^{-1} ; ^1H NMR (DMSO- d_6): δ 8.94 (s, 1H), 8.69 (s, 1H), 8.30 (d, $J = 9.2$ Hz, 1H), 8.01 (d, $J = 9.3$ Hz, 1H), 7.55 (t, $J = 8.0$ Hz, 1H), 7.37 (d, $J = 8.0$ Hz, 1H), 7.32 (s, 1H), 7.08 (d, $J = 8.2$ Hz, 1H), 3.87 (s, 3H); ^{13}C NMR (DMSO- d_6): δ 160.6, 142.8, 140.5, 140.2, 130.8, 131.2, 124.8, 122.7, 119.8, 115.3, 114.1, 112.0, 109.0, 56.0; MS: m/z 269 (M^+). Anal. Calcd for $\text{C}_{14}\text{H}_{11}\text{N}_3\text{O}_3$: C, 62.45; H, 4.12; N, 15.61. Found: C, 62.37; H, 4.06; N, 15.74.

1-(4-Methoxyphenyl)-5-nitro-1H-indazole (53d). Yield: 199 mg (0.74 mmol, 74%) as a light yellow solid; m.p. 181-182 °C; IR: 1516, 1342 cm^{-1} ; ^1H NMR (DMSO- d_6): δ 8.92 (d, $J = 2.2$ Hz, 1H), 8.64 (s, 1H), 8.27 (d, $J = 9.2, 2.2$ Hz, 1H), 7.84 (d, $J = 9.2$ Hz, 1H), 7.68 (d, $J = 8.7$ Hz, 2H), 7.18 (d, $J = 8.7$ Hz, 2H), 3.86 (s, 3H); ^{13}C NMR (DMSO- d_6): δ 159.2, 142.6, 141.6, 138.3, 132.1,

125.2, 124.3, 122.4, 119.8, 115.6, 111.6, 56.2, ; MS: m/z 269 (M^+). Anal. Calcd for $C_{14}H_{11}N_3O_3$: C, 62.45; H, 4.12; N, 15.61. Found: C, 62.41; H, 4.07; N, 15.56.

1-(4-Bromophenyl)-5-nitro-1H-indazole (53e). Yield: 222 mg (0.70 mmol, 70%) as a tan solid; m.p. 169-170 °C; IR: 1511, 1348 cm^{-1} ; 1H NMR (DMSO- d_6): δ 8.95 (s, 1H), 8.71 (s, 1H), 8.32 (d, $J = 9.3$ Hz, 1H), 8.01 (d, $J = 9.2$ Hz, 1H), 7.84 (d, $J = 8.4$ Hz, 2H), 7.79 (d, $J = 8.4$ Hz, 2H); ^{13}C NMR (DMSO- d_6): δ 142.9, 140.4, 139.2, 138.4, 133.2, 125.2, 125.0, 122.8, 120.7, 119.9, 111.9; MS: m/z 317 (M^+). Anal. Calcd for $C_{13}H_8BrN_3O_2$: C, 49.08; H, 2.53; N, 13.21. Found: C, 48.97; H, 2.59; N, 13.25.

1-(3-Chlorophenyl)-5-nitro-1H-indazole (53f). Yield: 164 mg (0.60 mmol, 60%) as an off-white solid; m.p. 143-144 °C; IR: 1514, 1346 cm^{-1} ; 1H NMR (DMSO- d_6): δ 8.95 (s, 1H), 8.72 (s, 1H), 8.32 (d, $J = 9.2$ Hz, 1H), 8.03 (d, $J = 9.2$ Hz, 1H), 7.88 (s, 1H), 7.82 (d, $J = 8.0$ Hz, 1H), 7.67 (t, $J = 8.1$ Hz, 1H), 7.57 (d, $J = 8.2$ Hz, 1H); ^{13}C NMR (DMSO- d_6): δ 142.9, 140.5, 140.3, 139.4, 134.6, 132.0, 128.0, 125.0, 123.0, 122.9, 121.7, 119.8, 112.0; MS: m/z 273 (M^+). Anal. Calcd for $C_{13}H_8ClN_3O_2$: C, 57.05; H, 2.95; N, 15.35. Found: C, 56.96; H, 3.00; N, 15.29.

1-(4-Chlorophenyl)-5-nitro-1H-indazole (53g). Yield: 191 mg (0.70 mmol, 70%) as a light yellow solid; m.p. 179-180 °C; IR: 1509, 1343 cm^{-1} ; 1H NMR (DMSO- d_6): δ 8.95 (d, $J = 2.2$ Hz, 1H), 8.71 (s, 1H), 8.31 (dd, $J = 9.3, 2.2$ Hz, 1H), 7.99 (d, $J = 9.3$ Hz, 1H), 7.85 (d, $J = 8.6$ Hz, 2H), 7.70 (d, $J = 8.6$ Hz, 2H); ^{13}C NMR (DMSO- d_6): δ 142.9, 140.5, 139.2, 138.0, 132.4, 130.3, 124.9, 122.8, 119.9, 111.9 (one carbon unresolved); MS: m/z 273 (M^+). Anal. Calcd for $C_{13}H_8ClN_3O_2$: C, 57.05; H, 2.95; N, 15.35. Found: C, 57.12; H, 2.97; N, 15.33.

1-(2,4-Dichlorophenyl)-5-nitro-1H-indazole (53h). Yield: 215 mg (0.70 mmol, 70%) as a light pink solid; m.p. 101-102 °C. IR: 1517, 1344 cm^{-1} ; 1H NMR (DMSO- d_6): δ 8.96 (s, 1H), 8.72 (s, 1H), 8.29 (d, $J = 9.2$ Hz, 1H), 8.03 (s, 1H), 7.78 (d, $J = 8.3$ Hz, 1H), 7.73 (d, $J = 8.3$ Hz, 1H), 7.52 (d, $J = 9.2$ Hz, 1H); ^{13}C NMR (DMSO- d_6): δ 143.0, 142.3, 139.2, 135.7, 135.0, 132.2, 131.6, 130.8, 129.3, 123.9, 122.7, 119.8, 111.7; MS: m/z 307 (M^+). Anal. Calcd for $C_{13}H_7Cl_2N_3O_2$: C, 50.68; H, 2.29; N, 13.64. Found: C, 50.67; H, 2.34; N, 13.53.

1-(3-(Trifluoromethyl)phenyl)-5-nitro-1H-indazole (53i). Yield: 190 mg (0.62 mmol, 62%) as a light yellow solid; m.p. 118-119 °C. IR: 1513, 1347 cm⁻¹; ¹H NMR (DMSO-*d*₆): δ 8.97 (s, 1H), 8.75 (s, 1H), 8.35 (d, *J* = 9.2 Hz, 1H), 8.18 (d, *J* = 7.2 Hz, 1H), 8.13 (s, 1H), 8.05 (d, *J* = 9.3 Hz, 1H), 7.94-7.85 (complex, 2H); ¹³C NMR (DMSO-*d*₆): δ 143.0, 140.6, 139.8, 139.6, 131.7, 131.0 (q, *J* = 32.7 Hz), 126.9, 125.2, 124.6 (q, *J* = 4.3 Hz), 124.1 (q, *J* = 272.6 Hz), 123.0, 119.8 (q, *J* = 4.9 Hz), 112.0 (one carbon unresolved); MS: *m/z* 307 (M⁺). Anal. Calcd for C₁₄H₈F₃N₃O₂: C, 54.73; H, 2.62; N, 13.68. Found: C, 54.66; H, 2.64; N, 13.57.

1-(4-(Trifluoromethyl)phenyl)-5-nitro-1H-indazole (53j). Yield: 209 mg (0.68 mmol, 68%) as a light yellow solid; m.p. 151-152 °C. IR: 1519, 1327 cm⁻¹; ¹H NMR (DMSO-*d*₆): δ 8.95 (s, 1H), 8.76 (s, 1H), 8.34 (d, *J* = 9.5 Hz, 1H), 8.11 (obscured d, *J* = 9.5 Hz, 1H), 8.08 (d, *J* = 8.5 Hz, 2H), 8.00 (d, *J* = 8.5 Hz, 2H); ¹³C NMR (DMSO-*d*₆): δ 143.1, 142.3, 140.5, 139.8, 127.9, (q, *J* = 32.3 Hz), 127.5 (q, *J* = 3.5 Hz), 125.4, 124.4 (q, *J* = 273.7 Hz), 123.3, 123.1, 119.9, 112.1; MS: *m/z* 307 (M⁺). Anal. Calcd for C₁₄H₈F₃N₃O₂: C, 54.73; H, 2.62; N, 13.68. Found: C, 54.68; H, 2.61; N, 13.64.

1-(4-Cyanophenyl)-5-nitro-1H-indazole (53k). Yield: 158 mg (0.60 mmol, 60%) as a light yellow solid; m.p. 250-251 °C. IR: 2227, 1512, 1344 cm⁻¹; ¹H NMR (DMSO-*d*₆): δ 8.97 (d, *J* = 2.2 Hz, 1H), 8.78 (s, 1H), 8.36 (dd, *J* = 9.3, 2.2 Hz, 1H), 8.15 (d, *J* = 9.3 Hz, 1H), 8.12 (d, *J* = 8.8 Hz, 2H), 8.07 (d, *J* = 8.8 Hz, 2H); ¹³C NMR (DMSO-*d*₆): δ 142.1, 141.6, 139.4, 139.1, 133.6, 124.5, 122.1, 120.0, 118.9, 117.7, 111.3, 109.0; MS: *m/z* 264 (M⁺). Anal. Calcd for C₁₄H₈N₄O₂: C, 63.64; H, 3.05; N, 21.20. Found: C, 63.55; H, 3.09; N, 21.08.

4-(5-Nitro-1H-indazol-1-yl)benzenesulfonamide (53l). Yield: 159 mg (0.50 mmol, 50%); m.p. 237-238 °C; IR: 3329, 3241, 1512, 1339 cm⁻¹; ¹H NMR (DMSO-*d*₆): δ 8.97 (d, *J* = 2.2 Hz, 1H), 8.76 (s, 1H), 8.35 (dd, *J* = 9.3, 2.2 Hz, 1H), 8.13 (d, *J* = 9.3 Hz, 1H), 8.06 (s, 4H), 7.53 (br s, 2H); ¹³C NMR (DMSO-*d*₆): δ 143.1, 141.60, 141.55, 140.5, 139.8, 128.0, 125.3, 123.1, 122.2, 119.9, 112.2; MS: *m/z* 318 (M⁺). Anal. Calcd for C₁₃H₁₀N₄O₄S: C, 49.05; H, 3.17; N, 17.60. Found: C, 49.11; H, 3.16; N, 17.66.

4-(5-Nitro-1*H*-indazol-1-yl)benzoic acid (53m). This product was formed only using the two-step procedure. Yield: 142 mg (0.50 mmol, 50%) as a brown product; m.p. 158-159 °C; IR: 3395-2372, 1694, 1518, 1345 cm⁻¹; ¹H NMR (DMSO-*d*₆): δ 13.3 (br s, 1H), 8.97 (d, *J* = 2.2 Hz, 1H), 8.76 (s, 1H), 8.35 (dd, *J* = 9.3, 2.2 Hz, 1H), 8.18 (d, *J* = 8.4 Hz, 2H), 8.13 (d, *J* = 9.3 Hz, 1H), 7.98 (d, *J* = 8.4 Hz, 2H); ¹³C NMR (DMSO-*d*₆): δ 167.0, 143.0, 142.5, 140.4, 139.7, 131.5, 129.8, 125.3, 123.0, 122.5, 119.9, 112.2; MS: *m/z* 283 (M⁺). Anal. Calcd for C₁₄H₉N₃O₄: C, 59.37; H, 3.20; N, 14.84. Found: C, 59.32; H, 3.23; N, 14.75.

Representative procedure for the general indazole synthesis.

To a stirred solution of the carbonyl compound (**54**, **55** or **56**, 1.0 mmol) in DMPU (5 mL) were added powdered 4Å molecular sieves (30 wt% relative to the carbonyl substrate) and ArNHNH₂·HCl (1.5 mmol). The mixture was heated at 90 °C (oil bath) for 1.5 h at which time CuI (0.2 mmol) and K₂CO₃ (2.5 mmol) were added and heating was continued at this temperature for 16 h. The crude reaction mixture was cooled to 23 °C and filtered through a Celite[®] pad. The pad was rinsed with ether (2 × 20 mL) and the combined filtrate was washed with water (25 mL), saturated NaCl (25 mL), dried (MgSO₄), filtered, and concentrated under vacuum. The products were purified by silica gel chromatography using increasing concentrations of EtOAc in hexanes. Yields as well as physical and spectral data are given below.

3-Methyl-1-phenyl-1*H*-indazole (57a). Yield: 169 mg (0.81 mmol, 81%) as tan solid; m.p. 72-73 °C (lit⁸⁶ m.p. 73-74 °C); IR: 1597, 1505 cm⁻¹; ¹H NMR (CDCl₃): δ 7.75-7.96 (complex, 4H), 7.52 (t, *J* = 7.3 Hz, 2H), 7.42 (t, *J* = 7.5 Hz, 1H), 7.32 (t, *J* = 7.3 Hz, 1H), 7.21 (t, *J* = 7.5 Hz, 1H), 2.65 (s, 3H); ¹³C NMR (CDCl₃): δ 144.0, 140.3, 139.5, 129.4, 127.1, 126.1, 124.9, 122.4, 120.8, 120.6, 110.3, 12.0; MS: *m/z* 208 (M⁺). Anal. Calcd for C₁₄H₁₂N₂: C, 80.74; H, 5.81; N, 13.45. Found: C, 81.01; H, 6.08; N, 13.23.

1-(4-Methoxyphenyl)-3-methyl-1H-indazole (57d). Yield: 207 mg (0.87 mmol, 87%) as a yellow oil; IR: 2845, 1517 cm^{-1} ; ^1H NMR (CDCl_3): δ 7.72 (d, $J = 8.1$ Hz, 1H), 7.60 (d, $J = 7.7$ Hz, 1H), 7.59 (d, $J = 8.9$ Hz, 2H), 7.39 (t, $J = 7.4$ Hz, 1H), 7.18 (t, $J = 7.5$ Hz, 1H), 7.04 (d, $J = 8.9$ Hz, 2H), 3.87 (s, 3H), 2.65 (s, 3H); ^{13}C NMR (CDCl_3): δ 158.1, 143.8, 139.7, 133.5, 126.9, 124.4, 124.3, 120.50, 120.47, 114.6, 110.1, 56.6, 11.9; MS: m/z 238 (M^+). Anal. Calcd for $\text{C}_{15}\text{H}_{14}\text{N}_2\text{O}$: C, 75.61; H, 5.92; N, 11.76. Found: C, 75.35; H, 6.18; N, 11.25.

4-(3-Methyl-1H-indazol-1-yl)benzotrile (57l). Yield: 198 mg (0.85 mmol, 85%) as tan solid; m.p. 124-126 $^\circ\text{C}$; IR: 2224, 1604, 1517 cm^{-1} ; ^1H NMR (CDCl_3): δ 7.91 (d, $J = 8.6$ Hz, 2H), 7.80 (d, $J = 8.6$ Hz, 2H), 7.78 (d, $J = 8.4$ Hz, 1H), 7.75 (d, $J = 7.9$ Hz, 1H), 7.50 (t, $J = 8.3$ Hz, 1H), 7.28 (t, $J = 7.4$ Hz, 1H), 2.65 (s, 3H); ^{13}C NMR (CDCl_3): δ 146.1, 143.9, 139.1, 133.5, 128.0, 125.9, 121.9, 121.3, 121.1, 118.7, 110.5, 108.5, 12.0; MS: m/z 233 (M^+). Anal. Calcd for $\text{C}_{15}\text{H}_{11}\text{N}_3$: C, 77.23; H, 4.75; N, 18.01. Found: C, 77.35; H, 4.31; N, 18.32.

1-Phenyl-1H-indazole (58a). Yield: 149 mg (0.77 mmol, 77%) as off-white solid; m.p. 77-78 $^\circ\text{C}$ (lit⁸⁸ m.p. 78 $^\circ\text{C}$); IR: 1595, 1500 cm^{-1} ; ^1H NMR (CDCl_3): δ 8.21 (s, 1H), 7.81 (d, $J = 8.1$ Hz, 1H), 7.77 (d, $J = 8.4$ Hz, 1H), 7.75 (d, $J = 8.7$ Hz, 2H), 7.54 (t, $J = 8.4$ Hz, 2H), 7.43 (t, $J = 8.3$ Hz, 1H), 7.37 (t, $J = 8.3$ Hz, 1H), 7.23 (t, $J = 8.1$ Hz, 1H); ^{13}C NMR (CDCl_3): δ 140.2, 138.8, 135.4, 129.5, 127.1, 126.6, 125.3, 122.8, 121.5, 121.3, 110.4; MS: m/z 194 (M^+). Anal. Calcd for $\text{C}_{13}\text{H}_{10}\text{N}_2$: C, 80.39; H, 5.19; N, 14.42. Found: C, 80.15; H, 5.31; N, 14.69.

1-(4-Methoxyphenyl)-1H-indazole (58d). Yield: 177 mg (0.79 mmol, 79%) as a yellow oil; IR: 2836, 1515 cm^{-1} ; ^1H NMR (CDCl_3): δ 8.17 (s, 1H), 7.79 (d, $J = 8.1$ Hz, 1H), 7.65 (d, $J = 8.5$ Hz, 1H), 7.62 (d, $J = 8.9$ Hz, 2H), 7.41 (t, $J = 8.3$ Hz, 1H), 7.21 (t, $J = 8.0$ Hz, 1H), 7.06 (d, $J = 8.9$ Hz, 2H), 3.88 (s, 3H); ^{13}C NMR (CDCl_3): δ 158.4, 139.0, 134.8, 133.4, 126.9, 124.9, 124.5, 121.23, 121.21, 114.6, 110.2, 55.6; MS: m/z 224 (M^+). Anal. Calcd for $\text{C}_{14}\text{H}_{12}\text{N}_2\text{O}$: C, 74.98; H, 5.39; N, 12.49. Found: C, 74.63; H, 5.52; N, 12.63.

4-(1*H*-Indazol-1-yl)benzotrile (58I). Yield: 164 mg (0.75 mmol, 75%) as a white solid; m.p. 104-106 °C; IR: 2225, 1604, 1510 cm⁻¹; ¹H NMR (CDCl₃): δ 8.26 (s, 1H), 7.94 (d, *J* = 8.6 Hz, 2H), 7.84 (d, *J* = 8.6 Hz, 2H), 7.86-7.81 (complex, 2H), 7.51 (t, *J* = 8.4 Hz, 1H), 7.31 (t, *J* = 8.0 Hz, 1H); ¹³C NMR (CDCl₃): δ 143.8, 138.5, 137.3, 133.6, 128.1, 126.1, 122.5, 121.9, 121.8, 118.5, 110.4, 109.3; MS: m/z 219 (M⁺). Anal. Calcd for C₁₄H₉N₃: C, 76.70; H, 4.14; N, 19.17. Found: C, 76.85; H, 4.31; N, 19.32.

1-Phenyl-1*H*-pyrazolo[3,4-*b*]pyridine (59a). Yield: 133 mg (0.68 mmol, 68%) as a white solid; m.p. 52-54 °C (lit⁸⁶ 53-55 °C); IR: 1595, 1499 cm⁻¹; ¹H NMR (CDCl₃): δ 8.65 (dd, *J* = 4.5, 1.7 Hz, 1H), 8.28 (dd, *J* = 7.7, 1.2 Hz, 2H), 8.21 (s, 1H), 8.14 (dd, *J* = 8.0, 1.7 Hz, 1H), 7.54 (t, *J* = 7.7 Hz, 1H), 7.33 (t, *J* = 7.5 Hz, 1H), 7.22 (dd, *J* = 8.0, 4.5 Hz, 1H); ¹³C NMR (CDCl₃): δ 150.1, 149.2, 139.5, 133.8, 130.2, 129.1, 126.1, 121.4, 117.6, 117.2; MS: m/z 195 (M⁺). Anal. Calcd for C₁₂H₉N₃: C, 73.83; H, 4.65; N, 21.52. Found: C, 73.95; H, 4.87; N, 21.78.

1-(4-Methoxyphenyl)-1*H*-pyrazolo[3,4-*b*]pyridine (59d). Yield: 140 mg (0.62 mmol, 62%) as a purple solid; m.p. 204-205 °C; IR: 2833, 1513 cm⁻¹; ¹H NMR (CDCl₃): δ 9.00 (dd, *J* = 8.0, 1.7 Hz, 1H), 8.70 (dd, *J* = 4.5, 1.7 Hz, 1H), 8.28 (d, *J* = 9.0 Hz, 2H), 7.35 (dd, *J* = 8.0, 4.5 Hz, 1H), 7.26 (s, 1H), 7.14 (d, *J* = 9.0 Hz, 2H), 3.91 (s, 3H); ¹³C NMR (CDCl₃): δ 158.0, 150.6, 149.6, 138.7, 132.9, 132.6, 123.0, 118.3, 115.3, 114.4, 55.6; MS: m/z 225 (M⁺). Anal. Calcd for C₁₃H₁₁N₃O: C, 69.32; H, 4.92; N, 18.66. Found: C, 69.68; H, 5.11; N, 19.82.

4-(1*H*-Pyrazolo[3,4-*b*]pyridine-1-yl)benzotrile (59I). Yield: 172 mg (0.78 mmol, 78%) as a white solid; m.p. 125-127 °C; IR: 2222, 1603, 1450 cm⁻¹; ¹H NMR (CDCl₃): δ 8.68 (dd, *J* = 4.5, 1.6 Hz, 1H), 8.66 (d, *J* = 8.8 Hz, 2H), 8.25 (s, 1H), 8.17 (dd, *J* = 8.0, 1.6 Hz, 1H), 7.82 (d, *J* = 8.8 Hz, 2H), 7.30 (dd, *J* = 8.0, 4.5 Hz, 1H); ¹³C NMR (CDCl₃): δ 150.7, 149.4, 143.1, 135.4, 133.2, 130.6, 120.3, 11.89, 118.4, 117.9, 108.7; MS: m/z 220 (M⁺). Anal. Calcd for C₁₃H₈N₄: C, 70.90; H, 3.66; N, 25.44. Found: C, 71.23; H, 3.82; N, 25.67.

2.3.2. 4*H*-Benzo[*d*][1,3]oxazin-4-ones and dihydro analogs.

Representative procedure under thermal conditions. Method 1.

The anthranilic acid (1.0 mmol) and the orthoester (4.5 mmol) were placed in a 15-mL Chemglass screw-cap pressure tube (CG-1880-01). Glacial acetic acid (2.6 mmol) was added, N₂ was introduced to the vessel and the cap was tightened. The vessel was heated at 100 °C under neat conditions for 4-48 h, and then cooled to room temperature. Upon cooling, the crude product crystallized from the reaction mixture and was purified by trituration from 5% ether in pentane.

Representative procedure under microwave conditions. Method 2.

A solution of the anthranilic acid (1.0 mmol) in the orthoester (0.45 mL, 2.0-2.7 equiv) was prepared in a 5-mL microwave tube and stirred for 30 s prior to irradiation at the "high absorption" setting. The reaction was performed under N₂ at 100 °C (400 W) for 0.75-3 h. Upon cooling, the crude product crystallized from the reaction mixture and was purified by trituration from 5% ether in pentane.

The following compounds were prepared:

2-Methyl-4*H*-benzo[*d*][1,3]oxazin-4-one (67a). Yield: 130 mg (81%, method 1) and 132 mg (82%, method 2) as white crystals; m.p. 79-80 °C (lit.¹¹³ 80-81 °C); IR: 1700, 1624 cm⁻¹; ¹H NMR (400 MHz, CDCl₃): δ 8.29 (dd, 1H, *J* = 7.5, 1.6 Hz, ArH), 7.78 (ddd, 1H, *J* = 8.4, 7.1, 1.6 Hz, ArH), 7.69 (d, 1H, *J* = 8.4 Hz, ArH), 7.48 (ddd, 1H, *J* = 8.1, 7.1, 1.2 Hz, ArH), 2.60 (s, 3H, CH₃); ¹³C NMR (101 MHz, CDCl₃): δ 164.1, 153.2, 149.4, 134.9, 127.0, 126.5, 126.3, 120.3, 22.2; HRMS (ESI): *m/z* [M+H]⁺ calcd for C₉H₇NO₂: 162.0555, found: 162.0553.

2-Ethyl-4*H*-benzo[*d*][1,3]oxazin-4-one (67b). Yield: 140 mg (80%, method 1) and 145 mg (83%, method 2) as white crystals; m.p. 83-84 °C (lit.¹¹³ m.p. 85-86 °C); IR: 1750, 1645 cm⁻¹; ¹H NMR (400 MHz, CDCl₃): δ 8.20 (dd, 1H, *J* = 7.9, 1.5 Hz, ArH), 7.80 (ddd, 1H, *J* = 8.4, 7.5, 1.5 Hz, ArH), 7.57 (d, 1H, *J* = 8.4 Hz, ArH), 7.50 (ddd, 1H, *J* = 8.2, 7.5, 1.2 Hz, ArH), 2.73 (q, 2H, *J* = 7.5 Hz, CH₂CH₃), 1.37 (t, 3H, *J* = 7.5 Hz, CH₂CH₃); ¹³C NMR (101 MHz, CDCl₃): δ 163.9,

159.9, 146.5, 136.5, 128.4, 128.1, 126.6, 116.9, 28.2, 10.3; HRMS (ESI): m/z $[M+H]^+$ calcd for $C_{10}H_9NO_2$: 176.0712, found: 176.0713.

2-Phenyl-4H-benzo[d][1,3]oxazin-4-one (67d). Yield: 174 mg (78%, method 1) and 179 mg (80%, method 2) as off-white crystals; m.p. 121-122 °C (lit.¹¹³ m.p. 123 °C); IR: 1762, 1615 cm^{-1} ; 1H NMR (400 MHz, $CDCl_3$): δ 8.34-8.30 (complex, 2H, ArH), 8.25 (dd, 1H, $J = 7.9, 1.5$, ArH), 7.84 (ddd, 1H, $J = 8.1, 7.3, 1.5$ Hz, ArH), 7.70 (d, $J = 8.1$ Hz, ArH), 7.62-7.48 (complex, 4H, ArH); ^{13}C NMR (101 MHz, $CDCl_3$): δ 159.6, 157.1, 147.0, 136.6, 132.6, 130.3, 128.8, 128.6, 128.32, 128.26, 127.2, 117.0; HRMS (ESI): m/z $[M+H]^+$ calcd for $C_{14}H_9NO_2$: 224.0712, found: 224.0709.

2,6-Dimethyl-4H-benzo[d][1,3]oxazin-4-one (68a). Yield: 119 mg (68%, method 2) as off-white crystals; m.p. 122-123 °C; IR: 1682, 1595 cm^{-1} ; 1H NMR (400 MHz, $CDCl_3$): δ 7.98 (s, 1H, ArH), 7.61 (d, 1H, $J = 8.2$ Hz, ArH), 7.44 (d, 1H, $J = 8.2$ Hz, ArH), 2.47 (s, 3H, CH_3), 2.45 (s, 3H, CH_3); ^{13}C NMR (101 MHz, $CDCl_3$): δ 159.9, 159.4, 144.3, 138.5, 137.7, 128.0, 126.2, 116.3, 21.3, 21.2; HRMS (ESI): m/z $[M+H]^+$ calcd for $C_{10}H_9NO_2$: 176.0712, found: 176.0709.

2-Ethyl-6-methyl-4H-benzo[d][1,3]oxazin-4-one (68b). Yield: 125 mg (66%, method 2) as white crystals; m.p. 103-104 °C; IR: 1686, 1596 cm^{-1} ; 1H NMR (400 MHz, $CDCl_3$): δ 7.98 (s, 1H, ArH), 7.60 (d, 1H, $J = 8.2$ Hz, ArH), 7.46 (d, 1H, $J = 8.2$ Hz, ArH), 2.71 (q, 2H, $J = 7.5$ Hz, CH_2CH_3), 2.47 (s, 3H, Ar CH_3), 1.36 (t, 3H, $J = 7.5$ Hz, CH_2CH_3); ^{13}C NMR (101 MHz, $CDCl_3$): δ 163.1, 160.1, 144.3, 138.4, 137.7, 128.0, 126.4, 116.5, 26.1, 21.2, 10.3; HRMS (ESI): m/z $[M+H]^+$ calcd for $C_{11}H_{11}NO_2$: 190.0868, found: 190.0865.

6-Methyl-2-phenyl-4H-benzo[d][1,3]oxazin-4-one (68d). Yield: 202 mg (85%, method 2) as off-white crystals; m.p. 144-145 °C; IR: 1752, 1607 cm^{-1} ; 1H NMR (400 MHz, $CDCl_3$): δ 8.29 (d, 2H, $J = 8.2$ Hz, ArH), 8.04 (s, 1H, ArH), 7.66-7.47 (complex, 5H, ArH), 2.49 (s, 3H, Ar CH_3); ^{13}C NMR (101 MHz, $CDCl_3$): δ 159.8, 156.4, 144.8, 138.7, 137.8, 132.4, 130.4, 128.7, 128.19,

128.17, 127.0, 116.7, 21.2; HRMS (ESI): m/z $[M+H]^+$ for $C_{15}H_{11}NO_2$: 238.0868, found: 238.0870.

7-Methoxy-2-methyl-4H-benzo[d][1,3]oxazin-4-one (69a). Yield: 166 mg (87%, method 1) and 168 mg (88%, method 2) as light yellow crystals; m.p. 119-120 °C; IR (nujol): 2830, 1747, 1610 cm^{-1} ; 1H NMR (400 MHz, DMSO- d_6): δ 8.00 (d, 1H, $J = 8.8$ Hz, ArH), 7.14 (dd, 1H, $J = 8.8, 2.5$ Hz, ArH), 7.05 (d, 1H, $J = 2.5$ Hz, ArH), 3.91 (s, 3H, OCH₃), 2.38 (s, 3H, CH₃); ^{13}C NMR (101 MHz, DMSO- d_6): δ 166.3, 161.5, 159.2, 149.0, 130.2, 117.1, 109.5, 109.1, 56.5, 21.5; HRMS (ESI): m/z $[M+H]^+$ calcd for $C_{10}H_9NO_3$: 192.0661, found: 192.0659.

2-Ethyl-7-methoxy-4H-benzo[d][1,3]oxazin-4-one (69b). Yield: 176 mg (86%, method 1) and 181 mg (88%, method 2) as light yellow crystals; m.p. 89-90 °C; IR (nujol): 2840, 1767, 1644, 1609 cm^{-1} ; 1H NMR (400 MHz, DMSO- d_6): δ 7.99 (d, 1H, $J = 8.8$ Hz, ArH) 7.14 (dd, 1H, $J = 8.8, 2.5$ Hz, ArH), 7.07 (d, 1H, $J = 2.5$ Hz, ArH), 3.92 (s, 3H, OCH₃), 2.68 (q, 2H, $J = 7.5$ Hz, CH₂CH₃), 1.24 (t, 3H, $J = 7.5$ Hz, CH₂CH₃); ^{13}C NMR (101 MHz, DMSO- d_6): δ 166.3, 164.9, 159.2, 149.0, 130.1, 117.3, 109.7, 109.1, 56.6, 27.7, 10.2; HRMS (ESI): m/z $[M+H]^+$ calcd for $C_{11}H_{11}NO_3$: 206.0817, found: 206.0817.

7-Methoxy-2-propyl-4H-benzo[d][1,3]oxazin-4-one (69c). Yield: 189 mg (86%, method 1) and 191 mg (87%, method 2) as light yellow crystals; m.p. 77-78 °C; IR (nujol): 2841, 1766, 1643, 1609 cm^{-1} ; 1H NMR (400 MHz, DMSO- d_6): δ 8.00 (d, 1H, $J = 8.8$ Hz, ArH), 7.14 (dd, 1H, $J = 8.8, 2.5$ Hz, ArH), 7.07 (d, 1H, $J = 2.5$ Hz, ArH), 3.92 (s, 3H, OCH₃), 2.63 (t, 2H, $J = 7.4$ Hz, CH₂CH₂CH₃), 1.75 (sextet, 2H, $J = 7.4$ Hz, CH₂CH₂CH₃); 0.98 (t, 3H, $J = 7.4$ Hz, CH₂CH₂CH₃); ^{13}C NMR (101 MHz, DMSO- d_6): δ 166.3, 163.9, 159.2, 148.9, 130.1, 117.3, 109.7, 109.1, 56.6, 36.2, 19.2, 13.9; HRMS (ESI): m/z $[M+H]^+$ calcd for $C_{12}H_{13}NO_3$: 220.0974, found: 220.0971.

7-Methoxy-2-phenyl-4H-benzo[d][1,3]oxazin-4-one (69d). Yield: 210 mg (83%, method 1) and 215 mg (85%, method 2) as light yellow crystals; m.p. 149-150 °C; IR (nujol): 2842, 1744, 1607 cm^{-1} ; 1H NMR (400 MHz, DMSO- d_6): δ 8.17 (d, 2H, $J = 8.1$ Hz, ArH), 8.03 (d, 1H, $J = 9.4$ Hz,

ArH), 7.67 (d, 1H, $J = 7.3$ Hz, ArH), 7.59 (t, 2H, $J = 8.1$ Hz, ArH), 7.15 (m, 2H, ArH), 3.94 (s, 3H, OCH₃); ¹³C NMR (101 MHz, DMSO-*d*₆): δ 166.4, 158.8, 157.6, 149.2, 133.2, 130.5, 130.3, 129.4, 128.3, 117.6, 109.9, 109.6, 56.6; HRMS (ESI): m/z [M+H]⁺ calcd for C₁₅H₁₁NO₃: 254.0817, found: 254.0814.

7-Nitro-2-phenyl-4H-benzo[*d*][1,3]oxazin-4-one (70d). Yield: 244 mg (91%, method 2) as light orange crystals; m.p. 175-176 °C; IR: 1757, 1629, 1608, 1530, 1349 cm⁻¹; ¹H NMR (400 MHz, CDCl₃): δ 8.52 (d, 1H, $J = 2.2$ Hz, ArH), 8.41 (d, 1H, $J = 8.6$ Hz, ArH), 8.33 (d, 2H, $J = 7.4$ Hz, ArH), 8.29 (dd, 1H, $J = 8.6, 2.2$ Hz, ArH), 7.64 (t, 1H, $J = 7.4$ Hz, ArH), 7.55 (t, 2H, $J = 7.4$ Hz, ArH); ¹³C NMR (101 MHz, CDCl₃): δ 159.0, 157.9, 152.9, 148.1, 133.6, 130.4, 129.3, 129.0, 128.7, 122.5, 122.0, 121.3; HRMS (ESI): m/z [M+H]⁺ calcd for C₁₄H₈N₂O₄: 269.0562, found: 269.0558.

7-Chloro-2-methyl-4H-benzo[*d*][1,3]oxazin-4-one (71a). Yield: 166 mg (85%, method 2) as white crystals; m.p. 149-150 °C; IR: 1762, 1696, 1642, 1596 cm⁻¹; ¹H NMR (400 MHz, CDCl₃): δ 8.11 (d, 1H, $J = 8.4$ Hz, ArH), 7.54 (d, 1H, $J = 2.0$ Hz, ArH), 7.46 (dd, 1H, $J = 8.4, 2.0$ Hz, ArH), 2.47 (s, 3H CH₃); ¹³C NMR (101 MHz, CDCl₃): δ 161.6, 158.9, 147.5, 142.9, 129.7, 128.8, 126.3, 115.1, 21.4; HRMS (ESI): m/z [M+H]⁺ calcd for C₉H₆³⁵ClNO₂: 196.0165, found: 196.0166.

7-Chloro-2-phenyl-4H-benzo[*d*][1,3]oxazin-4-one (71d). Yield: 237 mg (92%, method 2) as off-white crystals; m.p. 188-189 °C; IR: 1760, 1619, 1596 cm⁻¹; ¹H NMR (400 MHz, CDCl₃): δ 8.31 (d, 2H, $J = 7.4$ Hz, ArH), 8.17 (d, 1H, $J = 8.4$ Hz, ArH), 7.70 (d, 1H, $J = 2.0$ Hz, ArH), 7.60 (tt, 1H, $J = 7.4, 1.4$ Hz, ArH), 7.52 (t, 2H, $J = 7.4$ Hz, ArH), 7.48 (dd, 1H, $J = 8.4, 2.0$ Hz, ArH); ¹³C NMR (101 MHz, CDCl₃): δ 158.8, 158.3, 148.1, 143.0, 133.0, 129.9, 129.86, 128.83, 128.79, 128.5, 127.0, 115.4; HRMS (ESI): m/z [M+H]⁺ calcd for C₁₄H₈³⁵ClNO₂: 258.0322, found: 258.0317.

(±)-2-Ethoxy-2-phenyl-1,2-dihydro-4H-benzo[*d*][1,3]oxazin-4-one (73d). Yield: 232 mg (86%, method 1) as white crystals; m.p. 92-93 °C; IR: 3254, 1668, 1595 cm⁻¹; ¹H NMR (400 MHz,

CDCl₃): δ 12.09 (br s, 1H, NH), 8.94 (dd, 1H, $J = 8.5, 1.1$ Hz, ArH), 8.1 (dd, 1H, $J = 8.0, 1.7$ Hz, ArH), 8.06 (dd, 2H, $J = 7.8, 1.5$ Hz, ArH), 7.64-7.49 (complex, 4H, ArH), 7.13 (td, 1H, $J = 7.4, 1.2$ Hz, ArH), 4.43 (q, 2H, $J = 7.1$ Hz, OCH₂CH₃), 1.43 (t, 3H, $J = 7.1$ Hz, OCH₂CH₃); ¹³C NMR (101 MHz, CDCl₃): δ 168.6, 165.4, 141.9, 134.9, 134.7, 131.9, 130.9, 128.8, 127.4, 122.6, 120.5, 115.5, 61.5, 14.2; HRMS (ESI): m/z [M+H]⁺ calcd for C₁₆H₁₅NO₂: 254.1181, found: 254.1177.

(±)-2-Ethoxy-2,6-dimethyl-1,2-dihydro-4H-benzo[d][1,3]oxazin-4-one (74a): Yield: 195 mg (88%, method 1) as white crystals; m.p. 110-111 °C; IR: 3266, 1677, 1595 cm⁻¹; ¹H NMR (400 MHz, CDCl₃): δ 10.97 (br s, 1H, NH), 8.57 (d, 1H, $J = 8.6$ Hz, ArH), 7.83 (s, 1H, ArH), 7.34 (d, 1H, $J = 8.6$ Hz, ArH), 4.37 (q, 2H, $J = 7.1$ Hz, OCH₂CH₃), 2.33 (s, 3H, ArCH₃), 2.22 (s, 3H, CH₃), 1.42 (t, 3H, $J = 7.1$ Hz, OCH₂CH₃); ¹³C NMR (101 MHz, CDCl₃): δ 168.9, 168.4, 139.2, 135.3, 131.9, 130.8, 120.3, 115.0, 61.3, 25.5, 20.7, 14.2; HRMS (ESI): m/z [M+H]⁺ calcd for C₁₂H₁₅NO₃: 222.1130, found: 222.1128.

(±)-2-Ethoxy-2-ethyl-6-methyl-1,2-dihydro-4H-benzo[d][1,3]oxazin-4-one (74b). Yield: 205 mg (87%, method 1) as white crystals; m.p. 78-79 °C; IR: 3261, 1677, 1596 cm⁻¹; ¹H NMR (400 MHz, CDCl₃): δ 11.0 (br s, 1H, NH), 8.62 (d, 1H, $J = 8.6$ Hz, ArH), 7.83 (s, 1H, ArH), 7.34 (d, 1H, $J = 8.6$ Hz, ArH), 4.37 (q, 2H, $J = 7.0$ Hz, OCH₂CH₃), 2.46 (q, 2H, $J = 7.5$ Hz, CH₂CH₃), 2.33 (s, 3H, ArCH₃), 1.42 (t, 3H, $J = 7.0$ Hz, OCH₂CH₃), 1.27 (t, 3H, $J = 7.5$ Hz, CH₂CH₃); ¹³C NMR (101 MHz, CDCl₃): δ 172.7, 168.4, 139.4, 135.3, 131.7, 130.8, 120.3, 114.9, 61.3, 31.7, 20.7, 14.2, 9.7; HRMS (ESI): m/z [M+H]⁺ calcd for C₁₃H₁₇NO₃: 236.1287, found: 236.1284.

(±)-2-Ethoxy-6-methyl-2-propyl-1,2-dihydro-4H-benzo[d][1,3]oxazin-4-one (74c): Yield: 219 mg (88%, method 1) and 222 mg (89%, method 2) as off-white crystals; m.p. 39-40 °C; IR: 3265, 1682, 1599 cm⁻¹; ¹H NMR (400 MHz, CDCl₃): δ 10.98 (br s, 1H, NH), 8.62 (d, 1H, $J = 8.6$ Hz, ArH), 7.83 (s, 1H, ArH), 7.35 (d, 1H, $J = 8.6$ Hz, ArH), 4.38 (q, 2H, $J = 7.1$ Hz, OCH₂CH₃), 2.41 (q, 2H, $J = 7.5$ Hz, CH₂CH₂CH₃), 2.33 (s, 3H, ArCH₃), 1.78 (sextet, 2H, $J = 7.5$ Hz, CH₂CH₂CH₃), 1.42 (t, 3H, $J = 7.1$ Hz, OCH₂CH₃), 1.01 (t, 3H, $J = 7.5$ Hz, CH₂CH₂CH₃); ¹³C

NMR (101 MHz, CDCl₃): δ 171.9, 168.4, 139.3, 135.3, 131.7, 130.8, 120.3, 114.9, 61.3, 40.6, 20.7, 19.0, 14.2, 13.8; HRMS (ESI): m/z [M+H]⁺ calcd for C₁₄H₁₉NO₃: 250.1443, found: 250.1441.

(±)-2-Ethoxy-6-methyl-2-phenyl-1,2-dihydro-4H-benzo[d][1,3]oxazin-4-one (74d). Yield: 249 mg (88%, method 1) as white crystals; m.p. 117-118 °C; IR: 3249, 1662, 1602 cm⁻¹; ¹H NMR (400 MHz, CDCl₃): δ 11.98 (br s, 1H, NH), 8.82 (d, 1H, J = 8.5 Hz, ArH), 8.05 (d, 2H, J = 6.8 Hz, ArH), 7.89 (s, 1H, ArH), 7.58-7.47 (complex, 3H), 7.42 (d, 1H, J = 8.5 Hz, ArH), 4.42 (q, 2H, J = 7.1 Hz, OCH₂CH₃), 3.36 (s, 3H, ArCH₃), 1.44 (q, 3H, J = 7.1 Hz, OCH₂CH₃); ¹³C NMR (101 MHz, CDCl₃): δ 168.9, 165.5, 139.5, 135.4, 135.1, 132.1, 131.8, 131.0, 128.8, 127.3, 120.4, 115.4, 61.5, 20.8, 14.3; HRMS (ESI): m/z [M+H]⁺ calcd for C₁₇H₁₇NO₃: 284.1287, found: 284.1283.

(±)-2-Ethoxy-2-methyl-7-nitro-1,2-dihydro-4H-benzo[d][1,3]oxazin-4-one (76a): Yield: 212 mg (84%, method 1) and 219 mg (87%, method 2) as light tan crystals; m.p. 108-109 °C; IR: 3270, 1702, 1604, 1538, 1350 cm⁻¹; ¹H NMR (400 MHz, CDCl₃): δ 11.16 (br s, 1H, NH), 9.60 (d, 1H, J = 2.4 Hz, ArH), 8.20 (d, 1H, J = 8.8 Hz, ArH), 7.87 (dd, 1H, J = 8.8, 2.4 Hz, ArH), 4.45 (q, 2H, J = 7.1 Hz, OCH₂CH₃), 2.28 (s, 3H, CH₃), 1.46 (t, 3H, J = 7.1 Hz, OCH₂CH₃); ¹³C NMR (101 MHz, CDCl₃): δ 169.2, 166.9, 151.2, 142.2, 131.9, 119.3, 116.4, 115.2, 62.5, 25.5, 14.1; HRMS (ESI): m/z [M+H]⁺ calcd for C₁₁H₁₂N₂O₅: 253.0825, found: 253.0824.

(±)-2-Ethoxy-2-ethyl-7-nitro-1,2-dihydro-4H-benzo[d][1,3]oxazin-4-one (76b). Yield: 229 mg (86%, method 1) and 234 mg (88%, method 2) as light tan crystals; m.p. 74-75 °C; IR: 3273, 1694, 1600, 1538, 1349 cm⁻¹; ¹H NMR (400 MHz, CDCl₃): δ 11.18 (br s, 1H, NH), 9.65 (d, 1H, J = 2.4 Hz, ArH), 8.20 (d, 1H, J = 8.8 Hz, ArH), 7.86 (dd, 1H, J = 8.8, 2.4 Hz, ArH), 4.45 (q, 2H, J = 7.1 Hz, OCH₂CH₃), 2.53 (q, 2H, J = 7.5 Hz, CH₂CH₃), 1.46 (t, 3H, J = 7.1 Hz, OCH₂CH₃), 1.30 (t, 3H, J = 7.5 Hz, CH₂CH₃); ¹³C NMR (101 MHz, CDCl₃): δ 173.1, 166.9, 151.2, 142.5, 131.9,

119.3, 116.3, 115.3, 62.4, 31.6, 14.1, 9.3; HRMS (ESI): m/z $[M+H]^+$ calcd for $C_{12}H_{14}N_2O_5$: 267.0981, found: 267.0977.

(±)-2-Ethoxy-2-propyl-7-nitro-1,2-dihydro-4H-benzo[*d*][1,3]oxazin-4-one (76c). Yield: 238 mg (85%, method 1) and 245 mg (88%, method 2) as light tan crystals; m.p. 66-67°C; IR: 3270, 1697, 1604, 1538, 1349 cm^{-1} ; 1H NMR (400 MHz, $CDCl_3$): δ 11.17 (br s, 1H, NH), 9.65 (d, 1H, $J = 2.4$ Hz, ArH), 8.20 (d, 1H, $J = 8.8$ Hz, ArH), 7.86 (dd, 1H, $J = 8.8, 2.4$ Hz, ArH), 4.45 (q, 2H, $J = 7.1$ Hz, OCH_2CH_3), 2.47 (q, 2H, $J = 7.4$ Hz, $CH_2CH_2CH_3$), 1.81 (sextet, 2H, $J = 7.4$ Hz, $CH_2CH_2CH_3$), 1.46 (t, 3H, $J = 7.1$ Hz, OCH_2CH_3), 1.04 (t, 3H, $J = 7.4$ Hz, $CH_2CH_2CH_3$); ^{13}C NMR (101 MHz, $CDCl_3$): δ 172.3, 166.9, 151.2, 142.5, 131.9, 119.3, 116.3, 115.3, 62.4, 40.4, 18.8, 14.1, 13.7; HRMS (ESI): m/z $[M+H]^+$ calcd for $C_{13}H_{16}N_2O_5$: 281.1138, found: 281.1140.

(±)-2-Ethoxy-7-nitro-2-phenyl-1,2-dihydro-4H-benzo[*d*][1,3]oxazin-4-one (76d): Yield: 283 mg (90%, method 1) as off-white crystals; m.p. 180-181 °C; IR: 3257, 1673, 1651, 1600, 1538, 1346 cm^{-1} ; 1H NMR (400 MHz, $CDCl_3$): δ 11.62 (br s, 1H, NH), 9.31 (d, 1H, $J = 2.4$ Hz, ArH), 8.20 (d, 1H, $J = 8.8$ Hz, ArH), 8.03 (dd, 1H, $J = 8.8, 2.4$ Hz, ArH), 7.97 (d, 2H, $J = 7.4$ Hz, ArH), 7.69 (t, 1H, $J = 7.4$ Hz, ArH), 7.61 (t, 2H, $J = 7.4$ Hz, ArH), 4.38 (q, 2H, $J = 7.1$ Hz, OCH_2CH_3), 1.33 (t, 3H, $J = 7.1$ Hz, OCH_2CH_3); ^{13}C NMR (101 MHz, $CDCl_3$): δ 166.7, 165.7, 150.6, 141.0, 134.1, 133.1, 132.7, 129.5, 127.7, 1239, 118.2, 116.0, 62.6, 14.3; HRMS (ESI): m/z $[M+H]^+$ calcd for $C_{16}H_{14}N_2O_5$: 315.0981, found: 315.0975.

(±)-7-Chloro-2-ethoxy-2-methyl-1,2-dihydro-4H-benzo[*d*][1,3]oxazin-4-one (77a). Yield: 203 mg (84%, method 1) as white crystals; m.p. 75-76 °C; IR: 3262, 1681, 1578 cm^{-1} ; 1H NMR (400 MHz, $CDCl_3$): δ 10.70 (br s, 1H, NH), 8.43 (d, 1H, $J = 2.2$ Hz, ArH), 7.92 (d, 1H, $J = 8.6$ Hz, ArH), 7.23 (dd, 1H, $J = 8.6, 2.2$ Hz, ArH), 4.83 (q, 2H, $J = 7.1$ Hz, OCH_2CH_3), 2.15 (s, 3H, CH_3), 1.34 (t, 3H, $J = 7.1$ Hz, OCH_2CH_3); ^{13}C NMR (101 MHz, $CDCl_3$): δ 169.1, 167.7, 142.4, 140.8, 131.8, 122.6, 120.1, 113.2, 61.6, 25.5, 14.2; HRMS (ESI): m/z $[M+H]^+$ calcd for $C_{11}H_{12}^{35}ClNO_3$: 242.0584, found: 242.0582.

(±)-7-Chloro-2-ethoxy-2-ethyl-1,2-dihydro-4*H*-benzo[*d*][1,3]oxazin-4-one (77b). Yield: 215 mg (84%, method 1) and 220 mg (86%, method 2) as white crystals; m.p. 69-70 °C; IR: 3238, 1685, 1581 cm⁻¹; ¹H NMR (400 MHz, CDCl₃): δ 11.17 (br s, 1H, NH), 8.86 (d, 1H, *J* = 2.2 Hz, ArH), 7.96 (d, 1H, *J* = 8.6 Hz, ArH), 7.04 (dd, 1H, *J* = 8.6, 2.2 Hz, ArH), 4.38 (q, 2H, *J* = 7.1 Hz, OCH₂CH₃), 2.48 (q, 2H, *J* = 7.5 Hz, CH₂CH₃), 1.41 (t, 3H, *J* = 7.1 Hz, OCH₂CH₃), 1.27 (t, 3H, *J* = 7.5 Hz, CH₂CH₃); ¹³C NMR (101 MHz, CDCl₃): δ 173.0, 167.8, 142.6, 140.9, 131.8, 122.5, 120.2, 113.2, 61.6, 31.7, 14.2, 9.5; HRMS (ESI): *m/z* [M+H]⁺ calcd for C₁₂H₁₄³⁵ClNO₃: 256.0741, found: 256.0743.

(±)-7-Chloro-2-ethoxy-2-propyl-1,2-dihydro-4*H*-benzo[*d*][1,3]oxazin-4-one (77c). Yield: 224 mg (83%, method 1) and 227 mg (84%, method 2) as white semisolid; m.p. 25-26 °C; IR: 3280, 1691, 1581 cm⁻¹; ¹H NMR (400 MHz, CDCl₃): δ 11.16 (br s, 1H, NH), 8.85 (s, 1H, ArH), 7.96 (d, 1H, *J* = 8.6 Hz, ArH), 7.04 (dd, 1H, *J* = 8.6, 2.2 Hz, ArH), 4.38 (q, 2H, *J* = 7.1 Hz, OCH₂CH₃), 2.42 (q, 2H, *J* = 7.4 Hz, CH₂CH₂CH₃), 1.78 (sextet, 2H, *J* = 7.4 Hz, CH₂CH₂CH₃), 1.42 (t, 3H, *J* = 7.1 Hz, OCH₂CH₃), 1.02 (t, 3H, *J* = 7.4 Hz, CH₂CH₂CH₃); ¹³C NMR (101 MHz, CDCl₃): δ 172.2, 167.7, 142.5, 140.8, 131.8, 122.5, 120.2, 113.2, 61.6, 40.5, 18.9, 14.2, 13.2; HRMS (ESI): *m/z* [M+H]⁺ calcd for C₁₃H₁₆³⁵ClNO₃: 270.0897, found: 270.0893.

(±)-7-Chloro-2-ethoxy-2-phenyl-1,2-dihydro-4*H*-benzo[*d*][1,3]oxazin-4-one (77d). Yield: 258 mg (85%, method 1) as white crystals; m.p. 128-129 °C; IR: 3241, 1673, 1585 cm⁻¹; ¹H NMR (400 MHz, CDCl₃): δ 12.13 (br s, 1H, NH), 9.05 (d, 1H, *J* = 2.1 Hz, ArH), 8.03 (overlapping signals, apparent t, 3H, *J* ≈ 8.4 Hz, ArH), 7.60-7.49 (complex, 3H, ArH), 7.08 (dd, 1H, *J* = 8.6, 2.1 Hz, ArH), 4.42 (q, 2H, *J* = 7.1 Hz, OCH₂CH₃), 1.43 (t, 3H, *J* = 7.1 Hz, OCH₂CH₃); ¹³C NMR (101 MHz, CDCl₃): δ 168.1, 165.7, 142.7, 141.0, 134.4, 132.2, 132.0, 128.9, 127.4, 122.8, 120.3, 113.6, 61.8, 14.2; HRMS (ESI): *m/z* [M+H]⁺ calcd for C₁₆H₁₄³⁵ClNO₃: 304.0741, found: 304.0737.

(±)-2-Ethoxy-2-methyl-1,2-dihydro-4H-pyrido[2,3-*d*][1,3]oxazin-4-one (78a). Yield: 177 mg (85%, method 1) as white crystals; m.p. 55-56 °C; IR: 3270, 1680, 1589 cm⁻¹; ¹H NMR (400 MHz, CDCl₃): δ 10.79 (br s, 1H, NH), 8.59 (dd, 1H, *J* = 4.8, 2.0 Hz, PyH), 8.33 (dd, 1H, *J* = 7.9, 2.0 Hz, PyH), 7.06 (dd, 1H, *J* = 7.9, 4.8 Hz, PyH), 4.41 (q, 2H, *J* = 2.1 Hz, OCH₂CH₃), 2.42 (s, 3H, CH₃), 1.42 (t, 3H, *J* = 7.1 Hz, OCH₂CH₃); ¹³C NMR (101 MHz, CDCl₃): δ 169.6, 166.6, 152.9, 152.5, 140.0, 118.0, 111.1, 62.0, 26.0, 14.2; HRMS (ESI): *m/z* [M+H]⁺ calcd for C₁₀H₁₂N₂O₃: 209.0926, found: 209.0925.

2.3.3. Bis- and mono-1,3,4-oxadiazole synthesis promoted by catalytic NH₄Cl.

Representative procedure for the preparation bis- and mono-1,3,4-oxadiazoles.

The orthoester (2.2 equiv for **79-83** and 1.1 equiv for **85-91**) was added to a mixture of **79**, **81**, **83**, **85**, **86**, **89** or **91** (1.0 mmol) and ammonium chloride (60 mol% for **79-83** and 30 mol% for **85-91**) in DMSO (5 mL). The reaction was heated at 100 °C (oil bath) until TLC (10% MeOH in DCM) indicated complete conversion (1.5-96 h). The crude reaction mixture was cooled, added to water and extracted with DCM (2 x 15 mL). The combined organic layers were washed with saturated aq NaCl, dried (MgSO₄), and concentrated under vacuum to give the crude oxadiazoles. The crude products were stirred with 25% ether/hexane for 1 h, filtered and dried to give the bis-oxadiazoles **80**, **82** and **84** as well as the mono-1,3,4-oxadiazoles **87-90** and **92**.

1,4-Di(1,3,4-oxadiazol-2-yl)benzene (80a). Yield: 182 mg (0.85 mmol, 85%) as white crystals; m.p. 257-258 °C; IR (nujol): 1577 cm⁻¹; ¹H NMR (400 MHz, DMSO-*d*₆): δ 9.44 (s, 2H), 8.26 (s, 4H); ¹³C NMR (100 MHz, DMSO-*d*₆): δ 163.4, 155.5, 128.2, 126.5.

1,4-Bis(5-methyl-1,3,4-oxadiazol-2-yl)benzene (80b). Yield: 216 mg (0.89 mmol, 89%) as off-white crystals; m.p. 256-257 °C; IR (nujol): 1582 cm⁻¹; ¹H NMR (400 MHz, DMSO-*d*₆): δ 8.17 (s, 4H), 2.62 (s, 6H); ¹³C NMR (100 MHz, DMSO-*d*₆): δ 163.9, 162.6, 126.7, 125.4, 10.1.

1,4-Bis(5-ethyl-1,3,4-oxadiazol-2-yl)benzene (80c). Yield: 219 mg (0.81 mmol, 81%) as a white solid; m.p. 163-164 °C; IR (nujol): 1570 cm⁻¹; ¹H NMR (400 MHz, DMSO-*d*₆): δ 8.19 (s, 4H),

2.98 (q, $J = 7.5$ Hz, 4H), 1.35 (t, $J = 7.5$ Hz, 6H); ^{13}C NMR (100 MHz, DMSO- d_6): δ 168.7, 163.6, 127.8, 126.5, 18.9, 10.9.

1,4-Bis(5-propyl-1,3,4-oxadiazol-2-yl)benzene (80d). Yield: 239 mg (0.80 mmol, 80%) as a white flaky solid; m.p. 128-129 °C; IR (nujol): 1582, 1562 cm^{-1} ; ^1H NMR (400 MHz, DMSO- d_6): δ 8.18 (s, 4H), 2.94 (t, $J = 7.4$ Hz, 4H), 1.81 (sextet, $J = 7.4$ Hz, 4H), 1.00 (t, $J = 7.4$ Hz, 6H); ^{13}C NMR (100 MHz, DMSO- d_6): δ 167.2, 163.6, 127.8, 126.5, 26.9, 19.8, 13.8.

1,4-Bis(5-phenyl-1,3,4-oxadiazol-2-yl)benzene (80e). Yield: 278 mg (0.76 mmol, 76%) as a white solid; m.p. 321-322 °C; IR (nujol): 1585, 1559 cm^{-1} ; ^1H NMR (400 MHz, DMSO- d_6): δ 8.40 (s, 4H), 8.21-8.18 (complex, 4H), 7.70-7.64 (complex, 6H), ^{13}C NMR (100 MHz, DMSO- d_6): δ 164.4, 156.0, 131.9, 129.2, 126.7, 126.1, 119.3.

1,3-Di(1,3,4-oxadiazol-2-yl)benzene (82a). Yield: 180 mg (0.84 mmol, 84%) as a white solid; m.p. 189-190 °C; IR (nujol): 1535 cm^{-1} ; ^1H NMR (400 MHz, DMSO- d_6): δ 9.45 (s, 2H), 8.59 (t, $J = 1.8$ Hz, 1H), 8.28 (dd, $J = 7.9, 1.8$ Hz, 2H), 7.87 (t, $J = 7.9$ Hz, 1H); ^{13}C NMR (100 MHz, DMSO- d_6): δ 162.2, 154.3, 130.3, 129.3, 123.9, 123.8.

1,3-Bis(5-methyl-1,3,4-oxadiazol-2-yl)benzene (82b). Yield: 213 mg (0.88 mmol, 88%) as a white solid; m.p. 160-161 °C; IR (nujol): 1579 cm^{-1} ; ^1H NMR (400 MHz, DMSO- d_6): δ 8.47 (t, $J = 1.7$ Hz, 1H), 8.20 (dd, $J = 7.9, 1.7$ Hz, 2H), 7.82 (t, $J = 7.9$ Hz, 1H), 2.62 (s, 3H); ^{13}C NMR (100 MHz, DMSO- d_6): δ 164.9, 163.5, 131.3, 129.6, 125.1, 124.1, 11.1.

1,3-Bis(5-ethyl-1,3,4-oxadiazol-2-yl)benzene (82c). Yield: 232 mg (0.86 mmol, 86%) as a white solid; m.p. 139-140 °C; IR (nujol): 1570 cm^{-1} ; ^1H NMR (400 MHz, DMSO- d_6): δ 8.48 (t, $J = 1.8$ Hz, 1H), 8.20 (dd, $J = 7.9, 1.8$ Hz, 2H), 7.82 (t, $J = 7.9$ Hz, 1H), 2.99 (q, $J = 7.5$ Hz, 4H), 1.36 (t, $J = 7.5$ Hz, 6H); ^{13}C NMR (100 MHz, DMSO- d_6): δ 167.6, 162.4, 130.2, 128.6, 124.1, 123.1, 17.9, 9.8.

1,3-Bis(5-propyl-1,3,4-oxadiazol-2-yl)benzene (82d). Yield: 253 mg (0.85 mmol, 85%) as a white solid; m.p. 63-64 °C; IR (nujol): 1568 cm^{-1} ; ^1H NMR (400 MHz, DMSO- d_6): δ 8.49 (s, 1H), 8.21 (d, $J = 7.9$ Hz, 2H), 7.83 (t, $J = 7.9, 2.5$ Hz, 1H), 2.95 (t, $J = 7.3$ Hz, 4H), 1.82 (sextet, $J =$

7.3 Hz, 4H), 1.01 (t, $J = 7.3$ Hz, 6H); ^{13}C NMR (100 MHz, DMSO- d_6): δ 167.3, 163.5, 131.2, 129.7, 125.1, 124.2, 26.9, 19.9, 13.8.

1,3-Bis(5-phenyl-1,3,4-oxadiazol-2-yl)benzene (82e). Yield: 282 mg (0.77 mmol, 77%) as a white flaky solid; m.p. 235-236 °C; IR (nujol): 1550 cm^{-1} ; ^1H NMR (400 MHz, DMSO- d_6): δ 8.80 (t, $J = 1.7$ Hz, 1H), 8.41 (dd, $J = 7.9, 1.7$ Hz, 2H), 8.23-8.19 (complex, 4H), 7.92 (t, $J = 7.9$ Hz, 1H), 7.74-7.65 (complex, 6H); ^{13}C NMR (100 MHz, DMSO- d_6): δ 164.9, 163.8, 132.7, 131.3, 130.4, 130.0, 127.4, 125.1, 124.8, 123.7.

1,4-Di(1,3,4-oxadiazol-2-yl)butane (84a). Yield: 102 mg (0.53 mmol, 53%) as a light pink solid; m.p. 59-61 °C; IR (nujol): 3139, 1580, 1517 cm^{-1} ; ^1H NMR (400 MHz, DMSO- d_6): δ 9.13 (s, 2H), 2.93 (m, 4H), 1.78 (m, 4H); ^{13}C NMR (100 MHz, DMSO- d_6): δ 165.4, 153.7, 24.5, 23.2.

1,4-Bis(5-methyl-1,3,4-oxadiazol-2-yl)butane (84b). Yield: 44 mg (0.20 mmol, 20%) as a tan solid; m.p. 41-42 °C; IR (nujol): 1598, 1566 cm^{-1} ; ^1H NMR (400 MHz, DMSO- d_6): δ 2.85 (m, 4H), 2.44 (s, 6H), 1.76 (m, 4H); ^{13}C NMR (100 MHz, DMSO- d_6): δ 165.5, 162.8, 24.4, 23.3, 9.8.

1,4-Bis(5-ethyl-1,3,4-oxadiazol-2-yl)butane (84c). Yield: 198 mg (0.79 mmol, 79%) as a white solid; m.p. 34-35 °C; IR (nujol): 1594, 1563 cm^{-1} ; ^1H NMR (400 MHz, DMSO- d_6): δ 2.86 (m, 4H), 2.83 (q, $J = 7.5$ Hz, 4H), 1.76 (m, 4H), 1.24 (t, $J = 7.5$ Hz, 6H); ^{13}C NMR (100 MHz, DMSO- d_6): δ 166.7, 165.5, 24.5, 23.4, 17.6, 9.9.

1,4-Bis(5-phenyl-1,3,4-oxadiazol-2-yl)butane (84e). Yield: 194 mg (0.56 mmol, 56%) as a cream solid; m.p. 133-135 °C; IR (nujol): 1569, 1546 cm^{-1} ; ^1H NMR (400 MHz, DMSO- d_6): δ 7.98 (dd, $J = 8.1, 1.9$ Hz, 4H), 7.65-7.55 (complex, 6H), 3.03 (m, 4H), 1.91 (m, 4H); ^{13}C NMR (100 MHz, DMSO- d_6): δ 167.1, 164.3, 132.2, 129.9, 126.8, 124.0, 25.5, 24.6.

2-(4-Nitrophenyl)-1,3,4-oxadiazole (87a). Yield: 176 mg (0.92 mmol, 92%) as an off-white solid; m.p. 152-153 °C; IR (nujol): 1554, 1538, 1525, 1341 cm^{-1} ; ^1H NMR (400 MHz, DMSO- d_6): δ 9.49 (s, 1H), 8.44 (d, $J = 8.9$ Hz, 2H), 8.30 (d, $J = 8.9$ Hz, 2H); ^{13}C NMR (100 MHz, DMSO- d_6): δ 162.9, 155.9, 149.7, 129.2, 128.6, 125.1.

2-Methyl-5-(4-nitrophenyl)-1,3,4-oxadiazole (87b). Yield: 174 mg (0.85 mmol, 85%) as an off-white solid; m.p. 163-164 °C; IR (nujol): 1573, 1551, 1522, 1354 cm⁻¹; ¹H NMR (400 MHz, DMSO-*d*₆): δ 8.42 (d, *J* = 8.9 Hz, 2H), 8.24 (d, *J* = 8.9 Hz, 2H), 2.63 (s, 3H); ¹³C NMR (100 MHz, DMSO-*d*₆): δ 165.5, 163.1, 149.5, 129.5, 128.2, 125.1, 11.2.

2-Ethyl-5-(4-nitrophenyl)-1,3,4-oxadiazole (87c). Yield: 193 mg (0.88 mmol, 88%) as an off-white solid; m.p. 113-114 °C; IR (nujol): 1564, 1540, 1514, 1353 cm⁻¹; ¹H NMR (400 MHz, DMSO-*d*₆): δ 8.42 (d, *J* = 8.9 Hz, 2H), 8.24 (d, *J* = 8.9 Hz, 2H), 2.99 (q, *J* = 7.5 Hz, 2H), 1.35 (t, *J* = 7.5 Hz, 3H); ¹³C NMR (100 MHz, DMSO-*d*₆): δ 169.2, 163.0, 149.5, 129.5, 128.2, 125.0, 19.0, 10.8.

2-(4-Nitrophenyl)-5-propyl-1,3,4-oxadiazole (87d). Yield: 210 mg (0.90 mmol, 90%) as an off-white solid; m.p. 109-110 °C; IR (nujol): 1568, 1548, 1512, 1352 cm⁻¹; ¹H NMR (400 MHz, DMSO-*d*₆): δ 8.42 (d, *J* = 8.9 Hz, 2H), 8.24 (d, *J* = 8.9 Hz, 2H), 2.95 (t, *J* = 7.4 Hz, 2H), 1.81 (sextet, *J* = 7.4 Hz, 2H), 1.00 (t, *J* = 7.4 Hz, 3H); ¹³C NMR (100 MHz, DMSO-*d*₆): δ 168.2, 163.0, 149.5, 129.5, 128.2, 125.1, 26.9, 19.8, 13.8.

2-(4-Nitrophenyl)-5-phenyl-1,3,4-oxadiazole (87e). Yield: 208 mg (0.78 mmol, 78%) as yellow crystals; m.p. 203-204 °C; IR (nujol): 1548, 1513, 1344 cm⁻¹; ¹H NMR (400 MHz, DMSO-*d*₆): δ 8.47 (d, *J* = 8.9 Hz, 2H), 8.41 (d, *J* = 8.9 Hz, 2H), 8.19 (dd, *J* = 6.0, 1.7 Hz, 2H), 7.72-7.64 (complex, 3H); ¹³C NMR (100 MHz, DMSO-*d*₆): δ 165.3, 163.2, 149.7, 132.9, 130.0, 129.4, 128.5, 127.4, 125.1, 123.5.

2-(4-Methoxyphenyl)-1,3,4-oxadiazole (88a). Yield: 166 mg (0.94 mmol, 94%) as white crystals; m.p. 54-55 °C; IR (nujol): 2839, 1613, 1596, 1263 cm⁻¹; ¹H NMR (400 MHz, DMSO-*d*₆): δ 9.27 (s, 1H), 7.97 (d, *J* = 8.9 Hz, 2H), 7.16 (d, *J* = 8.9 Hz, 2H), 3.85 (s, 3H); ¹³C NMR (100 MHz, DMSO-*d*₆): δ 164.0, 162.5, 154.5, 129.0, 116.0, 115.4, 56.0.

2-(4-Methoxyphenyl)-5-methyl-1,3,4-oxadiazole (88b). Yield: 177 mg (0.93 mmol, 93%) as white crystals; m.p. 79-80 °C; IR (nujol): 2835, 1609, 1589, 1508, 1256 cm⁻¹; ¹H NMR (400

MHz, DMSO-*d*₆): δ 7.91 (d, *J* = 8.9 Hz, 2H), 7.13 (d, *J* = 8.9 Hz, 2H), 3.85 (s, 3H), 2.56 (s, 3H); ¹³C NMR (100 MHz, DMSO-*d*₆): δ 1643, 163.8, 162.3, 128.6, 116.4, 115.3, 56.0, 11.1.

2-Ethyl-5-(4-methoxyphenyl)-1,3,4-oxadiazole (88c). Yield: 188 mg (0.92 mmol, 92%) as white crystals; m.p. 48-49 °C; IR (nujol): 2834, 1615, 1591, 1581, 1255 cm⁻¹; ¹H NMR (400 MHz, DMSO-*d*₆): δ 7.92, (d, *J* = 8.8 Hz, 2H), 7.13 (d, *J* = 8.8 Hz, 2H), 3.85 (s, 3H), 2.92 (q, *J* = 7.5 Hz, 2H), 1.32 (t, *J* = 7.5 Hz, 3H); ¹³C NMR (100 MHz, DMSO-*d*₆): δ 167.6, 164.2, 162.3, 128.6, 116.4, 115.3, 55.9, 18.9, 11.0.

2-(4-Methoxyphenyl)-5-propyl-1,3,4-oxadiazole (88d). Yield: 192 mg (0.88 mmol, 88%) as white crystals; m.p. 50-51 °C; IR (nujol): 2841, 1621, 1599, 1579, 1259 cm⁻¹; ¹H NMR (400 MHz, DMSO-*d*₆): δ 7.91 (d, *J* = 8.9 Hz, 2H), 7.13 (d, *J* = 8.9 Hz, 2H), 3.85 (s, 3H), 2.88 (t, *J* = 7.4 Hz, 2H), 1.77 (sextet, *J* = 7.4 Hz, 2H), 0.99 (t, *J* = 7.4 Hz, 3H); ¹³C NMR (100 MHz, DMSO-*d*₆): δ 165.5, 163.1, 161.2, 127.6, 115.3, 114.2, 54.9, 25.8, 18.8, 12.8.

2-(4-Methoxyphenyl)-5-phenyl-1,3,4-oxadiazole (88e). Yield: 203 mg (0.80 mmol, 80%) as a white flaky solid; m.p. 141-142 °C; IR (nujol): 2840, 1611, 1551, 1263 cm⁻¹; ¹H NMR (400 MHz, DMSO-*d*₆): δ 8.16-8.11 (complex, 2H), 8.10 (d, *J* = 8.9 Hz, 2H), 8.09 (d, *J* = 8.9 Hz, 2H), 7.68-7.60 (complex, 3H), 3.87 (s, 3H); ¹³C NMR (100 MHz, DMSO-*d*₆): δ 163.4, 162.9, 161.5, 131.9, 128.8, 128.0, 126.0, 122.9, 115.1, 114.3, 55.0.

2-(Pyridin-3-yl)-1,3,4-oxadiazole (90a). Yield: 141 mg (0.96 mmol, 96%) as a white solid; m.p. 68-69 °C; IR: 3070, 1568, 1514, 1436 cm⁻¹; ¹H NMR (400 MHz, CDCl₃): δ 9.32 (d, *J* = 2.1 Hz, 1H), 8.81 (dd, *J* = 4.9, 1.7 Hz, 1H), 8.55 (s, 1H), 8.40 (dt, *J* = 8.0, 2.1 Hz, 1H), 7.50 (dd, *J* = 8.0, 4.9 Hz, 1H); ¹³C NMR (100 MHz, CDCl₃): δ 162.8, 153.0, 152.8, 148.1, 134.4, 123.9, 120.6.

2-Methyl-5-(pyridin-3-yl)-1,3,4-oxadiazole (90b). Yield: 113 mg (0.70 mmol, 70%) as a light pink solid; m.p. 109-110 °C; IR: 3073, 1585, 1430 cm⁻¹; ¹H NMR (400 MHz, CDCl₃): δ 9.25 (d, *J* = 2.2 Hz, 1H), 8.77 (dd, *J* = 4.9, 1.7 Hz, 1H), 8.34 (dt, *J* = 8.1, 2.2 Hz, 1H), 7.47 (dd, *J* = 8.1, 4.9 Hz, 1H), 2.66 (s, 3H); ¹³C NMR (100 MHz, CDCl₃): δ 164.2, 162.9, 152.3, 147.8, 134.0, 123.8, 120.5, 11.1.

2-Ethyl-5-(pyridin-3-yl)-1,3,4-oxadiazole (90c). Yield: 140 mg (0.80 mmol, 80%) as a pale yellow slurry; IR: 3057, 1578, 1434 cm^{-1} ; ^1H NMR (400 MHz, CDCl_3): δ 9.25 (s, 1H), 8.76 (dd, $J = 4.9, 1.7$ Hz, 1H), 8.35 (dq, $J = 8.1, 2.1$ Hz, 1H), 7.47 (dd, $J = 8.1, 4.9$ Hz, 1H), 3.00 (q, $J = 7.6$ Hz, 2H); 1.47 (t, $J = 7.6$ Hz, 2H); ^{13}C NMR (100 MHz, CDCl_3): δ 168.3, 162.6, 152.2, 147.7, 134.0, 123.8, 19.2, 10.8.

2-Propyl-5-(pyridin-3-yl)-1,3,4-oxadiazole (90d). Yield: 157 mg (0.83 mmol, 83%) as an orange oil; IR: 3047, 1578, 1464 cm^{-1} ; ^1H NMR (400 MHz, CDCl_3): δ 9.26 (d, $J = 2.2$ Hz, 1H), 8.77 (dd, $J = 4.9, 1.7$ Hz, 1H), 8.35 (dt, $J = 8.1, 2.0$ Hz, 1H), 7.47 (dd, $J = 8.1, 4.9$ Hz, 1H), 2.94 (t, $J = 7.4$ Hz, 2H), 1.90 (sextet, $J = 7.4$ Hz, 2H), 1.08 (t, $J = 7.4$ Hz, 3H); ^{13}C NMR (100 MHz, CDCl_3): δ 167.5, 162.7, 152.3, 147.8, 134.0, 123.8, 120.6, 27.3, 20.1, 13.6.

2-Phenyl-5-(pyridin-3-yl)-1,3,4-oxadiazole (90e). Yield: 179 mg (0.80 mmol, 80%) as a white solid; m.p. 119-120 $^\circ\text{C}$; IR: 3058, 1597, 1448 cm^{-1} ; ^1H NMR (400 MHz, CDCl_3): δ 9.37 (d, $J = 2.2$ Hz, 1H), 8.81 (dd, $J = 4.9, 1.7$ Hz, 1H), 8.46 (dt, $J = 8.0, 2.1$ Hz, 1H), 8.17 (d, $J = 8.1$ Hz, 2H), 7.60-7.54 (complex, 3H); 7.51 (dd, $J = 8.0, 4.9$ Hz, 1H); ^{13}C NMR (100 MHz, CDCl_3): δ 165.1, 162.5, 152.5, 147.9, 134.2, 132.1, 129.2, 127.1, 123.9, 123.5, 120.5.

2-(Pyridin-4-yl)-1,3,4-oxadiazole (92a). Yield: 125 mg (0.85 mmol, 85%) as light tan crystals; m.p. 116-117 $^\circ\text{C}$; IR: 3061, 1538, 1497, 1411 cm^{-1} ; ^1H NMR (400 MHz, CDCl_3): δ 8.86 (br s, 2H), 8.58 (s, 1H), 7.96 (d, $J = 6.1$ Hz, 2H); ^{13}C NMR (100 MHz, CDCl_3): δ 163.1, 153.4, 151.0, 130.6, 120.5.

2-Methyl-5-(pyridin-4-yl)-1,3,4-oxadiazole (92b). Yield: 139 mg (0.86 mmol, 86%) as a light tan solid; m.p. 147-148 $^\circ\text{C}$; IR: 3059, 1572, 1411 cm^{-1} ; ^1H NMR (400 MHz, CDCl_3): δ 8.81 (d, $J = 6.1$ Hz, 2H), 7.89 (d, $J = 6.1$ Hz, 2H), 2.67 (s, 3H); ^{13}C NMR (100 MHz, CDCl_3): δ 164.7, 163.2, 150.9, 131.0, 120.2, 11.2.

2-Ethyl-5-(pyridin-4-yl)-1,3,4-oxadiazole (92c). Yield: 149 mg (0.85 mmol, 85%) as a pale yellow solid; m.p. 51-52 $^\circ\text{C}$; IR: 3046, 1563, 1413 cm^{-1} ; ^1H NMR (400 MHz, CDCl_3): δ 8.81 (d, J

= 6.1 Hz, 2H), 7.90 (d, $J = 6.1$ Hz, 2H), 3.00 (q, $J = 7.6$ Hz, 2H), 1.47 (t, $J = 7.6$ Hz, 3H); ^{13}C NMR (100 MHz, CDCl_3): δ 168.8, 163.0, 150.9, 131.2, 120.3, 19.3, 10.8.

2-Propyl-5-(pyridin-4-yl)-1,3,4-oxadiazole (92d). Yield: 163 mg (0.86 mmol, 86%) as a pale yellow solid; m.p. 41-42 °C; IR: 3041, 1563, 1414 cm^{-1} ; ^1H NMR (400 MHz, CDCl_3): δ 8.81 (d, $J = 6.1$ Hz, 2H), 7.90 (d, $J = 6.1$ Hz, 2H), 2.95 (t, $J = 7.4$ Hz, 2H), 1.91 (sextet, $J = 7.4$ Hz, 2H), 1.08 (t, $J = 7.4$ Hz, 3H); ^{13}C NMR (100 MHz, CDCl_3): δ 167.9, 163.0, 150.9, 131.2, 120.2, 27.3, 20.1, 13.6.

2-Phenyl-5-(pyridin-4-yl)-1,3,4-oxadiazole (92e). Yield: 196 mg (0.88 mmol, 88%) as a pale yellow solid; m.p. 133-134 °C; IR: 3038, 1542, 1449, 1411 cm^{-1} ; ^1H NMR (400 MHz, CDCl_3): δ 8.86 (d, $J = 6.1$ Hz, 2H), 8.17 (d, $J = 7.9$ Hz, 2H), 8.01 (d, $J = 6.1$ Hz, 2H), 7.63-7.54 (complex, 3H); ^{13}C NMR (100 MHz, CDCl_3): δ 165.1, 162.5, 152.5, 147.9, 134.2, 132.1, 129.2, 127.1, 123.9, 123.5, 120.5.

2.3.4. Naphthalenes and heterocycles from Morita-Baylis-Hillman (MBH) acetates by domino Michael addition-elimination- $\text{S}_{\text{N}}\text{Ar}$ reactions.

Representative procedure for the synthesis of MBH alcohols (95a-h).

To a stirred solution of the aldehyde **47a-c** (1 equiv) and DABCO (1.5 equiv) in CH_3CN (8 mL) under N_2 was added the corresponding acrylate **94a** or acrylonitrile **94b** (2 equiv) at room temperature. After 24-48 h, TLC analysis (10% EtOAc/hexane) indicated completion of reaction, and the solution was partitioned between H_2O and EtOAc. The organic layer was washed with 1M HCl (2 \times), and saturated NaHCO_3 . The combined aqueous layers were back extracted with EtOAc (3 \times), and all of the combined organic layers were washed with saturated NaCl and dried (Na_2SO_4). Removal of the solvent under vacuum resulted in pure MBH alcohols **95a-h**, which were used without any further purification.

Representative procedure for the synthesis of MBH acetates (96a-f).

A solution of the corresponding MBH alcohol **95a-f** (1 mmol) in CH₂Cl₂ (2 mL) was treated with acetic anhydride (1.5 mmol) at 0 °C, followed by a CH₂Cl₂ solution of TMSOTf (1 M; 20 μL). After 30 minutes, TLC analysis (10% ether/hexane) showed completion of reaction. Treatment of the reaction mixture with NaHCO₃ gave two phases, of which the organic extracts were washed with water and dried (Na₂SO₄). Evaporation of the solvent under vacuum afforded clean MBH acetates **96a-f**, which did not require any further purification.

Ethyl 2-(acetoxymethyl(2-fluoro-5-nitrophenyl)methyl)acrylate (96a). Yield: 305 mg (0.98 mmol, 98%) as a colorless oil; IR: 1751, 1723, 1639, 1532, 1351 cm⁻¹; ¹H NMR (400 MHz, CDCl₃): δ 8.26 (dd, *J* = 6.0, 2.8 Hz, 1H), 8.23 (ddd, *J* = 8.9, 4.3, 2.9 Hz, 1H), 7.22 (t, *J* = 8.9 Hz, 2H), 6.91 (s, 1H), 6.54 (s, 1H), 4.18 (qd, *J* = 7.1, 1.3 Hz, 2H), 2.15 (s, 3H), 1.25 (q, *J* = 7.1 Hz, 3H); ¹³C NMR (100 MHz, CDCl₃): δ 182.6, 169.0, 164.22 (d, *J* = 232.5 Hz), 144.2, 137.4, 127.4, 126.0 (d, *J* = 10.2 Hz), 125.2 (d, *J* = 5.2 Hz), 116.9, 116.7, 66.6, 61.4, 20.9, 13.9.

2-Cyano-1-(2-fluoro-5-nitrophenyl)allyl acetate (96b). Yield: 259 mg (0.98 mmol, 98%) as off-white crystals; m.p. 66-67 °C; IR: 2232, 1759, 1632, 1532, 1535, 1352 cm⁻¹; ¹H NMR (400 MHz, CDCl₃): δ 8.42 (dd, *J* = 6.1, 2.8 Hz, 1H), 8.31 (ddd, *J* = 9.0, 4.4, 2.8 Hz, 1H), 7.29 (t, *J* = 9.0 Hz, 1H), 6.64 (s, 1H), 6.19 (s, 1H), 6.18 (s, 1H), 2.26 (s, 3H); ¹³C NMR (100 MHz, CDCl₃): δ 168.8, 163.1 (d, *J* = 260.1 Hz), 144.7, 133.7, 126.8 (d, *J* = 10.3 Hz), 125.3 (d, *J* = 15.1 Hz), 124.1 (d, *J* = 4.9 Hz), 120.9, 117.1 (d, *J* = 23.7 Hz), 115.2, 67.8 (d, *J* = 3.0 Hz), 20.8.

2-Cyano-1-(5-cyano-2-fluorophenyl)allyl acetate (96c). Yield: 259 mg (0.98 mmol, 98%) as off-white crystals; m.p. 74-75 °C; IR: 2255, 2235, 1757, 1613 cm⁻¹; ¹H NMR (400 MHz, CDCl₃): δ 7.86 (dd, *J* = 6.6, 2.1 Hz, 1H), 7.72 (ddd, *J* = 8.4, 4.8, 2.1 Hz, 1H), 7.24 (t, *J* = 9.3 Hz, 1H), 6.60 (s, 1H), 6.16 (s, 1H), 6.15 (s, 1H), 2.24 (s, 3H); ¹³C NMR (100 MHz, CDCl₃): δ 168.8, 161.9 (d, *J* = 259.0 Hz), 135.2 (d, *J* = 9.8 Hz), 133.7, 132.3 (d, *J* = 4.3 Hz), 125.6 (d, *J* = 14.2 Hz), 120.9, 117.44 (d, *J* = 22.8 Hz), 117.41, 115.3, 109.6 (d, *J* = 4.0 Hz), 67.8 (d, *J* = 3.2 Hz), 20.8.

Ethyl 2-(acetoxymethyl(5-cyano-2-fluorophenyl)methyl)acrylate (96d). Yield: 285 mg (0.98 mmol, 98%) as a colorless oil; IR: 2234, 1752, 1729, 1637 cm^{-1} ; ^1H NMR (400 MHz, CDCl_3): δ 7.69 (dd, $J = 6.6, 2.1$ Hz, 1H), 7.64 (ddd, $J = 8.5, 4.7, 2.1$ Hz, 1H), 7.19 (t, $J = 9.3$ Hz, 1H), 6.88 (s, 1H), 6.51 (s, 1H), 5.92 (s, 1H), 4.19 (q, $J = 7.1$ Hz, 2H), 2.15 (s, 3H), 1.25 (t, $J = 7.1$ Hz, 3H); ^{13}C NMR (100 MHz, CDCl_3): δ 169.0, 164.2, 162.6 (d, $J = 260.3$ Hz), 137.6, 134.4 (d, $J = 9.8$ Hz), 133.6 (d, $J = 4.8$ Hz), 127.7 (d, $J = 14.9$ Hz), 127.3, 117.8, 117.2 (d, $J = 23.4$ Hz), 108.7 (d, $J = 4.0$ Hz), 66.6 (d, $J = 2.9$ Hz), 61.3, 20.8, 14.0.

2-Cyano-1-(2,5-difluorophenyl)allyl acetate (96e). Yield: 232 mg (0.98 mmol, 98%) as a white solid; m.p. 49-50 $^\circ\text{C}$; IR: 2256, 2232, 1752, 1627 cm^{-1} ; ^1H NMR (400 MHz, CDCl_3): δ 7.22 (m, 1H), 7.07 (m, 2H), 6.58 (s, 1H), 6.12 (s, 1H), 6.10 (s, 1H), 2.21 (s, 3H); ^{13}C NMR (100 MHz, CDCl_3): δ 168.8, 158.8 (d, $J = 244.2$ Hz), 155.7 (d, $J = 243.7$ Hz), 133.2, 124.9 (dd, $J = 15.4, 7.4$ Hz), 121.5, 117.4 (dd, $J = 24.2, 8.7$ Hz), 117.1 (dd, $J = 24.1, 8.5$ Hz), 115.6, 114.6 (dd, $J = 25.6, 3.3$ Hz), 68.1 (d, $J = 3.1$ Hz), 20.8.

Ethyl 2-(acetoxymethyl(2,5-difluorophenyl)methyl)acrylate (96f). Yield: 278 mg (0.98 mmol, 98%) as a colorless oil; IR: 1752, 1723, 1638 cm^{-1} ; ^1H NMR (400 MHz, CDCl_3): δ 7.05-6.95 (complex, 3H), 6.88 (s, 1H), 6.47 (s, 1H), 5.82 (s, 1H), 4.18 (q, $J = 7.1$ Hz, 2H), 2.12 (s, 3H), 1.24 (t, $J = 7.1$ Hz, 3H); ^{13}C NMR (100 MHz, CDCl_3): δ 169.1, 164.5 (d, $J = 242.2$ Hz), 158.5, 156.2, 148.8, 138.2, 133.5, 126.9, 116.7 (ddd, 24.7, 24.7, 8.5 Hz), 115.4 (dd, $J = 25.0, 3.8$ Hz), 62.0, 61.2, 20.9, 14.0.

Representative procedure for the synthesis of MBH acetates (96g and 96h) using MBH alcohols derived from 2-fluoronicotinaldehyde.

To a solution of the corresponding MBH alcohol **95g,h** (1 mmol) in CH_2Cl_2 (2 mL) at 0 $^\circ\text{C}$, was added acetic anhydride (4.5 mmol), and a CH_2Cl_2 solution of TMSOTf (1 M; 6 mmol), in a portionwise fashion over 1 h. Upon completion of reaction (TLC analysis using 20% EtOAc/hexane), the reaction mixture was quenched with stoichiometric amount of methanol (relative to acetic anhydride used). Treatment of the mixture with NaHCO_3 gave two phases, of

which the organic extracts were washed with water, and dried (Na₂SO₄). Evaporation of the solvent under vacuum afforded clean MBH acetates **96g,h**, which did not require any further purification.

2-Cyano-1-(2-fluoropyridin-3-yl)allyl acetate (96g). Yield: 209 mg (0.95 mmol, 95%) as a colorless oil; IR: 2231, 1756, 1609 cm⁻¹; ¹H NMR (400 MHz, CDCl₃): δ 8.26 (m, 1H), 7.99 (tm, *J* = 8.5 Hz, 1H), 7.30 (m, 1H), 6.53 (s, 1H), 6.19 (m, 1H), 6.17 (m, 1H), 2.21 (s, 3H); ¹³C NMR (100 MHz, CDCl₃): δ 168.8, 160.2 (d, *J* = 240.0 Hz), 148.4 (d, *J* = 15.0 Hz), 138.8 (d, *J* = 3.7 Hz), 133.8, 122.0 (d, *J* = 4.4 Hz), 120.9, 118.5 (d, *J* = 27.9 Hz), 115.4, 68.5 (d, *J* = 2.9, 3.3 Hz), 20.8.

Ethyl 2-(acetoxymethyl)acrylate (96h). Yield: 254 mg (0.95 mmol, 95%) as a colorless oil; IR: 1758, 1727, 1637 cm⁻¹; ¹H NMR (400 MHz, CDCl₃): δ 8.19 (m, 1H), 7.81 (ddd, *J* = 9.4, 7.4, 2.0 Hz, 1H), 7.20 (ddd, *J* = 6.5, 4.8, 1.6 Hz, 1H), 6.81 (s, 1H), 6.50 (s, 1H), 5.92 (s, 1H), 4.18 (q, *J* = 7.1 Hz, 2H), 2.14 (s, 3H), 1.24 (t, *J* = 7.1 Hz, 3H); ¹³C NMR (100 MHz, CDCl₃): δ 169.1, 164.4, 161.0 (d, *J* = 241.9 Hz), 147.6 (d, *J* = 14.9 Hz), 140.1 (d, *J* = 4.3 Hz), 137.5, 127.2 (d, *J* = 1.2 Hz), 121.4 (d, *J* = 4.4 Hz), 120.5 (d, *J* = 27.9 Hz), 61.2, 20.8, 14.0.

Representative procedure for the synthesis of naphthalene derivatives using MBH acetates and active methylene compounds.

A 50-mL, round-bottomed flask equipped with a condenser, stir bar and vacuum adapter, was charged with MBH acetate **96b** (1 mmol) in 1 mL of DMF under N₂. The corresponding active methylene compound (1.5 mmol) and K₂CO₃ (1.5 mmol) were added at room temperature with continued stirring. TLC analysis (30% EtOAc/hexane) indicated complete consumption of the starting material after 1 h. The solution was poured into 15 mL of de-ionized water, of which the mixture was extracted with EtOAc (3×). The combined organic layers were washed with saturated NaCl and dried (Na₂SO₄). Removal of the solvent under vacuum gave the crude product, which was purified by silica gel column chromatography to afford the pure naphthalene derivatives.

6-Nitronaphthalene-1,3-dicarbonitrile (98a) from 96b and ethyl cyanoacetate. Yield: 178 mg (0.80 mmol, 80%) as a white solid; m.p. 224 °C (dec.); IR: 2250, 1541, 1354 cm^{-1} ; ^1H NMR (400 MHz, CDCl_3): δ 8.97 (d, $J = 2.2$ Hz, 1H), 8.67 (s, 1H), 8.65 (dd, $J = 9.1, 2.2$ Hz, 1H), 8.51 (d, $J = 9.2$ Hz, 1H), 8.26 (d, $J = 1.6$ Hz, 1H); ^{13}C NMR (100 MHz, CDCl_3): δ 147.6, 139.7, 135.7, 135.5, 131.4, 127.9, 125.3, 125.0, 116.0, 114.9, 113.2, 112.0.

Methyl 3-cyano-6-nitro-1-naphthoate (98b) from 96b and methyl phenylsulfonylacetate. Yield: 220 mg (0.86 mmol, 86%) as a white solid; m.p. 219-220 °C; IR: 2254, 1708, 1534, 1350 cm^{-1} ; ^1H NMR (400 MHz, CDCl_3): δ 9.26 (d, $J = 9.5$ Hz, 1H), 8.89 (d, $J = 2.4$ Hz, 1H), 8.58 (s, 1H), 8.54 (d, $J = 1.7$ Hz, 1H), 8.51 (dd, $J = 9.5, 2.4$ Hz, 1H), 4.08 (s, 3H); ^{13}C NMR (100 MHz, CDCl_3): δ 165.3, 146.5, 139.8, 135.0, 133.8, 132.2, 129.1, 128.6, 125.0, 123.8, 117.1, 111.3, 53.1.

Ethyl 3-cyano-6-nitro-1-naphthoate (98c) from 96b and ethyl nitroacetate. Yield: 238 mg (0.88 mmol, 88%) as a white solid; m.p. 156-157 °C; IR: 2254, 1722, 1629, 1535, 1350 cm^{-1} ; ^1H NMR (400 MHz, CDCl_3): δ 9.26 (d, $J = 9.5$ Hz, 1H), 8.89 (d, $J = 2.4$ Hz, 1H), 8.58 (s, 1H), 8.53 (s, 1H), 8.51 (dd, $J = 9.5, 2.4$ Hz, 1H), 4.54 (q, $J = 7.1$ Hz, 2H), 1.50 (t, $J = 7.1$ Hz, 3H); ^{13}C NMR (100 MHz, CDCl_3): δ 164.9, 146.5, 139.6, 135.0, 133.7, 132.1, 129.5, 128.7, 125.0, 123.7, 117.2, 111.3, 62.4, 14.3.

Representative procedure for the synthesis of dihydroheteroaromatics using MBH acetates and 1° alkyl or aromatic amines.

To a solution of MBH acetate (1 mmol) in 1 mL of DMF under N_2 was added the corresponding amine (1.5 mmol), and the mixture was stirred at room temperature for 2 h. K_2CO_3 (1.5 mmol) was added at 23 °C, and the temperature was gradually increased to 50 °C, with continued stirring for 2 h (alternatively, only 2.0 equiv of the corresponding amine can be used without K_2CO_3 , and the temperature can gradually be increased to 50 °C immediately after addition of the amine). After TLC (20% EtOAc/hexane) has indicated complete consumption of the starting material, the solution was poured into 15 mL of DI water, and extracted with EtOAc (3×). The organic layer was washed with 1M HCl (2×), followed by saturated NaHCO_3 (2×). The combined organic

layers were washed with saturated NaCl and dried (Na₂SO₄). Removal of the solvent under vacuum gave a crude product, which was further purified by column chromatograph to afford the dihydroheteroaromatic compounds.

1-Methyl-6-nitro-1,2-dihydroquinoline-3-carbonitrile (100a) from 96b and methylamine.

Yield: 189 mg (0.88 mmol, 88%) as an orange solid; m.p. 186-187 °C; IR: 2210, 1640, 1515, 1321 cm⁻¹; ¹H NMR (400 MHz, CDCl₃): δ 8.05 (dd, *J* = 9.2, 2.7 Hz, 1H), 7.82 (d, *J* = 2.7 Hz, 1H), 7.00 (br s, 1H), 6.47 (d, *J* = 9.2 Hz, 1H), 4.41 (d, *J* = 1.6 Hz, 2H), 2.94 (s, 3H); ¹³C NMR (100 MHz, CDCl₃): δ 150.5, 139.0, 137.7, 128.7, 125.0, 117.5, 116.5, 109.6, 103.7, 51.5, 37.6.

1-Hexyl-6-nitro-1,2-dihydroquinoline-3-carbonitrile (100b) from 96b and *n*-hexylamine.

Yield: 222 mg (0.78 mmol, 78%) as a yellow solid; m.p. 110-111 °C; IR: 2228, 1647, 1532, 1344 cm⁻¹; ¹H NMR (400 MHz, CDCl₃): δ 8.02 (dd, *J* = 9.3, 2.7 Hz, 1H), 7.80 (d, *J* = 2.7 Hz, 1H), 6.97 (br s, 1H), 6.44 (d, *J* = 9.3 Hz, 1H), 4.43 (s, 3H), 3.25 (t, *J* = 7.2 Hz, 2H), 1.62 (quintet, *J* = 7.5 Hz, 2H), 1.36 (m, 6H), 0.92 (t, *J* = 6.8 Hz, 3H); ¹³C NMR (100 MHz, CDCl₃): δ 149.8, 139.2, 137.6, 128.9, 125.5, 117.4, 116.7, 109.6, 103.3, 50.9, 50.3, 31.5, 26.6, 25.0, 22.6, 14.0.

1-isoButyl-6-nitro-1,2-dihydroquinoline-3-carbonitrile (100c) from 96b and isobutylamine.

Yield: 203 mg (0.79 mmol, 79%) as a yellow solid; m.p. 158-159 °C; IR: 2208, 1642, 1519, 1324 cm⁻¹; ¹H NMR (400 MHz, CDCl₃): δ 8.00 (d, *J* = 9.3 Hz, 1H), 7.80 (s, 1H), 6.96 (s, 1H), 6.47 (d, *J* = 9.3 Hz, 1H), 4.44 (s, 2H), 3.08 (d, *J* = 7.5 Hz, 2H), 2.11 (septet, *J* = 6.7 Hz, 1H), 1.02 (d, *J* = 6.7 Hz, 6H); ¹³C NMR (100 MHz, CDCl₃): δ 150.3, 139.3, 137.6, 128.7, 125.6, 117.4, 116.7, 110.2, 103.1, 58.4, 51.3, 26.2, 20.2.

1-Benzyl-6-nitro-1,2-dihydroquinoline-3-carbonitrile (100d) from 96b and benzylamine.

Yield: 233 mg (0.80 mmol, 80%) as a yellow solid; m.p. 154-155 °C; IR: 2231, 1648, 1530, 1345 cm⁻¹; ¹H NMR (400 MHz, CDCl₃): δ 7.99 (dd, *J* = 9.2, 2.6 Hz, 1H), 7.86 (d, *J* = 2.6 Hz, 1H), 7.43-7.32 (complex, 3H), 7.23 (d, *J* = 8.5 Hz, 2H), 7.04 (s, 1H), 6.54 (d, *J* = 9.2 Hz, 1H), 4.52 (s, 2H), 4.44 (d, *J* = 1.6 Hz, 2H); ¹³C NMR (100 MHz, CDCl₃): δ 150.1, 139.0, 138.3, 133.8, 129.3, 128.3, 126.8, 125.5, 117.6, 116.5, 110.4, 103.9, 54.1, 50.4.

6-Nitro-1-phenethyl-1,2-dihydroquinoline-3-carbonitrile (100e) from 96b and phenethylamine. Yield: 250 mg (0.82 mmol, 82%) as a yellow solid; m.p. 121-122 °C; IR: 2239, 1623, 1526, 1344 cm^{-1} ; ^1H NMR (400 MHz, CDCl_3): δ 8.02 (dd, $J = 9.2, 2.7$ Hz, 1H), 7.81 (d, $J = 2.7$ Hz, 1H), 7.38-7.18 (complex, 5H), 6.95 (s, 1H), 6.47 (d, $J = 9.3$ Hz, 1H), 4.28 (s, 2H), 3.52 (t, $J = 7.4$ Hz, 2H), 2.92 (t, $J = 7.4$ Hz, 2H); ^{13}C NMR (100 MHz, CDCl_3): δ 149.5, 139.0, 137.9, 137.5, 129.1, 128.9, 128.7, 127.2, 125.6, 117.5, 116.5, 109.6, 103.4, 52.6, 50.7, 31.8.

1-Methyl-1,2-dihydroquinoline-3,6-dicarbonitrile (101a) from 96c and methylamine. Yield: 160 mg (0.82 mmol, 82%) as a yellow solid; m.p. 205-206 °C; IR: 2253, 1625 cm^{-1} ; ^1H NMR (400 MHz, CDCl_3): δ 7.39 (d, $J = 8.6$ Hz, 1H), 7.15 (s, 1H), 6.94 (s, 1H), 6.48 (d, $J = 8.6$ Hz, 1H), 4.33 (s, 2H), 2.87 (s, 2H); ^{13}C NMR (100 MHz, CDCl_3): δ 148.9, 139.0, 136.4, 132.7, 119.2, 119.0, 116.8, 110.8, 103.7, 99.8, 51.4, 37.4.

1-Hexyl-1,2-dihydroquinoline-3,6-dicarbonitrile (101b) from 96c and *n*-hexylamine. Yield: 204 mg (0.77 mmol, 77%) as a yellow solid; m.p. 178-179 °C; IR: 2254, 1651 cm^{-1} ; ^1H NMR (400 MHz, CDCl_3): δ 8.76 (s, 1H), 8.09 (s, 1H), 7.96 (d, $J = 8.9$ Hz, 1H), 7.60 (d, $J = 8.9$ Hz, 1H), 4.22 (t, $J = 7.4$ Hz, 2H), 1.91 (quintet, $J = 7.4$ Hz, 2H), 1.50-1.28 (complex, 6H), 0.91 (t, $J = 6.7$ Hz, 3H); ^{13}C NMR (100 MHz, CDCl_3): δ 172.8, 149.5, 141.2, 135.5, 132.9, 127.0, 117.5, 117.3, 114.5, 109.7, 97.9, 54.8, 31.2, 28.8, 26.3, 22.4, 13.9.

1-isoButyl-1,2-dihydroquinoline-3,6-dicarbonitrile (101c) from 96c and isobutylamine. Yield: 192 mg (0.81 mmol, 81%) as a yellow solid; m.p. 131-132 °C; IR: 2229, 1626 cm^{-1} ; ^1H NMR (400 MHz, CDCl_3): δ 7.33 (dd, $J = 8.8, 2.1$ Hz, 1H), 7.14 (d, $J = 2.1$ Hz, 1H), 6.92 (s, 1H), 6.48 (d, $J = 8.8$ Hz, 1H), 4.38 (d, $J = 1.5$ Hz, 2H), 3.02 (d, $J = 7.5$ Hz, 2H), 2.06 (septet, $J = 6.6$ Hz, 1H), 1.00 (d, $J = 6.6$ Hz, 6H); ^{13}C NMR (100 MHz, CDCl_3): δ 148.6, 139.1, 136.1, 133.2, 119.3, 118.7, 116.9, 111.2, 102.7, 98.9, 58.1, 50.9, 26.2, 20.2.

Ethyl 6-cyano-1-methyl-1,2-dihydroquinoline-3-carboxylate (102a) from 96d and methylamine. Yield: 209 mg (0.91 mmol, 91%) as a yellow solid; m.p. 140-141 °C; IR: 2201, 1708, 1652 cm^{-1} ; ^1H NMR (400 MHz, CDCl_3): δ 7.35 (dd, $J = 8.6, 2.1$ Hz, 1H), 7.23 (s, 1H), 7.17 (d, J

= 2.1 Hz, 1H), 6.42 (d, $J = 8.6$ Hz, 1H), 4.41 (d, $J = 1.5$ Hz, 2H), 4.27 (q, $J = 7.1$ Hz, 2H), 2.87 (s, 3H), 1.34 (t, $J = 7.1$ Hz, 3H); ^{13}C NMR (100 MHz, CDCl_3): δ 164.8, 149.6, 135.9, 133.7, 133.0, 122.7, 119.9, 119.8, 109.9, 98.6, 61.0, 51.0, 37.4.

Ethyl 6-cyano-1-phenethyl-1,2-dihydroquinoline-3-carboxylate (102e) from 96d and phenethylamine. Yield: 270 mg (0.85 mmol, 85%) as a yellow solid; m.p. 131-132 °C; IR: 2217, 1701, 1650 cm^{-1} ; ^1H NMR (400 MHz, CDCl_3): δ 7.36-7.29 (complex, 3H), 7.25-7.18 (complex, 4H), 7.18 (d, $J = 2.1$ Hz, 1H), 6.44 (d, $J = 8.7$ Hz, 1H), 4.43 (d, $J = 1.6$ Hz, 2H), 4.26 (q, $J = 7.1$ Hz, 2H), 3.45 (t, $J = 7.9$ Hz, 2H), 2.88 (t, $J = 7.9$ Hz, 2H), 1.33 (t, $J = 7.1$ Hz, 3H); ^{13}C NMR (100 MHz, CDCl_3): δ 164.8, 148.5, 138.1, 135.8, 132.7, 133.4, 128.9, 128.7, 126.8, 122.1, 119.9, 119.7, 109.8, 98.2, 61.0, 52.1, 49.6, 31.3, 14.3.

Ethyl 6-cyano-1-phenyl-1,2-dihydroquinoline-3-carboxylate (102f) from 96d and aniline. Yield: 252 mg (0.83 mmol, 83%) as a yellow solid; m.p. 129-130 °C; IR: 2254, 1698, 1644 cm^{-1} ; ^1H NMR (400 MHz, CDCl_3): δ 7.47 (t, $J = 7.8$ Hz, 2H), 7.36 (s, 1H), 7.33-7.24 (complex, 4H), 7.19 (dd, $J = 8.7, 2.0$ Hz, 1H), 6.44 (d, $J = 8.7$ Hz, 1H), 4.71 (d, $J = 1.5$ Hz, 2H), 4.27 (q, $J = 7.1$ Hz, 2H), 1.33 (t, $J = 7.1$ Hz, 3H); ^{13}C NMR (100 MHz, CDCl_3): δ 164.6, 148.8, 143.9, 134.8, 133.22, 133.16, 130.2, 126.8, 125.4, 123.1, 121.1, 119.6, 113.8, 100.3, 61.1, 50.4, 14.3.

1-Hexyl-1,2-dihydro-1,8-naphthyridine-3-carbonitrile (103b) from 96g and *n*-hexylamine. Yield: 198 mg (0.82 mmol, 82%) as a yellow semisolid; IR: 2254, 1639 cm^{-1} ; ^1H NMR (400 MHz, CDCl_3): δ 7.97 (dd, $J = 5.0, 1.8$ Hz, 1H), 7.04 (dd, $J = 7.3, 1.8$ Hz, 1H), 6.87 (t, $J = 1.4$ Hz, 1H), 6.42 (dd, $J = 7.3, 5.0$ Hz, 1H), 4.44 (d, $J = 1.4$ Hz, 2H), 3.45 (t, $J = 7.4$ Hz, 2H), 1.58 (quintet, $J = 7.2$ Hz, 2H), 1.38-1.28 (complex, 6H), 0.90 (t, $J = 6.9$ Hz, 3H); ^{13}C NMR (100 MHz, CDCl_3): δ 155.5, 151.0, 139.8, 135.9, 117.5, 113.4, 112.7, 102.4, 49.6, 47.4, 31.7, 26.6, 25.7, 22.6, 14.1.

1-Phenethyl-1,2-dihydro-1,8-naphthyridine-3-carbonitrile (103e) from 96g and phenethylamine. Yield: 209 mg (0.80 mmol, 80%) as a yellow semisolid; IR: 2254, 1639 cm^{-1} ; ^1H NMR (400 MHz, CDCl_3): δ 8.02 (dd, $J = 5.0, 1.9$ Hz, 1H), 7.35-7.21 (complex, 5H), 7.06 (dd, $J =$

7.3, 1.9 Hz, 1H), 6.86 (t, $J = 1.4$ Hz, 1H), 6.46 (dd, $J = 7.3, 5.0$ Hz, 1H), 4.32 (d, $J = 1.4$ Hz, 2H), 3.68 (t, $J = 7.4$ Hz, 2H), 2.92 (t, $J = 7.1$ Hz, 2H); ^{13}C NMR (100 MHz, CDCl_3): δ 155.2, 151.1, 139.6, 135.8, 128.9, 128.6, 126.5, 117.3, 113.5, 113.0, 102.5, 50.3, 49.6, 32.4.

Representative procedure for the synthesis of 4-oxo-1,4-dihydroquinolines using MBH acetates and 1° alkyl or aromatic amines.

To a solution of MBH acetate (1 mmol) in 1 mL of DMF under N_2 was added the corresponding amine (1.5 mmol), and the mixture was stirred at room temperature for 2 h. K_2CO_3 (1.5 mmol) was added at 23 °C, and the temperature was gradually increased to 90 °C, with continued stirring for 2 h (alternatively, only 2.0 equiv of the corresponding amine can be used without K_2CO_3 , and the temperature can gradually be increased to 90 °C immediately after addition of the amine). After TLC (20% EtOAc/hexane) has indicated complete consumption of the starting material, the solution was poured into 15 mL of DI water, and extracted with EtOAc (3×). The organic layer was washed with 1M HCl (2×), followed by saturated NaHCO_3 (2×). The combined organic layers were washed with saturated NaCl and dried (Na_2SO_4). Removal of the solvent under vacuum gave a crude product, which was further purified by column chromatograph to afford the 4-oxo-1,4-dihydroquinoline compounds.

Ethyl 6-fluoro-1-methyl-4-oxo-1,4-dihydroquinoline-3-carboxylate (104a) from 96f and methylamine. Yield: 210 mg (0.90 mmol, 90%) as a light tan solid; m.p. 203-204 °C; IR: 1728, 1694 cm^{-1} ; ^1H NMR (400 MHz, CDCl_3): δ 8.46 (s, 1H), 8.18 (d, $J = 8.9$ Hz, 1H), 7.44 (d, $J = 5.7$ Hz, 2H), 4.40 (q, $J = 7.1$ Hz, 2H), 3.90 (s, 3H), 1.42 (t, $J = 7.1$ Hz, 3H); ^{13}C NMR (100 MHz, CDCl_3): δ 173.5 (d, $J = 2.0$ Hz), 165.7, 160.1 (d, $J = 232.0$ Hz), 149.6, 136.3 (d, $J = 6.6$ Hz), 130.8 (d, $J = 6.8$ Hz), 121.0 (d, $J = 24.7$ Hz), 117.8 (d, $J = 7.7$ Hz), 113.0 (d, $J = 23.2$ Hz), 110.4, 61.6, 41.6, 14.4.

Ethyl 6-fluoro-1-isobutyl-4-oxo-1,4-dihydroquinoline-3-carboxylate (104c) from 96f and isobutylamine. Yield: 245 mg (0.89 mmol, 89%) as a light tan solid; m.p. 150-151 °C; IR: 1727, 1695

cm⁻¹; ¹H NMR (400 MHz, CDCl₃): δ 8.43 (s, 1H), 8.21 (m, 1H), 7.42 (m, 2H), 4.41 (q, *J* = 7.1 Hz, 2H), 3.97 (d, *J* = 7.5 Hz, 1H), 2.26 (nonet, *J* = 7.0 Hz, 1H), 1.42 (t, *J* = 7.1 Hz, 3H), 1.02 (d, *J* = 6.6 Hz, 6H); ¹³C NMR (100 MHz, CDCl₃): δ 173.4 (d, *J* = 2.4 Hz), 165.9, 159.9 (d, *J* = 247.8 Hz), 149.4, 135.4 (d, *J* = 1.9 Hz), 131.2 (d, *J* = 6.8 Hz), 120.8 (d, *J* = 28.1 Hz), 118.1 (d, *J* = 7.8 Hz), 113.1 (d, *J* = 23.0 Hz), 109.9, 61.6, 61.0, 19.9, 14.4.

Ethyl 1-benzyl-6-fluoro-4-oxo-1,4-dihydroquinoline-3-carboxylate (104d) from 96f and benzylamine. Yield: 266 mg (0.86 mmol, 86%) as a light tan solid; m.p. 169-170 °C; IR: 1727, 1691, 1619 cm⁻¹; ¹H NMR (400 MHz, CDCl₃): δ 8.60 (s, 1H), 8.18 (dd, *J* = 8.9, 2.9 Hz, 1H), 7.41-7.24 (complex, 5H), 7.16 (d, *J* = 6.3 Hz, 2H), 5.40 (s, 2H), 4.41 (q, *J* = 7.1 Hz, 2H), 1.42 (t, *J* = 7.1 Hz, 3H); ¹³C NMR (100 MHz, CDCl₃): δ 173.5 (d, *J* = 2.3 Hz), 165.8, 160.0 (d, *J* = 248.0 Hz), 149.6, 135.6 (d, *J* = 1.8 Hz), 133.9, 131.2 (d, *J* = 7.0 Hz), 129.5, 128.8, 126.0, 121.0 (d, *J* = 25.3 Hz), 118.9 (d, *J* = 7.8 Hz), 113.0 (d, *J* = 23.0 Hz), 110.6, 61.1, 57.8, 14.4.

Ethyl 6-fluoro-4-oxo-1-phenethyl-1,4-dihydroquinoline-3-carboxylate (104e) from 96f and phenethylamine. Yield: 284 mg (0.88 mmol, 88%) as a light tan solid; m.p. 151-152 °C; IR: 1736, 1691, 1618 cm⁻¹; ¹H NMR (400 MHz, CDCl₃): δ 8.21 (dd, *J* = 8.9, 3.0 Hz, 1H), 8.14 (s, 1H), 7.50 (dd, *J* = 9.2, 4.1 Hz, 1H), 7.44 (m, 1H), 7.33-7.23 (complex, 3H), 7.06 (d, *J* = 7.5 Hz, 2H), 4.40 (t, *J* = 7.1 Hz, 2H), 4.34 (q, *J* = 7.1 Hz, 2H), 3.16 (t, *J* = 7.1 Hz, 2H), 1.36 (t, *J* = 7.1 Hz, 3H); ¹³C NMR (100 MHz, CDCl₃): δ 173.3 (d, *J* = 2.3 Hz), 165.4, 159.9 (d, *J* = 247.9 Hz), 149.0, 136.1, 135.1 (d, *J* = 1.8 Hz), 131.2 (d, *J* = 6.8 Hz), 129.1, 128.7, 127.6, 121.0 (d, *J* = 25.2 Hz), 117.7 (d, *J* = 7.7 Hz), 113.3 (d, *J* = 23.0 Hz), 110.1, 60.9, 55.4, 35.2, 14.4.

REFERENCES

1. Punchi Hewage, A. N. D.; Yao, H.; Nammalwar, B.; Gnanasekaran, K. K.; Lovell, S.; Bunce, R. A.; Eshelman, K.; Phaniraj, S. M.; Lee, M. M.; Peterson, B. R.; Battaile, K. P.; Reitz, A. B.; Rivera, M. Small Molecule Inhibitors of the BfrB–Bfd Interaction Decrease *Pseudomonas aeruginosa* Fitness and Potentiate Fluoroquinolone Activity. *J. Am. Chem. Soc.* **2019**, *141*, 8171–8184.
2. Centers for Disease Control (CDC). Antibiotic Resistance Threats in the United States 2013. www.cdc.gov/drugresistance/threat-report-2013/.
3. Blaskovich, M. A.; Butler, M. S.; Cooper, M. A. Polishing the Tarnished Silver Bullet: The Quest for New Antibiotics. *Essays Biochem.* **2017**, *61*, 103–114.
4. Laxminarayan, R.; Duse, A.; Wattal, C.; Zaidi, A. K.; Wertheim, H. F.; Sumpradit, N.; Vlieghe, E.; Hara, G. L.; Gould, I. M.; Goossens, H.; Greko, C.; So, A. D.; Bigdeli, M.; Tomson, G.; Woodhouse, W.; Ombaka, E.; Peralta, A. Q.; Qamar, F. N.; Mir, F.; Kariuki, S.; Bhutta, Z. A.; Coates, A.; Bergstrom, R.; Wright, G. D.; Brown, E. D.; Cars, O. Antibiotic Resistance—the Need for Global Solutions. *Lancet Infect. Dis.* **2013**, *13*, 1057–98.
5. D’Costa, V. M.; King, C. E.; Kalan, L.; Morar, M.; Sung, W. W. L.; Schwarz, C. et al. Antibiotic Resistance is Ancient. *Nature* **2011**, *477*, 457–461.
6. Fair, R. J.; Tor, Y. Antibiotics and Bacterial Resistance in the 21st Century. *Perspective in Medicinal Chemistry* **2014**, *6*, 25–64.
7. O’Shea R.; Moser, H. E. Physicochemical Properties of Antibacterial Compounds: Implications for Drug Discovery. *J. Med. Chem.* **2008**, *51*, 2871–2878.

8. Tacconelli, E.; Carrara, E.; Savoldi, A.; Harbarth, S.; Mendelson, M.; Monnet, D. L.; Pulcini, C.; Kahlmeter, G.; Kluytmans, J.; Carmeli, Y.; Ouellette, M.; Outtersson, K.; Patel, J.; Cavaleri, M.; Cox, E. M.; Houchens, C. R.; Grayson, M. L.; Hansen, P.; Singh, N.; Theuretzbacher, U.; Magrini, N.; Group, W. H. O. P. P. L. W. Discovery, Research, and Development of New Antibiotics: The WHO Priority List of Antibiotic-resistant Bacteria and Tuberculosis. *Lancet Infect. Dis.* **2018**, *18*, 318–327.
9. Lomovskaya O.; Lewis K. Emr, an Escherichia coli Locus for Multidrug Resistance. *Proc. Natl. Acad. Sci. U.S.A.* **1992**, *89*, 8938–42.
10. Li, X. Z.; Nikaido H. Efflux-mediated Drug Resistance in Bacteria. *Drugs* **2004**, *64*, 159–204.
11. Burrows, L. L. The Therapeutic Pipeline for *Pseudomonas aeruginosa* Infections. *ACS Infect. Dis.* **2018**, *4*, 1041–1047.
12. Boucher, H. W.; Talbot, G. H.; Bradley, J. S.; Edwards, J. E.; Gilbert, D.; Rice, L. B.; Scheld, M.; Spellberg, B.; Bartlett, J. Bad Bugs, No Drugs: No ESKAPE! An Update from the Infectious Diseases Society of America. *Clin. Infect. Dis.* **2009**, *48*, 1–11.
13. Konstan, M. W.; Morgan, W. J.; Butler, S. M.; Pasta, D. J.; Craib, M. L.; Silva, S. J.; Stokes, D. C.; Wohl, M. E.; Wagener, J. S.; Regelman, W. E.; Johnson, C. A. MBCHB for the Scientific Advisory Group and the Investigators and Coordinators of the Epidemiologic Study of Cystic Fibrosis, Risk Factors for Rate of Decline in Forced Expiratory Volume in One Second in Children and Adolescents with Cystic Fibrosis. *J. Pediatr.* **2007**, *151*, 134–139.
14. Crull, M. R.; Ramos, K. J.; Caldwell, E.; Mayer-Hamblett, N.; Aitken, M. L.; Goss, C. H. Change in *Pseudomonas aeruginosa* Prevalence in Cystic Fibrosis Adults Over Time. *BMC Pulm. Med.* **2016**, *16*, 176.
15. Ballouche, M.; Cornelis, P.; Baysse, C. Iron Metabolism: A Promising Target for Antibacterial Strategies. *Recent Pat. Anti-Infect. Drug Discovery* **2009**, *4*, 190–205.

16. Foley, T. L.; Simeonov, A. Targeting Iron Assimilation to Develop New Antibacterials. *Expert Opin. Drug Discovery* **2012**, *7*, 831–847.
17. Goss, C. H.; Kaneko, Y.; Khuu, L.; Anderson, G. D.; Ravishankar, S.; Aitken, M. L.; Lechtzin, N.; Zhou, G.; Czyz, D. M.; McLean, K. Gallium Disrupts Bacterial Iron Metabolism and Has Therapeutic Effects in Mice and Humans with Lung Infections. *Sci. Transl. Med.* **2018**, *10*, 7520.
18. Heinzl, G. A.; Huang, W.; Yu, W.; Giardina, B. J.; Zhou, Y.; MacKerell, A. D., Jr.; Wilks, A.; Xue, F. Iminoguanidines as Allosteric Inhibitors of the Iron-Regulated Heme Oxygenase (HemO) of *Pseudomonas aeruginosa*. *J. Med. Chem.* **2016**, *59*, 6929–6942.
19. Lueangsakulthai, J.; Jangpromma, N.; Temsiripong, T.; McKendrick, J. E.; Khunkitti, W.; Maddocks, S. E.; Klaynongsruang, S. A Novel Antibacterial Peptide Derived from *Crocodylus siamensis* Haemoglobin Hydrolysate Induces Membrane Permeabilization Causing Iron Dysregulation, Oxidative Stress and Bacterial Death. *J. Appl. Microbiol.* **2017**, *123*, 819–831.
20. Cornelis, P.; Wei, Q.; Andrews, S. C.; Vinckx, T. Iron Homeostasis and Management of Oxidative Stress Response in Bacteria. *Metallomics* **2011**, *3*, 540–539.
21. Bullen, J. J.; Rogers, H. J.; Spalding, P. B.; Ward, C. G. Iron and Infection: The Heart of the Matter. *FEMS Immunol. Med. Microbiol.* **2005**, *43*, 325–330.
22. Weinberg, E. D. Iron Availability and Infection. *Biochim. Biophys. Acta, Gen. Subj.* **2009**, *1790*, 600–605.
23. Hood, M. I.; Skaar, E. P. Nutritional immunity: Transition Metals at the Pathogen-host Interface. *Nat. Rev. Microbiol.* **2012**, *10*, 525–537.
24. Benson, D. R.; Rivera, M. Heme Uptake and Metabolism in Bacteria. *Met. Ions Life Sci.* **2013**, *12*, 279–332.
25. Eshelman, K.; Yao, H.; Punchi Hewage, A. N. D.; Deay, J. J.; Chandler, J. R.; Rivera, M. Inhibiting the BfrB:Bfd Interaction in *Pseudomonas aeruginosa* Causes Irreversible Iron

- Accumulation in Bacterioferritin and Iron Deficiency in the Bacterial Cell. *Metallomics* **2017**, *9*, 646–659.
26. Keyer, K.; Imlay, J. A. Superoxide Accelerates DNA-Damage by Elevating Free-Iron Levels. *Proc. Natl. Acad. Sci. U. S. A.* **1996**, *93*, 13635–13649.
 27. Meraz, Kevin. Synthesis of Small Molecules as Antibiotic Candidates. Ph.D. Dissertation, Oklahoma State University: Stillwater, OK, **2019**.
 28. *Metallomics and the Cell*; Banci, L., Ed.; Metal ions in life sciences; Springer: Dordrecht, 2013.
 29. Köster, W. ABC Transporter-Mediated Uptake of Iron, Siderophores, Heme and Vitamin B12. *Research in Microbiology* **2001**, *152*, 291–301.
 30. Frawley, E. R.; Fang, F. C. The Ins and Outs of Bacterial Iron Metabolism: Bacterial Iron Efflux Transporters. *Mol. Microbiol.* **2014**, *93*, 609–616.
 31. Cartron, M. L.; Maddocks, S.; Gillingham, P.; Craven, C.J.; Andrews, S.C. Feo-transport of Ferrous Iron into Bacteria. *Biometals* **2006**, *19*, 143–157.
 32. Zhou, D.; Hardt, W. D.; and Galan, J. E. *Salmonella typhimurium* Encodes a Putative Iron Transport System within the Centisome 63 Pathogenicity Island. *Infect Immun.* **1999**, *67*, 1974–1981.
 33. Ma, J.-F.; Ochsner, U. A.; Klotz, M. G.; Nanayakkara, V. K.; Howell, M. L.; Johnson, Z.; Posey, J. E.; Vasil, M. L.; Monaco, J. J.; Hasset, D. J. Bacterioferritin A Modulates Catalase A (KatA) Activity and Resistance to Hydrogen Peroxide in *Pseudomonas aeruginosa*. *J. Bacteriol.* **1999**, *181*, 3730–3742.
 34. Weeratunga, S.; Lovell, S.; Yao, H.; Battaile, K. P.; Fischer, C. J.; Gee, C. E.; Rivera, M. Structural Studies of Bacterioferritin B (BfrB) from *Pseudomonas aeruginosa* Suggest a Gating Mechanism for Iron Uptake via the Ferroxidase Center. *Biochemistry* **2010**, *49*, 1160–1175.

35. Rivera, M. Bacterioferritin: Structure, Dynamics and Protein-Protein Interactions at Play in Iron Storage and Mobilization. *Acc. Chem. Res.* **2017**, *50*, 331–340.
36. Weeratunga, S.; Gee, C. E.; Lovell, S.; Zeng, Y.; Woodin, C. L.; Rivera, M. Binding of *Pseudomonas aeruginosa* Apobacterioferritin-Associated Ferredoxin to Bacterioferritin B Promotes Heme Mediation of Electron Delivery and Mobilization of Core Mineral Iron. *Biochemistry* **2009**, *48*, 7420–7431.
37. Wijerathne, H.; Yao, H.; Wang, Y.; Lovell, S.; Battaile, K. P.; Rivera, M. Bfd, a New Class of [2Fe-2S] Protein That Functions in Bacterial Iron Homeostasis, Requires a Structural Anion Binding Site. *Biochemistry* **2018**, *57*, 5533–5543.
38. Zughair, S. M.; Cornelis, P. Editorial: Role of Iron in Bacterial Pathogenesis. *Frontiers in Cellular and Infection Microbiology* **2018**, *8*.
39. Wang, Y.; Yao, H.; Cheng, Y.; Lovell, S.; Battaile, K. P.; Midaugh, C. R.; Rivera, M. Characterization of the Bacterioferritin/ Bacterioferritin Associated Ferredoxin Protein-Protein Interactions in Solution and Determination of Binding Energy Hot Spots. *Biochemistry* **2015**, *54*, 6162–6175.
40. Lepre, C. A.; Moore, J. M.; Peng, J. W. Theory and Applications of NMR-Based Screening in Pharmaceutical Research. *Chem. Rev.* **2004**, *104*, 3641–3675.
41. Silverman, R. B. *The Organic Chemistry of Drug Design and Drug Action*; Academic Press: San Diego, California, 1992, pp 55.
42. Spring, D. R. Chemical Genetics to Chemical Genomics: Small Molecules Offer Big Insights. *Chem. Soc. Rev.* **2005**, *34*, 472–482.
43. O'Connor, C. J.; Laraia, L.; Spring, D. R. Chemical Genetics. *Chem. Soc. Rev.* **2011**, *40*, 4332–4345.
44. Patschinski, P.; Zhang, C.; Zipse, H. The Lewis Base-Catalyzed Silylation of Alcohols—A Mechanistic Analysis. *J. Org. Chem.* **2014**, *79*, 8348–8357.

45. Wuts, P. G. M.; Greene, T. W. *Greene's Protective Groups in Organic Synthesis*; John Wiley & Sons, Inc.: Hoboken, NJ, USA, 2006.
46. Kim, S.; Chang, H. 1,8-Diazabicyclo[5.4.0]undec-7-ene. An Effective and Selective Catalyst for the *tert*-Butyldimethylsilylation of Alcohols. *Bull. Chem. Soc. Jpn.* **1985**, *58*, 3669–3670.
47. Lombardo, L. Diisopropylethylamine: An Effective Catalyst for the Introduction of the *t*-Butyldimethylsilyl Group. *Tetrahedron Lett.* **1984**, *25*, 227–228.
48. Akiba, K.; Iseki, Y.; Wada, M. A Convenient Method for the Regioselective Synthesis of 4-Alkyl(Aryl)Pyridines Using Pyridinium Salts. *Bull. Chem. Soc. Jpn.* **1984**, *57*, 1994–1999.
49. Fleming, I. et al. *Science of Synthesis. Category 1, Organometallics: Compounds of Groups 15 (As, Sb, Bi) and Silicon Compounds*, 1st Ed.; Thieme Verlagsgruppe: Stuttgart, 2002.
50. Ando, K. A Mechanistic Study of the Horner–Wadsworth–Emmons Reaction: Computational Investigation on the Reaction Pass and the Stereochemistry in the Reaction of Lithium Enolate Derived from Trimethyl Phosphonoacetate with Acetaldehyde. *J. Org. Chem.* **1999**, *64*, 6815–6821.
51. Kumar, P. Synthesis of Substituted 1-Tetralones. *Org. Prep. Proced. Int.* **1997**, *29*, 477–480.
52. Abdel-Magid, A. F.; Carson, K. G.; Harris, B. D.; Maryanoff, C. A.; Shah, R. D. Reductive Amination of Aldehydes and Ketones with Sodium Triacetoxyborohydride. Studies on Direct and Indirect Reductive Amination Procedures. *J. Org. Chem.* **1996**, *61*, 3849–3862.
53. Yang, L.-X.; Hofer, K. G. Reductive Amination of Nitroimidazole Aldehyde with Diamines Using Sodium Triacetoxyborohydride. *Tetrahedron Lett.* **1996**, *37*, 6081–6084.
54. Abdel-Magid, A. F.; Mehrman, S. J. A Review on the Use of Sodium Triacetoxyborohydride in the Reductive Amination of Ketones and Aldehydes. *Org. Process Res. Dev.* **2006**, *10*, 971–1031.

55. Evans, D. A.; Chapman, K. T.; Carreira, E. M. Directed Reduction of β -Hydroxy Ketones Employing Tetramethylammonium Triacetoxyborohydride. *J. Am. Chem. Soc.* **1988**, *110*, 3560–3578.
56. Private communication from Professor M. Rivera, Department of Chemistry, Louisiana State University, Baton Rouge, LA, U.S.A.
57. Tolkmith, H.; Britton, E. Some Heterocyclic Compounds Containing Phosphorus. *J. Org. Chem.* **1959**, *24*, 705–708.
58. Xu, W.; Chan, K. M.; Kool, E. T. Fluorescent Nucleobases as Tools for Studying DNA and RNA. *Nat. Chem.* **2017**, *9*, 1043–1055.
59. Senge, M. O.; Ryan, A. A.; Letchford, K. A.; MacGowan, S. A.; Mielke, T. Chlorophylls, Symmetry, Chirality, and Photosynthesis. *Symmetry* **2014**, *6*, 781–843.
60. Hartmann, R. W.; Hector, M.; Wachall, B. G.; Paluszczak, A.; Palzer, M.; Huch, V.; Veith, M. Synthesis and Evaluation of 17-Aliphatic Heterocycle-Substituted Steroidal Inhibitors of 17 α -Hydroxylase/C17–20-Lyase (P450 17). *J. Med. Chem.* **2000**, *43*, 4437–4445.
61. El-salam, N. M. A.; Mostafa, M. S.; Ahmed, G. A.; Alothman, O. Y. Synthesis and Antimicrobial Activities of Some New Heterocycle Compounds Based on 6-Chloropyridazine-3-(2H)-thione. *J. Med. Chem.* **2013**, *2013*, 1–8.
62. Azab, M. E.; Youssef, M. M.; El-Bordany, E. A. Synthesis and Antimicrobial Evaluation of Novel Heterocyclic Compounds Containing a Sulfonamido Moiety. *Molecules* **2013**, *18*, 832–844.
63. Salem, M. S.; Sakr, S. I.; El-Senousy, W. M.; Madkour, H. M. F. Synthesis, Antibacterial, and Antiviral Evaluation of New Heterocycles Containing the Pyridine Moiety. *Arch. Pharm. (Weinheim)*. **2013**, *346*, 766–773.
64. Cao, X.; Sun, Z.; Cao, Y.; Wang, R.; Cai, T.; Chu, W.; Yang, Y. Design, Synthesis, and Structure–Activity Relationship Studies of Novel Fused Heterocycles-Linked Triazoles with Good Activity and Water Solubility. *J. Med. Chem.* **2014**, *57*, 3687–3706.

65. El-Sawy, E. R.; Ebaid, M. S.; Abo-Salem, H. M.; Al-Sehemi, A. G.; Mandour, A. H. Synthesis, Anti-inflammatory, Analgesic and Anticonvulsant Activities of Some New 4,6-Dimethoxy-5-(heterocycles)benzofuran Starting from Naturally Occurring Visnagin. *J. Chem.* **2013**, *7*, 914–923.
66. Chen, Y.; Yu, K.; Tan, N. Y.; Qiu, R. H.; Liu, W.; Luo, N. L.; Tong, L.; Au, C. T.; Luo, Z. Q. Synthesis, Characterization and Anti-Proliferative Activity of Heterocyclic Hypervalent Organoantimony Compounds. *Eur. J. Med. Chem.* **2014**, *79*, 391–398.
67. El-Sawy, E. R.; Mandour, A. H.; El-Hallouty, S. M.; Shaker, K. H.; Abo-Salem, H. M. Synthesis, Antimicrobial and Anticancer Activities of Some New *N*-Methylsulphonyl and *N*-Benzenesulphonyl-3-indolyl Heterocycles. 1st Cancer Update. *Arab. J. Chem.* **2013**, *6*, 67–78.
68. Mabkhot, Y. N.; Barakat, A.; Al-Majid, A. M.; Alshahrani, S.; Yousuf, S.; Choudhary, M. I. Synthesis, Reactions and Biological Activity of Some New Bis-Heterocyclic Ring Compounds Containing Sulphur Atom. *Chem. Cent. J.* **2013**, *7*, 112–120.
69. Freeman, J. P.; Grabiak, R. C. Heterocyclic *N*-Oxides as Synthetic Intermediates. 5. Synthesis of 5-Aminopyridazine 1-Oxides. *J. Org. Chem.* **1997**, *41*.
70. Ager, D. J.; Prakash, I.; Schaad, D. R. 1,2-Amino Alcohols and Their Heterocyclic Derivatives as Chiral Auxiliaries in Asymmetric Synthesis. *Chem. Rev.* **1996**, *96*, 835–875.
71. Kollar, L.; Keglevich, G. *P*-Heterocycles as Ligands in Homogeneous Catalytic Reactions. *Chem. Rev.* **2010**, *110*, 4257–4302.
72. Lu, F. Some Heterocyclic Polymers and Polysiloxanes. *Polym. Rev.* **1998**, *38*, 143–205.
73. Ashok Kumar, S. L.; Saravana Kumar, M.; Sreeja, P. B.; Sreekanth, A. Novel Heterocyclic Thiosemicarbazones Derivatives as Colorimetric and “Turn On” Fluorescent Sensors for Fluoride Anion Sensing Employing Hydrogen Bonding. *Spectrochimica Acta Part A: Molecular Spectroscopy* **2013**, *113*, 123–129.

74. Dunn, P. J. The Importance of Green Chemistry in Process Research and Development. *Chem. Soc. Rev.* **2012**, *41*, 1452-1461.
75. Narendar Reddy, T.; Jayathirtha Rao, V. Importance of Baylis-Hillman Adducts in Modern Drug Discovery. *Tetrahedron Lett.* **2018**, *59*, 2859–2875.
76. Sumalatha, Y.; Ranga Reddy, T.; Pratap Reddy, P.; Satyanarayana, B. A Simple, Efficient and Scalable Synthesis of Hypnotic Agent, Zolpidem. *ARKIVOC* **2009**, *ii*, 315–320.
77. Annor-Gyamfi, J. K.; Gnanasekaran, K. K.; Bunce, R. A. Syntheses of 1-Aryl-5-nitro-1*H*-indazoles and a General One-pot Route to 1-Aryl-1*H*-indazoles. *Molecules* **2018**, *23*, 674.
78. Błaziak, K.; Danikiewicz, W.; Małkosza, M. How Does Nucleophilic Aromatic Substitution Really Proceed in Nitroarenes. Computational Prediction and Experimental Verification. *J. Am. Chem. Soc.* **2016**, *138*, 7276–7281.
79. Bruice, P. Y. *Organic Chemistry*. 6th Ed.; Pearson: United States, 2011.
80. a) Nammalwar, B.; Bunce R. A. Recent Syntheses of 1,2,3,4-Tetrahydroquinolines, 2,3-Dihydro-4(1*H*)-quinolinones and 4(1*H*)-Quinolinones Using a Domino Strategy. *Molecules* **2014**, *19*, 204–232. b) Bunce, R. A.; Nammalwar, B.; Gnanasekaran, K. K.; Cain, N. R. Isoquinolin-1(2*H*)-ones and 1,6-Naphthyridin-5(6*H*)-ones by an *N*-acylation-S_NAr Sequence. *Tetrahedron* **2014**, *70*, 838–844. c) Gnanasekaran, K. K.; Muddala, N. P.; Bunce, R. A. Pyrazoloquinazolinones and Pyrazolopyridopyrimidinones by a Sequential *N*-Acylation-S_NAr Reaction. *Tetrahedron Lett.* **2015**, *56*, 1367–1369. d) Gnanasekaran, K. K.; Muddala, N. P.; Bunce, R. A. Benzo[4,5]imidazo[2,1-*b*]quinazolin-12-ones and Benzo[4,5]imidazo[1,2-*a*]pyrido[2,3-*d*]pyrimidin-5-ones by a Sequential *N*-Acylation-S_NAr Reaction. *Tetrahedron Lett.* **2015**, *56*, 7180–7183.
81. Palazzo, G.; Corsi, G.; Baiocchi, L.; Silvestrini, B. Synthesis and Pharmacological Properties of 1-Substituted 3-Dimethylaminoalkoxy-1*H*-indazoles. *J. Med. Chem.* **1966**, *9*, 38–41.

82. Bai, M.; Carr, G.; DeOrazio, R. J.; Friedrich, T. D.; Dobritsa, S.; Fitzpatrick, K.; Guzzo, P. R.; Kitchen, D. B.; Lynch, M. A.; Peace, D.; Sajad, M.; Usyatinsky, A.; Wolf, M. 5-Functionalized Indazoles as Glucocorticoid Receptor Agonists. *Bioorg. Med. Chem. Lett.* **2010**, *20*, 3017–3020.
83. Zhao, C.; Wang, R.; Li, G.; Xue, X.; Sun, C.; Qu, X.; Li, W. Synthesis of Indazole Based Diarylurea Derivatives and Their Antiproliferative Activity Against Tumor Cell Lines. *Bioorg. Med. Chem. Lett.* **2013**, *23*, 1989–1992.
84. Dessole, G.; Branca, D.; Ferrigno, F.; Kinzel, O.; Muraglia, E.; Palumbi, M. C.; Rowley, M.; Serafini, S.; Steinkühler, C.; Jones, P. Discovery of *N*-[(1-Aryl-1*H*-indazol-5-yl)methyl]-amide Derivatives as Smoothed Antagonists for Inhibition of the Hedgehog Pathway. *Bioorg. Med. Chem. Lett.* **2009**, *19*, 4191–4195.
85. Mahindroo, N.; Punchihewa, C.; Fujii, N. Hedgehog-Gli Pathway Inhibitors as Anticancer Agents. *J. Med. Chem.* **2009**, *52*, 3829–3845.
86. Gao, M.; Liu, X.; Wang, X.; Cai, Q.; Ding, K. Synthesis of 1-Aryl-1*H*-indazoles via a Ligand-free Copper-catalyzed Intramolecular Amination Reaction. *Chin. J. Chem.* **2011**, *29*, 1199–1204.
87. Esmaeili-Marandi, F.; Saeedi, M.; Mahdavi, M.; Yavari, I.; Foroumadi, A.; Shafiee, A. Potassium *tert*-Butoxide Promoted Intramolecular Amination of 1-Aryl-2-(nitro-benzylidene)hydrazines: Efficient Synthesis of 1-Aryl-1*H*-indazoles. *Synlett.* **2014**, *25*, 2605–2608.
88. Lokhande, P. D.; Raheem, A.; Sabale, S. T.; Chabukswar, A. R.; Jagdale, S. C. An efficient Synthesis of 1*H*-indazoles. *Tetrahedron Lett.* **2007**, *48*, 6890–6892.
89. Xiong, X.; Jiang, Y.; Ma, D. Assembly of *N,N*-Disubstituted Hydrazines and 1-Aryl-1*H*-indazoles via Copper-catalyzed Coupling Reactions. *Org. Lett.* **2012**, *14*, 2552–2555.
90. Veerareddy, A.; Gogireddy, S.; Dubey, P. K. Regioselective Synthesis of 1-Substituted indazole-3-carboxylic Acids. *J. Heterocycl. Chem.* **2014**, *51*, 1311–1321.

91. Li, P.; Wu, C.; Zhao, J.; Rogness, D. C.; Shi, F. Synthesis of Substituted 1*H*-indazoles from Arynes and Hydrazones. *J. Org. Chem.* **2012**, *77*, 3149–3158.
92. Lebedev, A. Y.; Khartulyari, A. S.; Voskoboynikov, A. Z. Synthesis of 1-Aryl-1*H*-indazoles via a Palladium-catalyzed Intramolecular Amination of Aryl Halides. *J. Org. Chem.* **2005**, *70*, 596–602.
93. Xu, P.; Wang, G.; Wu, Z.; Li, S.; Zhu, C. Rh(III)-catalyzed Double C-H Activation of Aldehyde Hydrazones: A Route for Functionalized 1*H*-indazole Synthesis. *Chem. Sci.* **2017**, *8*, 1303–1308.
94. Schmidt, A.; Beutler, A.; Snovydyovych, B. Recent Advances in the Chemistry of Indazoles. *Eur. J. Org. Chem.* **2008**, 4073–4095.
95. Gaikwad, D. D.; Chapolikar, A. D.; Devkate, C. G.; Warad, K. D.; Tyade, A. P.; Pawar, R. P.; Domb, A. J. Synthesis of Indazole Motifs and their Medicinal Importance: An Overview. *Eur. J. Med. Chem.* **2015**, *90*, 707–731.
96. Cankarová, N.; Hlavác, J.; Krchnák, V. Recent Synthetic Approaches to 1*H*- and 2*H*-indazoles. A review. *Org. Prep. Proced. Int.* **2010**, *42*, 433–465.
97. Kim, S.; Yoon, J.-Y. *Science of Synthesis Houben-Weyl Methods of Molecular Transformations*; Padwa, A. Ed.; Thieme: Stuttgart; 2004, Vol 27, pp 671–722.
98. Bordwell, F. G. Equilibrium Acidities in Dimethyl Sulfoxide Solution. *Acc. Chem. Res.* **1988**, *21*, 456–463.
99. a) Reich, H. J.; Rigby, J. H. *Handbook of Reagents for Organic Synthesis: Acidic and Basic Reagents*; Wiley: New York, 1999, Vol 4, pp 296–298. b) Fieser, M; Fieser, L. F. *Reagents for Organic Synthesis*; Wiley: New York, 1975, Vol 5, pp 552–553.
100. Gribble, G. W. *Indole Ring Synthesis: From Natural Products to Drug Discovery*; Wiley: New York, NY, 2016; p 229.
101. Most ring closures to produce 6,5-fused aromatic rings involve reaction of an aryl-bound nucleophile with a side chain electrophilic center, see Katritsky, A. R.; Ramsden, C. A.;

- Joule, J. A.; Zhankin, V. V. *Handbook of Heterocyclic Chemistry*, 3rd Ed.; Elsevier: Amsterdam, 2010; for Indazoles, see pp 830-831; for Indoles, see pp 801-807.
102. Smith, M. B.; March, J. *March's Advanced Organic Chemistry: Reactions, Mechanism and Structure*, 6th Ed.; Wiley-Interscience: Hoboken, NJ, 2007; p 495.
103. a) Lukin, K.; Hsu, M. C.; Fernando, D.; Leanna, M. R. New Practical Synthesis of Indazoles via Condensation of *o*-Fluorobenzaldehydes and their *O*-Methyloximes with Hydrazine. *J. Org. Chem.* **2006**, *71*, 8166–8172. b) Sagitullina, G. P.; Garkushenko, A. K.; Poendaev, N. V.; Sagitullin, R. S. Simple and Efficient Synthesis of 1*H*-indazoles. *Mendeleev Commun.* **2012**, *22*, 167–168.
104. This statement is further substantiated by the fact that hydrazones bearing nitro groups at C2 and C4 failed to cyclize under our optimized conditions.
105. Gavin, J. T.; Annor-Gyamfi, J. K.; Bunce, R. A. Quinazolin-4(3*H*)-ones and 5,6-Dihydropyrimidin-4(3*H*)-ones from β -Aminoamides and Orthoesters. *Molecules* **2018**, *23*, 2925.
106. Annor-Gyamfi, J. K.; Bunce, R. A. 4*H*-Benzo[*d*][1,3]oxazin-4-ones and Dihydro Analogs from Substituted Anthranilic Acids and Orthoesters. *Molecules* **2019**, *24*, 3555.
107. Fenton, G.; Newton, C. G.; Wyman, B. M.; Bagge, P.; Dron, D. I.; Riddell, D.; Jones, G. D. Hypolipidemic 2-[4-(1,1-Dimethylethyl)phenyl]-4*H*-3,1-benzoxazin-4-one. Structure Activity Relationships of a Novel Series of High-Density Lipoprotein Elevators. *J. Med. Chem.* **1989**, *32*, 265–272.
108. Krantz, A.; Spencer, R. W.; Tam, T. F.; Liak, T. J.; Copp, L. J.; Thomas, E. M.; Rafferty, S. P. Design and Synthesis of 4*H*-3,1-Benzoxazin-4-ones as Potent Alternate Substrate Inhibitors of Human Leukocyte Elastase. *J. Med. Chem.* **1990**, *33*, 464–479.
109. Goel, P.; Jumpertz, T.; Tichá, A.; Ogorek, I.; Mikles, D. C.; Hubalek, M.; Piertrzik, C. U.; Strisovsky, K.; Schmidt, B.; Weggen, S. Discovery and Validation of 2-Styryl Substituted Benzoxazin-4-ones as a Novel Scaffold for Rhomboid Protease Inhibitors. *Bioorg. and Med. Chem. Lett.* **2018**, *28*, 1417–1422.

110. Yang, J.; Barniol-Xicotá, M.; Nguyen, M. T. N.; Ticha, A.; Strisovsky, K.; Verhelst, S. H. L. Benzoazin-4-ones as Novel, Easily Accessible Inhibitors for Rhomboid Proteases. *Bioorg. and Med. Chem. Lett.* **2018**, *28*, 1423–1427.
111. Madkour, H. M. F. Reactivity of 4*H*-3,1-Benzoxazin-4-ones Towards Nitrogen and Carbon Nucleophilic Reagents: Applications to the Synthesis of New Heterocycles. *ARKIVOC*, **2004**, (i), 36–54.
112. Baravkar, S. B.; Roy, A.; Gawade, R. L.; Puranik, V. G.; Sanjayan, G. J. Nucleophilic Ring Opening of Benzoxazinone by DBU: Some Observations. *Synth. Commun.* **2014**, *44*, 2955–2960.
113. Zentmeyer, D. T.; Wagner, E. C. The So-called Acylanthranils (3,1,4-benzoxazones). I. Preparation; Reactions with Water, Ammonia and Aniline; Structure. *J. Org. Chem.* **1949**, *14*, 967–981.
114. Bain, D. I.; Smalley, R. K. Synthesis of 2-Substituted-4*H*-3,1-benzoxazin-4-ones. *J. Chem. Soc.* **1968**, 1593.
115. Larksarp, C.; Alper, H. A Simple Synthesis of 2-Substituted 4*H*-3,1-Benzoxazin-4-ones by Palladium-catalyzed Cyclocarbonylation of *o*-Iodoanilines with Acid Chlorides. *Org. Lett.* **1999**, *1*, 1619–1622.
116. Yamashita, M.; Iida, A. One-pot Approach to 2-Arylbenzoxazinone Derivatives from 1-Alkynylanilines using Copper Mediated Tandem Reactions. *Tetrahedron* **2014**, *70*, 5746–5751.
117. Shang, X.-X.; Vu, H.-M.; Li, X.-Q. One-pot Synthesis of 2-Arylbenzoxazines from 2-Arylindoles with (Diacetoxyiodo)benzene as the Sole Oxidant. *Synthesis* **2018**, *50*, 377–383.
118. Plescia, S.; Raffa, D.; Plescia, F.; Casula, G.; Maggio, B.; Daidone, G.; Raimondi, M. V.; Cuismano, M. G.; Bombieri, G.; Meneghetti, F. Synthesis and Biological Evaluation of New Indazole Derivatives. *ARKIVOC* **2010**, (x), 163–177.

119. Deslongchamps, P. *Stereoelectronic Effects in Organic Chemistry*, Pergamon Press: Oxford, UK; 1983, Chapter 2 and references cited therein.
120. Smith M. B.; March, J. *March's Advanced Organic Chemistry*, 6th Ed.; Wiley-Interscience: New York, NY; 2007, pp 204–206.
121. Kleinpeter, E.; Thielemann, J. Synthesis and Conformational Analysis of Mono- and *Trans*-1,4-Dialkoxy Substituted Cyclohexanes-steric Substituent/skeleton Interactions. *Tetrahedron* **2007**, *63*, 9071–9081.
122. McElvain, S. N.; Nelson, J. W. The Preparation of Orthoesters. *J. Am. Chem. Soc.* **1942**, *64*, 1825–1827.
123. Noe, M.; Perosa, A.; Selva, M. A Flexible Pinner Preparation of Orthoesters: The Model Case of Trimethylorthoobenzoate. *Green Chem.* **2013**, *15*, 2252–2260.
124. Gnanasekaran, K. K.; Nammalwar, B.; Murie, M.; Bunce, R. A. Efficient Synthesis of 1,3,4-Oxadiazoles Promoted by NH₄Cl. *Tetrahedron Letters* **2014**, *55*, 6776–6778.
125. De Oliveira, C. S.; Lira, B. F.; Barbosa-Filho, J. M.; Lorenzo, J. G. F.; de Athayde-Filho, P. F. Synthetic Approaches and Pharmacological of 1,3,4-Oxadiazoles: A Review of the Literature from 2000–2012. *Molecules* **2012**, *17*, 10192.
126. Fortenberry, C.; Nammalwar, B.; Bunce, R. A. Ammonium Chloride-catalyzed Synthesis of Benzo-fused Heterocycles from *o*-Substituted Anilines and Orthoesters. *Org. Prep. Proced. Int.* **2013**, *45*, 57–65.
127. Nammalwar, B.; Fortenberry, C.; Bunce, R. A. Synthesis of α -Aminonitriles Under Mild Catalytic, Metal-free Conditions. *Tetrahedron Letters* **1968**, *55*, 379–381.
128. a) Bunce, R. A.; Nago, T. 1-Alkyl-2,3-dihydro-4(1*H*)-quinolinones by a Tandem Michael-S_NAr Annulation Reaction. *J. Heterocycl. Chem.* **2009**, *46*, 623. b) Bunce, R. A.; Rogers, D.; Nago, T.; Bryant, S. A. 4*H*-1-Benzopyran by a Tandem S_N2-S_NAr Reaction. *J. Heterocycl. Chem.* **2008**, *45*, 547. c) Bunce, R. A.; Nago, T.; Sonobe, N.; Slaughter, L. M. Benzo-fused

- Heterocycles and Carbocycles by Intramolecular S_NAr and Tandem S_N2-S_NAr Reactions. *J. Heterocycl. Chem.* **2008**, *45*, 551. d) Bunce, R. A.; Nago, T.; Sonobe, N. 6-Nitro-1,2,3,4-tetrahydroquinolines by Tandem Reductive Amination-S_NAr Reaction. *J. Heterocycl. Chem.* **2008**, *45*, 1155.
129. For reviews, see: a) Tsubaki, K. Synthesis and Properties of the Chiral Oligonaphthalenes. *Org. Biomol. Chem.* **2007**, *5*, 2179. b) Brasholz, M.; Sörgel, S.; Azap, C.; Reissig, H. Rubromycins: Structurally Intriguing, Biologically Valuable, Synthetically Challenging Antitumor Antibiotics. *Eur. J. Org. Chem.* **2007**, 3801. c) de Koning, C. B.; Rousseau, A. L.; van Otterlo, W. A. L. Modern Methods for the Synthesis of Substituted Naphthalenes. *Tetrahedron* **2003**, *59*, 7. d) Saito, S.; Yamamoto, Y. Recent Advances in the Transition-Metal-Catalyzed Regioselective Approaches to Polysubstituted Benzene Derivatives. *Chem. Rev.* **2000**, *100*, 2901. e) Katritzky, A. R.; Li, J.; Xie, L. [3 + 3] Benzannulations of Benzenoid- and Heteroaromatic-ring Systems. *Tetrahedron* **1999**, *55*, 8263. f) Bradsher, C. K. Formation of Six Membered Aromatic Rings by Cyclialkylation of Some Aldehydes and Ketones. *Chem. Rev.* **1987**, *87*, 1277.
130. Kang, D.; Kim, J.; Oh, S.; Lee, P. H. Synthesis of Naphthalenes via Platinum-catalyzed Hydroarylation of Aryl Enynes. *Org. Lett.* **2012**, *14*, 5636.
131. Manojveer, S.; Balamurugan, R. Synthesis of Naphthalene Derivatives from *ortho*-Alkynylacetophenone Derivatives via Tandem *in Situ* Incorporation of Acetal and Intramolecular Heteroalkyne Metathesis/Annulation. *Org. Lett.* **2014**, *16*, 1712–1715.
132. Liu, X.-Y.; Ding, P.; Huang, J.-S.; Che, C.-M. Synthesis of Substituted 1,2-Dihydroquinolines and Quinolines from Aromatic Amines and Alkynes by Gold(I)-Catalyzed Tandem Hydroamination–Hydroarylation under Microwave-Assisted Conditions. *Org. Lett.* **2007**, *9*, 2645–2648.

133. Gutiérrez, R. U.; Correa, H. C.; Bautista, R.; Vargas, J. L.; Jerezano, A. V.; Delgado, F.; Tamariz, J. Regioselective Synthesis of 1,2-Dihydroquinolines by a Solvent-free MgBr₂-Catalyzed Multicomponent Reaction. *J. Org. Chem.* **2013**, *78*, 9614–9626.
134. Vvedensky, V. Y.; Ivanov, Y. V.; Kysil, V.; Williams, C.; Tkachenko, S.; Kiselyov, A.; Khvat, A. V.; Ivachtchenko, A. V. Microwave-mediated Reactions of 3-Aminomethylpyridines with Acetylenedicarboxylates. A Novel Synthetic Route to Dihydronaphthyridines and Naphthyridine-1-ones. *Tetrahedron Lett.* **2005**, *46*, 3953–3956.
135. Johnson, J. V.; Rauckman, B. S.; Baccanari, D. P.; Roth, B. 2,4-Diamino-5-benzylpyrimidines and Analogs as Antibacterial Agents. 1,2-Dihydroquinolymethyl Analogs with High Activity and Specificity for Bacterial Dihydrofolate Reductase. *J. Med. Chem.* **1989**, *32*, 1942–1949.
136. Takahashi, H.; Bekkali, Y.; Capolino, A. J.; Gilmore, T.; Goldrick, S. E.; Kaplita, P. V.; Liu, L.; Nelson, R. M.; Terenzio, D.; Wang, J.; Zuvella-Jelaska, L.; Proudfoot, J.; Nabozny, G.; Thomson, D. Discovery and SAR Study of Novel Dihydroquinoline-Containing Glucocorticoid Receptors Agonists. *Bioorg. Med. Chem. Lett.* **2007**, *17*, 5091–5095.
137. a) Kumar, S.; Engman, L.; Valgimigli, L.; Amorati, R.; Fumo, M. G.; Pedulli, G. F. Regenerable Chain-Breaking 2,3-Dihydrobenzo[*b*]selenophene-5-ol Antioxidants. *J. Org. Chem.* **2007**, *72*, 6046–6055 and references cited therein. b) Lockhart, B.; Bonhomme, N.; Roger, A.; Dorey, G.; Casara, P.; Lestage, P. Protective Effect of the Antioxidant 6-ethoxy-2,2-pentamethylen-1,2-Dihydroquinoline (S33113) in Models of Cerebral Neurodegeneration. *Eur. J. Pharmacol.* **2001**, *416*, 59–68.
138. These compounds are also currently being evaluated for the treatment of: a) Central nervous system disorders: Gallery, G.; Groebke Zbinden, K. G.; Norcross, R.; Stalder, H. World Patent WO 2007085558 (2007), 85, *Chem. Abstr.*; b) Galley, G.; Groebke Zbinden, K. G.; Norcross, R.; Stalder, H. *Chem. Abstr.* 2007, 147, 841292; c) Potassium channel blockers: Gerlach, U.; Brendel, J.; Lang, H. J.; Weidmann, K. *Eur. Pat.* EP 857,724 (1998), 23; d)

- Gerlach, U.; Brendel, J.; Lang, H. J.; Weidmann, K. *Chem. Abstr.* 1998, 129, 175447; e)
Cancer: Vicker, N.; Day, J. M.; Bailey, H. V.; Heaton, W.; Gonzalez, A. M. R.; Sharland, C.
M.; Reed, M. J.; Purohit, A.; Potter, B. V. L. World Patent 2007003934 (2007), 266; f)
Vicker, N.; Day, J. M.; Bailey, H. V.; Heaton, W.; Gonzalez, A. M. R.; Sharland, C. M.;
Reed, M. J.; Purohit, A.; Potter, B. V. L. *Chem. Abstr.* 2007, 146, 142281.
139. Nair, D. K.; Mobin, S. M.; Namboothiri, I. N. N. Synthesis of Imidazopyridines from the
Morita–Baylis–Hillman Acetates of Nitroalkenes and Convenient Access to Alpidem and
Zolpidem. *Org. Lett.* **2012**, *14*, 4580–4583.
140. Morita, K.; Suzuki, Z.; Hirose, H. A Tertiary Phosphine-Catalyzed Reaction of Acrylic
Compounds with Aldehydes. *Bull. Chem. Soc. Jpn.* **1968**, *41*, 2815–2815.
141. Methanolic Trimethylamine Mediated Baylis-Hillman Reaction. *ARKIVOC* **2002**, *2002*, 136.
142. Brzezinski, L. J.; Rafel, S.; Leahy, J. W. The Asymmetric Baylis–Hillman Reaction. *J. Am.
Chem. Soc.* **1997**, *119*, 4317–4318.
143. Srihari, E.; Kumar, G. S.; Kumar, C. N. S. S. P.; Seth, R. K.; Biswas, S.; Sridhar, B.;
Jayathirtha Rao, V. Synthesis and Antimalarial Activity of Baylis-Hillman Adducts from
Substituted 2-Chloroquinoline-3-Carboxaldehydes. *Heterocycl. Commun.* **2011**, *17*.
144. Makar, S.; Saha, T.; Singh, S. K. Naphthalene, a Versatile Platform in Medicinal Chemistry:
Sky-High Perspective. *Eur. J. Med. Chem.* **2019**, *161*, 252–276.
145. Feng, C.; Loh, T.-P. Palladium-Catalyzed Bisolefination of C–C Triple Bonds: A Facile
Method for the Synthesis of Naphthalene Derivatives. *J. Am. Chem. Soc.* **2010**, *132*, 17710–
17712.
146. Viswanathan, G. S.; Wang, M.; Li, C.-J. A Highly Regioselective Synthesis of
Polysubstituted Naphthalene Derivatives Through Gallium Trichloride Catalyzed Alkyne–
Aldehyde Coupling. *Angew. Chem. Int. Ed.* **2002**, *41*, 2138.
147. Kabalka, G. W.; Ju, Y.; Wu, Z. A New Titanium Tetrachloride Mediated Annulation of α -
Aryl-Substituted Carbonyl Compounds with Alkynes: A Simple and Highly Efficient Method

- for the Regioselective Synthesis of Polysubstituted Naphthalene Derivatives. *J. Org. Chem.* **2003**, *68*, 7915–7917.
148. Singh, B.; Chandra, A.; Singh, R. M. Base-free Amination of Baylis–Hillman Acetates of 2-Chloroquinolinyl-3-Carboxaldehydes: A Facile Route to the Synthesis of *N*-Substituted-1,2-dihydrobenzo-*b*[[1,8]-naphthyridines. *Tetrahedron* **2011**, *67*, 2441–2446.
149. Gupta, T.; Singh, J. B.; Mishra, K.; Singh, R. M. Active Methylene Compounds (AMCs) Controlled Facile Synthesis of Acridine and Phenanthridine from Morita Baylis–Hillman Acetate. *RSC Adv.* **2017**, *7*, 54581–54585.
150. Bruice, P. Y. *Organic Chemistry*, 6th Ed.; Prentice Hall: Boston, 2011.
151. Procopiou, P. A.; Baugh, S. P. D.; Flack, S. S.; Inglis, G. G. A. An Extremely Powerful Acylation Reaction of Alcohols with Acid Anhydrides Catalyzed by Trimethylsilyl Trifluoromethanesulfonate. *J. Org. Chem.* **1998**, *63*, 2342–2347.
152. See, for example, a) Stork, G.; White, W. N. The Stereochemistry of the S_N2' Reaction II. *J. Am. Chem. Soc.* **1956**, *78*, 4609; b) Jefford, C. W.; Sweeney, A.; Delay, F. The Reaction of Bicyclo [3.2.1] octenyl Halides with Metal Hydrides. *Helv. Chim. Acta.* **1972**, *55*, 2214; c) Kirmse, W.; Scheidt, F.; Vater, H. S_N2' Reactions of cis-3,4-Dichlorocyclobutene. *J. Am. Chem. Soc.* **1978**, *100*, 3945; d) Gallina, C.; Ciattini, P. G. Conversion of Allylic Carbamates into Olefins with Lithium Dimethylcuprate. A New Formal S_N2' Reaction. *J. Am. Chem. Soc.* **1979**, *101*, 1035.
153. See, for example, a) Borden, W. T.; Corey, E. J. *Tetrahedron Lett.* **1969**, 313; b) Takahashi, T. T.; Satoh, J. Y. A Substituted 5β-Steroids. VI. trans-S_N2' Reaction in Acylolysis of 4β-Bromo-3-keto-5β-steroids. *Bull. Chem. Soc. Jpn.* **1975**, *48*, 69; c) Staroscik, J.; Rickborn, B. Reaction of 1,3- and 1,4-Cyclohexadiene Monoepoxides with Methyl Organometallic Reagents *J. Am. Chem. Soc.* **1971**, *93*, 3046; d) Stork, G.; Schoofs, A. R. Concerted Intramolecular Displacement with Rearrangement in Allylic Systems. Displacement of an Allylic Ester with a Carbanion. *J. Am. Chem. Soc.* **1979**, *101*, 5081.

154. Schenck, L. W.; Kuna, S. K.; Frank, W.; Albert, A.; Kuckleander, U. Dialkyl quinone-2,3-dicarboxylates in the Nenitzescu Reaction. *Tetrahedron* **2005**, *61*, 9129–9139.
155. Bunce, R. A.; Wamsley, E. J.; Pierce, J. D.; Shellhammer, A. J. Jr.; Drumright, R. E. Tandem Michael Reactions for the Construction of Highly Functionalized Five-membered Rings. *J. Org. Chem.* **1987**, *52*, 464–466.
156. Meegalla, S. K.; Rodrigo, R. A General Synthetic Route Isobenzofurans Bearing a Functionalized C-1 Substituent. *J. Org. Chem.* **1991**, *56*, 1882–1888.

APPENDICES

X-ray data for ethyl 6-fluoro-4-oxo-1-phenylethyl-1,4-dihydroquinoline-3-carboxylate (104e)

Table 1. Crystal data and structure refinement for KEVJAG-1-64.

Empirical formula	C ₂₀ H ₁₈ F N O ₃	
Formula weight	339.35	
Crystal system	orthorhombic	
Space group	<i>P</i> 2 ₁ 2 ₁ 2 ₁	
Unit cell dimensions	<i>a</i> = 5.5713(2) Å	$\alpha = 90^\circ$
	<i>b</i> = 14.9835(4) Å	$\beta = 90^\circ$
	<i>c</i> = 19.7736(5) Å	$\gamma = 90^\circ$
Volume	1650.65(8) Å ³	
Z, Z'	4, 1	
Density (calculated)	1.366 Mg/m ³	
Wavelength	0.71073 Å	
Temperature	110(2) K	
<i>F</i> (000)	712	
Absorption coefficient	0.099 mm ⁻¹	
Absorption correction	semi-empirical from equivalents	
Max. and min. transmission	0.8623 and 0.7806	
Theta range for data collection	2.468 to 32.644°	
Reflections collected	39073	
Independent reflections	6040 [R(int) = 0.0288]	
Data / restraints / parameters	6040 / 0 / 227	
<i>wR</i> (<i>F</i> ² all data)	<i>wR</i> 2 = 0.0896	
<i>R</i> (<i>F</i> obsd data)	<i>R</i> 1 = 0.0322	
Goodness-of-fit on <i>F</i> ²	1.005	
Observed data [<i>I</i> > 2σ(<i>I</i>)]	5695	
Absolute structure parameter	0.29(13)	
Largest and mean shift / s.u.	0.000 and 0.000	
Largest diff. peak and hole	0.357 and -0.192 e/Å ³	

 $wR2 = \{ \sum [w(F_o^2 - F_c^2)^2] / \sum [w(F_o^2)^2] \}^{1/2}$

$R1 = \sum ||F_o| - |F_c|| / \sum |F_o|$

Table 2. Atomic coordinates and equivalent isotropic displacement parameters for KEVJAG-1-64. $U(\text{eq})$ is defined as one third of the trace of the orthogonalized U_{ij} tensor.

	x	y	z	$U(\text{eq})$
F(1)	1.40527(15)	0.51268(6)	0.13182(4)	0.02518(17)
O(1)	0.83616(19)	0.32814(6)	0.26570(5)	0.0241(2)
O(2)	0.4676(2)	0.28816(6)	0.36053(5)	0.0253(2)
O(3)	0.22921(17)	0.40520(6)	0.38484(5)	0.01994(18)
N(1)	0.60123(18)	0.58733(6)	0.28431(5)	0.01392(17)
C(1)	1.2051(2)	0.53118(8)	0.16864(6)	0.0178(2)
C(2)	1.1310(2)	0.61959(8)	0.17376(6)	0.0179(2)
C(3)	0.9293(2)	0.63859(7)	0.21193(6)	0.0165(2)
C(4)	0.8050(2)	0.56957(7)	0.24507(5)	0.01350(18)
C(5)	0.4932(2)	0.52046(7)	0.31744(6)	0.01432(19)
C(6)	0.5600(2)	0.43207(7)	0.31470(6)	0.01496(19)
C(7)	0.7637(2)	0.40551(7)	0.27365(6)	0.0155(2)
C(8)	0.8851(2)	0.48092(7)	0.23940(6)	0.01425(19)
C(9)	1.0886(2)	0.46228(8)	0.20000(6)	0.0169(2)
C(10)	0.5137(2)	0.67913(7)	0.29476(6)	0.01584(19)
C(11)	0.6580(2)	0.72932(7)	0.34897(6)	0.0172(2)
C(12)	0.6691(2)	0.67848(7)	0.41471(6)	0.01520(19)
C(13)	0.4835(2)	0.68335(8)	0.46163(6)	0.0184(2)
C(14)	0.4897(2)	0.63222(9)	0.52050(7)	0.0221(2)
C(15)	0.6833(3)	0.57615(9)	0.53343(7)	0.0235(2)
C(16)	0.8705(2)	0.57144(9)	0.48726(7)	0.0236(2)
C(17)	0.8624(2)	0.62199(8)	0.42812(6)	0.0195(2)
C(18)	0.4205(2)	0.36674(7)	0.35465(6)	0.0171(2)
C(19)	0.0901(3)	0.34871(9)	0.42981(7)	0.0243(3)
C(20)	0.2063(3)	0.34486(9)	0.49878(7)	0.0278(3)

Table 3. Bond lengths [Å] and angles [°] for KEVJAG-1-64.

F(1)-C(1)	1.3605(14)	C(10)-H(10A)	0.9900
O(1)-C(7)	1.2377(13)	C(10)-H(10B)	0.9900
O(2)-C(18)	1.2120(14)	C(11)-C(12)	1.5078(16)
O(3)-C(18)	1.3505(15)	C(11)-H(11A)	0.9900
O(3)-C(19)	1.4519(15)	C(11)-H(11B)	0.9900
N(1)-C(5)	1.3398(14)	C(12)-C(13)	1.3915(16)
N(1)-C(4)	1.4005(14)	C(12)-C(17)	1.3952(16)
N(1)-C(10)	1.4738(13)	C(13)-C(14)	1.3940(18)
C(1)-C(9)	1.3680(17)	C(13)-H(13)	0.9500
C(1)-C(2)	1.3911(16)	C(14)-C(15)	1.3908(19)
C(2)-C(3)	1.3835(17)	C(14)-H(14)	0.9500
C(2)-H(2)	0.9500	C(15)-C(16)	1.3879(19)
C(3)-C(4)	1.4068(15)	C(15)-H(15)	0.9500
C(3)-H(3)	0.9500	C(16)-C(17)	1.3939(18)
C(4)-C(8)	1.4058(14)	C(16)-H(16)	0.9500
C(5)-C(6)	1.3768(14)	C(17)-H(17)	0.9500
C(5)-H(5)	0.9500	C(19)-C(20)	1.511(2)
C(6)-C(7)	1.4507(16)	C(19)-H(19A)	0.9900
C(6)-C(18)	1.4788(15)	C(19)-H(19B)	0.9900
C(7)-C(8)	1.4810(15)	C(20)-H(20A)	0.9800
C(8)-C(9)	1.4036(15)	C(20)-H(20B)	0.9800
C(9)-H(9)	0.9500	C(20)-H(20C)	0.9800
C(10)-C(11)	1.5365(16)		
C(18)-O(3)-C(19)	116.30(10)	C(6)-C(5)-H(5)	117.3
C(5)-N(1)-C(4)	119.53(9)	C(5)-C(6)-C(7)	119.82(10)
C(5)-N(1)-C(10)	118.74(9)	C(5)-C(6)-C(18)	118.27(10)
C(4)-N(1)-C(10)	121.53(9)	C(7)-C(6)-C(18)	121.90(10)
F(1)-C(1)-C(9)	118.53(11)	O(1)-C(7)-C(6)	125.68(11)
F(1)-C(1)-C(2)	118.43(11)	O(1)-C(7)-C(8)	120.49(11)
C(9)-C(1)-C(2)	123.03(11)	C(6)-C(7)-C(8)	113.83(9)
C(3)-C(2)-C(1)	118.46(11)	C(9)-C(8)-C(4)	119.27(10)
C(3)-C(2)-H(2)	120.8	C(9)-C(8)-C(7)	118.10(10)
C(1)-C(2)-H(2)	120.8	C(4)-C(8)-C(7)	122.63(10)
C(2)-C(3)-C(4)	120.19(10)	C(1)-C(9)-C(8)	118.98(11)
C(2)-C(3)-H(3)	119.9	C(1)-C(9)-H(9)	120.5
C(4)-C(3)-H(3)	119.9	C(8)-C(9)-H(9)	120.5
N(1)-C(4)-C(8)	118.77(9)	N(1)-C(10)-C(11)	112.43(9)
N(1)-C(4)-C(3)	121.17(10)	N(1)-C(10)-H(10A)	109.1
C(8)-C(4)-C(3)	120.06(10)	C(11)-C(10)-H(10A)	109.1
N(1)-C(5)-C(6)	125.35(11)	N(1)-C(10)-H(10B)	109.1
N(1)-C(5)-H(5)	117.3	C(11)-C(10)-H(10B)	109.1

H(10A)-C(10)-H(10B)	107.9	C(15)-C(16)-H(16)	120.0
C(12)-C(11)-C(10)	112.07(9)	C(17)-C(16)-H(16)	120.0
C(12)-C(11)-H(11A)	109.2	C(16)-C(17)-C(12)	120.93(11)
C(10)-C(11)-H(11A)	109.2	C(16)-C(17)-H(17)	119.5
C(12)-C(11)-H(11B)	109.2	C(12)-C(17)-H(17)	119.5
C(10)-C(11)-H(11B)	109.2	O(2)-C(18)-O(3)	122.91(11)
H(11A)-C(11)-H(11B)	107.9	O(2)-C(18)-C(6)	125.47(12)
C(13)-C(12)-C(17)	118.61(11)	O(3)-C(18)-C(6)	111.62(9)
C(13)-C(12)-C(11)	121.18(10)	O(3)-C(19)-C(20)	110.26(11)
C(17)-C(12)-C(11)	120.14(10)	O(3)-C(19)-H(19A)	109.6
C(12)-C(13)-C(14)	120.63(11)	C(20)-C(19)-H(19A)	109.6
C(12)-C(13)-H(13)	119.7	O(3)-C(19)-H(19B)	109.6
C(14)-C(13)-H(13)	119.7	C(20)-C(19)-H(19B)	109.6
C(15)-C(14)-C(13)	120.32(12)	H(19A)-C(19)-H(19B)	108.1
C(15)-C(14)-H(14)	119.8	C(19)-C(20)-H(20A)	109.5
C(13)-C(14)-H(14)	119.8	C(19)-C(20)-H(20B)	109.5
C(16)-C(15)-C(14)	119.50(12)	H(20A)-C(20)-H(20B)	109.5
C(16)-C(15)-H(15)	120.2	C(19)-C(20)-H(20C)	109.5
C(14)-C(15)-H(15)	120.2	H(20A)-C(20)-H(20C)	109.5
C(15)-C(16)-C(17)	120.00(12)	H(20B)-C(20)-H(20C)	109.5

Table 4. Anisotropic displacement parameters ($\text{\AA}^2 \times 10^3$) for KEVJAG-1-64. The anisotropic displacement factor exponent takes the form:
 $-2 \pi^2 [h^2 a^{*2} U_{11} + \dots + 2 h k a^* b^* U_{12}]$

	U_{11}	U_{22}	U_{33}	U_{23}	U_{13}	U_{12}
F(1)	21(1)	30(1)	25(1)	-1(1)	8(1)	3(1)
O(1)	29(1)	10(1)	33(1)	-2(1)	5(1)	2(1)
O(2)	39(1)	12(1)	26(1)	2(1)	6(1)	-2(1)
O(3)	22(1)	18(1)	21(1)	3(1)	3(1)	-2(1)
N(1)	17(1)	9(1)	15(1)	1(1)	0(1)	1(1)
C(1)	17(1)	22(1)	15(1)	-2(1)	1(1)	1(1)
C(2)	21(1)	18(1)	15(1)	1(1)	2(1)	-2(1)
C(3)	21(1)	12(1)	16(1)	1(1)	1(1)	0(1)
C(4)	16(1)	11(1)	13(1)	-1(1)	-1(1)	0(1)
C(5)	17(1)	11(1)	15(1)	0(1)	0(1)	-1(1)
C(6)	19(1)	10(1)	16(1)	1(1)	-1(1)	-1(1)
C(7)	18(1)	11(1)	17(1)	-1(1)	-2(1)	0(1)
C(8)	17(1)	12(1)	14(1)	-1(1)	-2(1)	1(1)
C(9)	19(1)	16(1)	16(1)	-2(1)	0(1)	2(1)
C(10)	20(1)	10(1)	17(1)	0(1)	0(1)	3(1)
C(11)	22(1)	11(1)	18(1)	-1(1)	1(1)	-1(1)
C(12)	16(1)	13(1)	16(1)	-2(1)	0(1)	-1(1)
C(13)	17(1)	19(1)	19(1)	-2(1)	1(1)	2(1)
C(14)	20(1)	27(1)	19(1)	0(1)	3(1)	0(1)
C(15)	26(1)	24(1)	21(1)	4(1)	-2(1)	-1(1)
C(16)	22(1)	23(1)	26(1)	2(1)	-2(1)	6(1)
C(17)	17(1)	20(1)	22(1)	-1(1)	2(1)	3(1)
C(18)	23(1)	14(1)	15(1)	-1(1)	-1(1)	-4(1)
C(19)	31(1)	22(1)	20(1)	2(1)	4(1)	-9(1)
C(20)	42(1)	22(1)	20(1)	2(1)	2(1)	1(1)

Table 5. Hydrogen coordinates and isotropic displacement parameters for KEVJAG-1-64.

	x	y	z	U(eq)
H(2)	1.217003	0.665844	0.151551	0.021
H(3)	0.874620	0.698431	0.215784	0.020
H(5)	0.359545	0.535257	0.345089	0.017
H(9)	1.144612	0.402728	0.195190	0.020
H(10A)	0.342888	0.677085	0.308438	0.019
H(10B)	0.523916	0.712218	0.251518	0.019
H(11A)	0.823167	0.739584	0.332217	0.021
H(11B)	0.583082	0.788269	0.357059	0.021
H(13)	0.351176	0.721884	0.453463	0.022
H(14)	0.361095	0.635699	0.551942	0.026
H(15)	0.687320	0.541340	0.573572	0.028
H(16)	1.004075	0.533760	0.495958	0.028
H(17)	0.990365	0.617922	0.396513	0.023
H(19A)	0.079435	0.287785	0.410675	0.029
H(19B)	-0.074802	0.372690	0.434038	0.029
H(20A)	0.360889	0.313940	0.495409	0.042
H(20B)	0.101376	0.312490	0.530087	0.042
H(20C)	0.232162	0.405636	0.515577	0.042

Table 6. Torsion angles [°] for KEVJAG-1-64.

F(1)-C(1)-C(2)-C(3)	-179.16(10)	F(1)-C(1)-C(9)-C(8)	178.54(10)
C(9)-C(1)-C(2)-C(3)	-0.47(18)	C(2)-C(1)-C(9)-C(8)	-0.15(18)
C(1)-C(2)-C(3)-C(4)	0.58(17)	C(4)-C(8)-C(9)-C(1)	0.64(16)
C(5)-N(1)-C(4)-C(8)	2.49(15)	C(7)-C(8)-C(9)-C(1)	-179.20(10)
C(10)-N(1)-C(4)-C(8)	177.34(10)	C(5)-N(1)-C(10)-C(11)	95.41(12)
C(5)-N(1)-C(4)-C(3)	-177.22(10)	C(4)-N(1)-C(10)-C(11)	-79.48(12)
C(10)-N(1)-C(4)-C(3)	-2.37(15)	N(1)-C(10)-C(11)-C(12)	-53.66(13)
C(2)-C(3)-C(4)-N(1)	179.60(10)	C(10)-C(11)-C(12)-C(13)	-83.29(13)
C(2)-C(3)-C(4)-C(8)	-0.10(16)	C(10)-C(11)-C(12)-C(17)	93.64(13)
C(4)-N(1)-C(5)-C(6)	-2.56(17)	C(17)-C(12)-C(13)-C(14)	-0.55(18)
C(10)-N(1)-C(5)-C(6)	-177.56(11)	C(11)-C(12)-C(13)-C(14)	176.42(11)
N(1)-C(5)-C(6)-C(7)	0.36(18)	C(12)-C(13)-C(14)-C(15)	0.61(19)
N(1)-C(5)-C(6)-C(18)	179.98(10)	C(13)-C(14)-C(15)-C(16)	0.0(2)
C(5)-C(6)-C(7)-O(1)	-177.80(12)	C(14)-C(15)-C(16)-C(17)	-0.6(2)
C(18)-C(6)-C(7)-O(1)	2.59(18)	C(15)-C(16)-C(17)-C(12)	0.7(2)
C(5)-C(6)-C(7)-C(8)	1.65(15)	C(13)-C(12)-C(17)-C(16)	-0.10(18)
C(18)-C(6)-C(7)-C(8)	-177.95(10)	C(11)-C(12)-C(17)-C(16)	-177.11(11)
N(1)-C(4)-C(8)-C(9)	179.77(10)	C(19)-O(3)-C(18)-O(2)	4.70(17)
C(3)-C(4)-C(8)-C(9)	-0.52(16)	C(19)-O(3)-C(18)-C(6)	-175.23(10)
N(1)-C(4)-C(8)-C(7)	-0.40(16)	C(5)-C(6)-C(18)-O(2)	-175.00(12)
C(3)-C(4)-C(8)-C(7)	179.31(10)	C(7)-C(6)-C(18)-O(2)	4.61(19)
O(1)-C(7)-C(8)-C(9)	-2.30(17)	C(5)-C(6)-C(18)-O(3)	4.93(15)
C(6)-C(7)-C(8)-C(9)	178.22(10)	C(7)-C(6)-C(18)-O(3)	-175.46(10)
O(1)-C(7)-C(8)-C(4)	177.88(11)	C(18)-O(3)-C(19)-C(20)	82.56(14)
C(6)-C(7)-C(8)-C(4)	-1.61(15)		

Table 7. Hydrogen bonds for KEVJAG-1-64[Å and °].

D-H...A	d(D-H)	d(H...A)	d(D...A)	<(DHA)
C(2)-H(2)...O(2)#1	0.95	2.55	3.4406(16)	156.2
C(3)-H(3)...O(1)#1	0.95	2.55	3.1574(15)	121.9
C(10)-H(10B)...O(2)#2	0.99	2.49	3.4796(15)	176.3

Symmetry transformations used to generate equivalent atoms:

#1 -x+2, y+1/2, -z+1/2 #2 -x+1, y+1/2, -z+1/2

VITA

Joel Kwame Annor-Gyamfi

Candidate for the Degree of

Doctor of Philosophy

Dissertation: RING-FUSED NITROGEN HETEROCYCLES BY EFFICIENT
SYNTHETIC STRATEGIES

Major Field: Organic Chemistry

Biographical:

Education:

Completed the requirements for the Doctor of Philosophy in Chemistry at Oklahoma State University, Stillwater, Oklahoma in May, 2020.

Completed the requirements for the Master of Science in Chemistry at East Tennessee State University, Johnson City, TN, U.S.A in 2016.

Completed the requirements for the Bachelor of Science in Chemistry at University of Cape Coast, Cape Coast, Ghana in 2012.

Experience:

Developed efficient and scalable synthetic routes to drug candidates that allow structural diversity around core scaffolds for biological evaluations. Skills include NMR, HPLC, GC-MS, UV-Vis, FT-IR

Professional Memberships:

American Chemical Society, Ghana Chemical Society